The role of the proteasome in endothelial cell senescence

Dissertation

To Fulfill the Requirements for the Degree of

Doctor of Philosophy (Ph.D.)

Submitted to the Council of the Faculty of Medicine,

Friedrich Schiller University, Jena

by

Master of Science Odeta Meçe

born on 08.05.1987 in Delvine, Sarande, Albania

May 2016

Gutachter:

1. **Prof. Dr. Regine Heller**

   Center for Molecular Biomedicine (CMB), Jena

2. **Prof. Dr. Aria Baniahmad**

   Institute for Human Genetics, Jena

3. **Prof. Dr. Tilman Grune**

   German Institute of Human Nutrition, Potsdam-Rehbrücke

Tag der öffentlichen Verteidigung: 01.11. 2016

Table of Contents

List of figures

List of tables

List of abbreviations

AGE	Advanced glycation end products
AMPK	AMP-activated kinase
ANOVA	Analysis of variance
BSA	Bovine serum albumin
BSO	DL-buthionine-[S.R]-sulfoximine
CPD	Cumulative population doublings
DAPI	4',6-Diamidino-2-phenylindole
DDR	DNA damage response
DMEM	Dubelcco's modified Eagle's Medium
DTNB	5,5'-Dithiobis-(2-nitrobenzoic acid)
DTT	DL-Dithiothreitol
ECL	Enhanced chemiluminescent
EM	Endothelial mitogen
eNOS	Endothelial nitric oxide synthase
ETC	Electron transport chain
FACS	Fluorescence-Activated Cell Sorting
FCS	Fetal calf serum
GSH	Glutathione
H_2O_2	Hydrogen peroxide
H_2SO_4	Sulphuric acid
HBP	Hexosamine biosynthetic pathway
HCl	Hydrochloric acid
HClO4	Perchloric acid
HEPES	4-(2-hydroxyethyl)-1-piperazine ethane sulfonic acid
HNE	4-hydroxy-2-nonenal
HSA	Human serum albumin
HUVEC	Human umbilical vein endothelial cells
iNOS	Inducible nitric oxide
IRS1	Insulin Receptor Substrate 1

LPM	Lactate production medium
M199	Medium 199
MLEC	Mouse lung endothelial cells
mTOR	mammalian or mechanistic Target of Rapamycin
NaCl	Sodium chloride
NaF	Sodium fluoride
NaOH	Sodium hydroxide
NFκB	Nuclear factor kappa-light-chain-enhancer of activated B cells
NO	Nitric oxide
O-GlcNAc	O-linked N-acetylglucosamine
PBS	Phosphate-buffered saline
PIC	Protease inhibitor cocktail
PMSF	Phenylmethylsulfonyl fluoride
PPP	Pentose phosphate pathway
PVDF	Polyvinylidene fluoride
Rb	Retinoblastoma protein
RNS	Reactive nitrogen species
ROS	Reactive oxygen species
RS	Replicative senescence
S6K	S6 kinase
SDS	Sodium dodecyl sulphate
SDS-PAGE	Sodium dodecyl sulfate-polyacrylamide gel electrophoresis
SIPS	Stress-induced premature senescence
TEMED	N,N,N,N-Tetraethyl ethylene diamine
TN(-T) buffer	Tris-HCl, NaCl buffer (with Tween®20)
TNB	2-Nitro-5-thiobenzoate
Tris	Tris(hydroxymethyl)aminomethane
UPS	Ubiquitin proteasome system

Summary

Endothelial cells undergo senescence *in vitro* and *in vivo,* which contributes to endothelial dysfunction and vascular diseases. Senescence may result from continuous cell division and mitotic exhaustion, known as replicative senescence or by cellular pathways responsive to stress especially in certain inflammatory or oxidative microenvironments. A decline in protein degradative systems leading to the accumulation of protein aggregates is suggested to represent one major factor driving cellular senescence during ageing.

The current project was aimed at characterising proteasomal protein degradation in endothelial cells undergoing replicative or premature senescence or chronological ageing in mice and to investigate the outcome of proteasome inhibition on endothelial senescence. Primary human umbilical vein endothelial cells (HUVECs) and primary mouse lung endothelial cells were employed in this study. *In vitro* replicative senescence was achieved by culturing HUVECs until they ceased to proliferate (15-17 cumulative population doublings) and premature senescence was obtained by subjecting HUVECs to H_2O_2. The role of the proteasome in the development of senescence was tested by applying the proteasome inhibitors MG132 and bortezomib.

We show that continuously passaged HUVECs develop features of senescence and dysfunction (positive senescence associated β-galactosidase staining, increased size and granularity, lipofuscin accumulation, upregulation of the p53/p21 pathway, decreased expression of endothelial NO synthase, increased expression of inducible NO synthase) and that chronic oxidative insult leads to premature senescence development. Simultaneously, endothelial cells isolated from old mice confirmed senescence *in vivo.* Senescent cells were characterised by a decline in the ubiquitin proteasome system. Both HUVECs undergoing senescence *in vitro* as well as endothelial cells aged *in vivo* showed a selective loss of the proteasome subunits β2 and β5 and a corresponding inhibition of trypsin-like and chymotrypsin-like activities. Furthermore, transient proteasome inhibition by MG132 or bortezomib rendered young endothelial cells prematurely senescent, which was accompanied by increased oxidative stress and most probably mediated via the p53/p21 pathway. Bortezomib application led to DNA damage apparently responsible, in part, for the activation of p53. These findings establish that proteasome inhibition is likely to be causally

related to endothelial senescence. Unravelling the molecular links between proteolytic decline and senescence will facilitate better understanding of age-associated pathologies of the cardiovascular system.

Zusammenfassung

Endothelzellen unterliegen *in vitro* und *in vivo* Seneszenz, welche vermutlich zur Entwicklung von endothelialer Dysfunktion und vaskulären Erkrankungen beiträgt. Seneszenz entsteht durch Verlust der Zellteilungsfähigkeit (replikative Seneszenz) oder nach Einwirkung von oxidativem oder inflammatorischem Stress, der in bestimmten Gefäßbereichen auftreten kann. Zu den wichtigen Faktoren, die zelluläre Seneszenz induzieren können, scheint eine Verminderung und/oder Insuffizienz der Proteinabbausysteme mit nachfolgender Akkumulation von Proteinaggregaten zu gehören.

Das vorliegende Projekt hatte das Ziel, das Proteasom, ein wichtiges Proteinabbau-System, in Endothelzellen, die replikativer oder stress-induzierter Seneszenz oder Alterungsprozessen in der Maus unterliegen, zu charakterisieren. Zudem sollte untersucht werden, ob eine Hemmung der proteasomalen Aktivität in Endothelzellen zur Entwicklung einer Seneszenz führt. Als Modelle dienten humane primäre Endothelzellen aus der Nabelschnurvene (HUVEC) und murine primäre Endothelzellen, die aus der Lunge von Mäusen gewonnen wurden. Replikative Seneszenz wurde durch Langzeitkultivierung der Zellen im Allgemeinen nach 15-17 kumulativen Populationsverdopplungen und vorzeitige Seneszenz durch Einwirkung von H_2O_2 induziert. Zur Untersuchung der Rolle des Proteasoms bei der Entwicklung von Seneszenz wurden die Proteasominhibitoren MG132 und Bortezomib eingesetzt.

Die hier vorgelegten Daten bestätigen anhand verschiedener Seneszenzmarker die Entstehung replikativer Seneszenz nach Langzeitkultur von Endothelzellen (positive Seneszenz-assoziierte β-Galaktosidase-Färbung, erhöhte Zellgröße und Granularität, Aktivierung des p53/p21-Signalweges, verminderte Expression der endothelialen NO-Synthase und erhöhte Expression der induzierbaren NO-Synthase). Ebenso führten chronischer oxidativer Stress und Zellalterung *in vivo* zu Seneszenz. Die Entwicklung der Seneszenz war durch eine Verminderung des Ubiquitin-Proteasom-Systems gekennzeichnet. In allen Modelle (replikative oder vorzeitige Seneszenz in HUVEC, *in-vivo*-Alterung) waren eine selektive Verminderung der β2 und β5-Untereinheiten des Proteasoms und eine entsprechende Reduktion der Trypsin- und Chymotrypsin-ähnlichen Aktivitäten zu beobachten. Eine transiente Hemmung des Proteasoms durch MG132 oder Bortezomib

führte zu vorzeitiger Seneszenz, die mit oxidativem Stress und einer Hochregulation des p53/p21-Signalweges einherging. Bortezomib-Behandlung von HUVEC führte zu einer DNA-Schädigung, die vermutlich, zumindest teilweise, für die Aktivierung von p53 verantwortlich ist. Diese Daten zeigen, dass eine Verminderung der proteolytischen Kapazität des Proteasoms ursächlich an der Entstehung der Seneszenz beteiligt ist. Die Aufdeckung des Zusammenhangs zwischen proteolytischer Insuffizienz und Zellalterung trägt zu einem besseren Verständnis von altersabhängigen Gefäßerkrankungen bei.

1 Introduction

Multicellular organisms are complex assemblies of cells organised in tissues and organ systems. Such biological systems, be it cells or whole organisms, are evolutionarily designed to perform with astounding precision and accuracy, with a great degree of conservation of processes and pathways controlling vital functions [1,2]. Despite such fail-safe mechanisms, several environmental/extrinsic factors and intrinsic programs lead to occasional errors. As a consequence, irreversible damages accumulate with time, and ageing results [3,4].

1.1 The endothelium – guardian of the vasculature

Proper functioning of the circulatory system ensuring continuous supply of blood and nutrients is a major determinant of an organism's health span. Being in direct contact with the bloodstream, the endothelium is of utmost importance in nutrient exchange and elimination of metabolic waste from surrounding tissues [5]. The endothelium is the innermost lining of the vascular system, and is a continuum of cells embraced by a connective basal lamina, and supported by a layer of smooth muscle cells [6] (Fig.1).

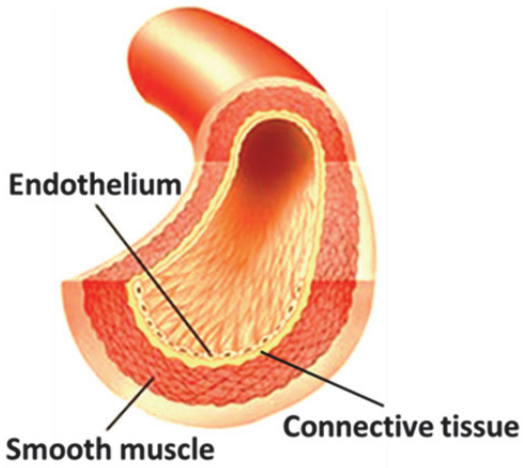

Figure 1: Morphology of a human artery

Schematic view of a vessel composed of the endothelium, smooth muscle cells and a layer of connective tissue between them. The outer layer is mainly composed of collagen and supported by an elastic lamina. Figure adopted from Subbotin et al [7].

Endothelial cells often come across chemical or physical signals, which stimulate them to produce and release factors that modulate physiological processes. These factors can act at

different levels and regulate processes such as angiogenesis, vasodilation and vasoconstriction, platelet adhesion and blood coagulation, smooth muscle cell growth and inflammation [8]Mounting evidence shows that apart from its principal function as a barrier mediating exchange between blood and tissues, the endothelium can function as an endocrine tissue and thereby regulate vascular homeostasis [9]. Despite commonality in their functions, endothelial cells are vastly heterogeneous owing to the diversity of vasculature, e.g., arterial *vs.* venous vasculature, macro- *vs.* microvasculature [10]. Morphologic and functional alterations of the endothelium resulting from physical injury or cytokine-mediated activation, is termed endothelial dysfunction. Balanced functioning of the endothelium is necessary to maintain vascular homeostasis, and ageing perturbs this equilibrium. Vascular ageing is associated with reduced nitric oxide (NO) bioavailability, increased superoxide production due to upregulation of NADPH oxidase, endothelial NO synthase (eNOS) uncoupling, increased endothelin-1 (ET-1), reduced production/responsiveness to dilatory prostaglandins, enhanced inflammation, advanced glycation end-products (AGE) formation, all of which contribute to endothelial dysfunction [11]. Age-related phenotypic changes in the vasculature are independent risk factors for atherosclerosis and other cardiovascular diseases [12]. Thus, understanding mechanisms of age-induced vascular alterations holds promise for reducing cardiovascular mortality in an ageing population.

1.2 Ageing and Senescence

By definition, the accumulation of diverse deleterious changes occurring in cells and tissues with advancing age, and being responsible for increased risk of disease and death has been termed ageing [13]. The ageing phenomenon is not only observed at the level of an organism, but also detectable at the cellular or biochemical level – termed “cellular senescence”. While cellular senescence in itself cannot be regarded as a deleterious phenomenon, its build-up certainly contributes to organismal ageing [14-16]. The ageing process progresses at variable rates such that life span of organisms is stratified very diversely among different species. The search for a single cause for ageing in general and endothelial dysfunction in particular, have long been replaced by the view that these processes are extremely complex and multifactorial.

Human evolution over eras and biomedical healthcare advances over the last century has made ageing more obvious among us. In fact, approximately two thirds of all deaths around the globe each day has an age-related cause, and ageing stands among the greatest risk factors for most of human diseases with cardiovascular diseases being the foremost [17]. In this context, ageing has profound implications for individuals, an entire population, the society and the economy, with immediate impact on the healthcare industry.

It has been a long-term research goal of gerontologists to identify common determinants of life span among species. The fact that the average life span is largely conserved within a certain species, immediately points to genetic underpinnings to the ageing process. The first ever report that cells underwent ageing in culture came from Leonard Hayflick in 1965 who hypothesised based on his observations that "The finite lifetime of diploid cell strains *in vitro* may be an expression of ageing or senescence at the cellular level" and coined the term "Hayflick's Limit" [18]. This discovery spurred extensive research over the last five decades on the genetic and environmental factors, and the mechanisms driving ageing of cells and organisms. More recently, attempts and means to improve cardiovascular performance and extend healthy lifespan of individuals have interested the ageing research community.

It is noteworthy, that the last three decades have shed enormous light on the molecular cues that induce, mediate and sustain cellular senescence, although with increasing complexity. Senescent cells are radically distinct from their proliferation-competent younger counterparts and they display genetic, morphological and behavioural differences. These differences are believed to have a detrimental impact on structural components, neighbouring cells and the extracellular matrix leading to aged tissues and increased disease risk [19]. Such deleterious effects of a build-up of senescent cells in ageing tissues is evident after attainment of reproductive maturity, when restorative functions begin to decline and tissue damage is enhanced (Fig.2). Indeed, metabolic syndromes including cancer, type 2 diabetes and cardiovascular diseases, termed lifestyle disorders, pose the highest healthcare risk in the 21st century and are associated with older ages, implying that ageing of the involved organ systems increases disease risk [20].

In this thesis, we have attempted to investigate how the cellular protein degradation systems and proteostasis impacts endothelial cell senescence, both in vitro and as part of physiological ageing.

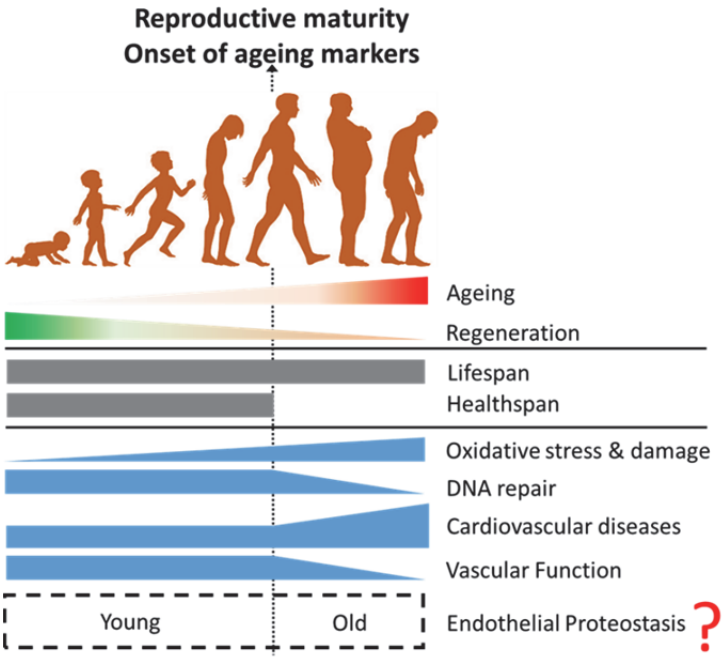

Figure 2: Alterations in physiology of humans during lifespan

Scheme depicting how increasing age in humans is associated with decreased regenerative capacity. Attainment of reproductive maturity marks the emergence of pathologies due to a decline in restorative functions. Exactly at what stage of the ageing process, protein homeostasis is lost, and whether this accelerates ageing, is the subject of focus in this thesis. Human ageing cartoon series (in brown) obtained from www.maxworkouts.com

1.3 Causes and consequences of senescence

Over the last century, several theories have been proposed, hypothesising the cause of ageing. Weak evolutionary negative selection pressure for deleterious traits, free radicals, mitochondrial dysfunction, anomalous gene regulation, telomere erosion, immune exhaustion and neuroendocrine effects have all been proposed [13]. In practise or reality, the precise cause of ageing is difficult to pinpoint. However, no two causes are mutually exclusive; in fact, all factors have to be considered as cumulative contributors.

Moreover, among known factors, defining the causes and consequences of senescence becomes difficult to dissect at some point, since the consequence becomes the cause in a vicious cycle.

This highly sought-after research problem, has not only thrown light on the factors, genetic or otherwise, that drive and accelerate the ageing process, but also uncovered subtypes of senescence in response to diverse inducers helping us understand the functional significance of senescence development [21,22]. With respect to endothelial cells, two major modes of senescence are predominant – replicative senescence (RS) and stress-induced premature senescence (SIPS).

1.3.1 Replicative senescence (RS):

The first described and classically view on senescence, comes from the so called "Hayflick limit", a measure of the finite number of cell divisions undergone before reaching growth stop. This type of cellular senescence, known as replicative senescence, is a state of irreversible growth arrest, caused by a sub-critical erosion of telomere length [18]. Telomeres are protective cap structures at linear chromosome ends, and their erosion triggers a DNA damage response (DDR), which is associated with the appearance of foci that stain positive for γH2AX (Ser 139 phosphorylated histone H2A variant X) [23,24]. Amplification of the DDR signals and further cascade of events activates several cell cycle regulatory proteins such as cell division cycle 25 (Cdc25) or tumour suppressor protein of 53 KiloDaltons (p53) to arrest the cell cycle [25,26] (Fig.3). This may lead to a transient proliferation arrest, allowing time for cells to repair their damage. Sustained damage inducers or damage response signalling, however, reinforces commitment to senescence or permanent growth arrest.

Telomerase is a ribonucleoprotein DNA polymerase complex that maintains telomere length. The complex comprises the protein telomerase reverse transcriptase (TERT) and a catalytic RNA molecule that is used as a template when to elongate telomeres. Human endothelial cells and vascular smooth muscle cells express telomerase activity and its activity is declined with *in vitro* ageing because of a decrease in the expression of TERT leading to vascular cell senescence [27]. On the other hand, introduction of telomerase extends lifespan of endothelial cells and vascular smooth muscle cells, suggesting a crucial role of telomerase in vascular cell senescence [28]

1.3.2 Stress-induced premature senescence (SIPS):

A variety of stress conditions can evoke a senescence response or a senescence-like long term arrest, called stress-induced premature senescence, in which telomere length is virtually unaltered and functionally intact. Factors pertaining to culture shock and stress conditions could be counted as a cause of premature senescence [29].

These include oxidative growth environment (for instance, culture in non-physiological partial O_2 pressure) [30,31], high glucose, persistent mitogenic stimulation, several genotoxic stressors, e.g., doxorubicin and platinum compounds, and oxidative agents e.g., hydrogen peroxide, paraquat etc. They are known to induce senescence in primary, non-transformed cells, by direct damage to cellular biomolecules or indirectly generating reactive species [22,32-34]. The most susceptible cellular targets of oxidative stress are DNA, proteins and the mitochondria, all of which, when damaged, induce senescence. Additionally, oxidized proteins may aggregate and generate non-degradable cellular debris known to impair functioning of organelles and accelerate senescence [35,36]. Several lines of evidence support the fact that endothelial cells undergo SIPS upon different stimuli in certain microenvironments. Farhat et al. (2008) have shown that endothelial cells isolated from chronic smokers with premature atherosclerosis undergoing coronary artery bypass graft surgery, exhibit cellular senescence and this is independent of telomere length and directly related to oxidative damage [37].

Moreover, Coleman at al. (2010) have shown that SIPS in endothelial cells caused either by H_2O_2 or by overexpression of the *SENEX* gene led to an anti-inflammatory phenotype thus suggesting a unique protective role of this type of senescence to inhibit uncontrolled proliferation and limit inflammatory response of endothelial cells [38]. Other reports in vascular biology highlight impaired glucose tolerance as a factor influencing atherosclerosis and senescence [39-42]. Intermittent high glucose was shown to promote vascular endothelial senescence more than constant high glucose independent of telomere attrition but partially dependent on superoxide production [39]. Regardless of the senescence trigger, cells engage either one or both the p53/p21 and p16/Rb tumour suppressor pathways, as the downstream effectors of the senescence program (Fig.3).

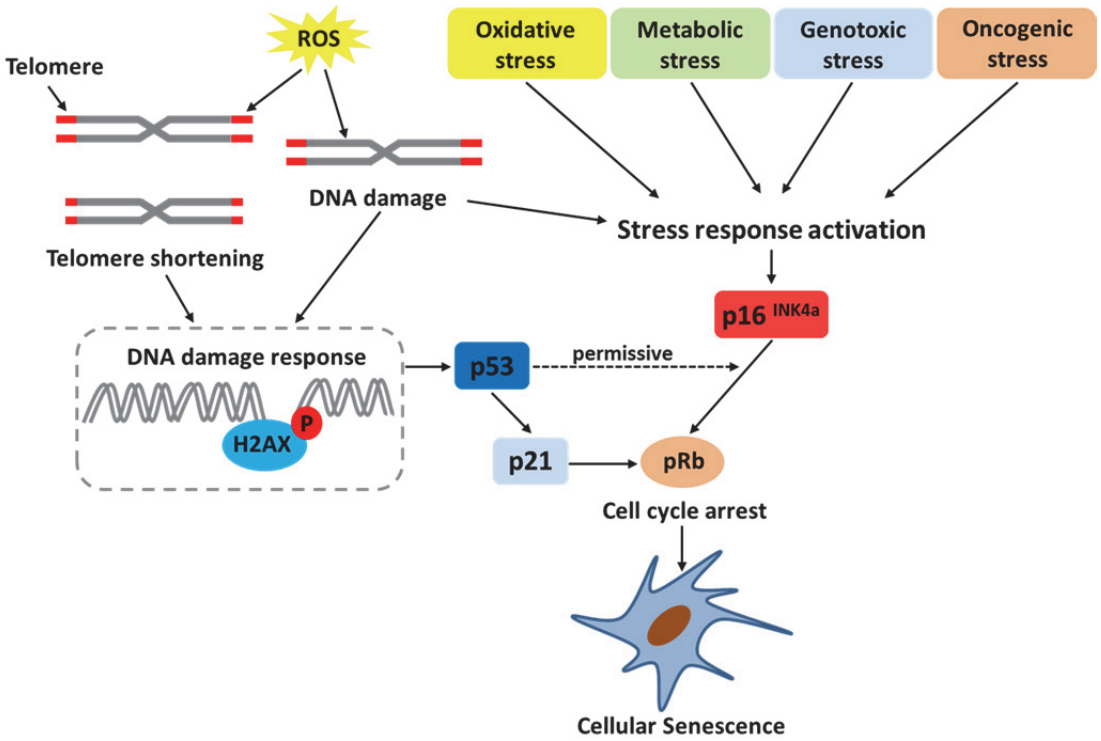

Figure 3: Modes of senescence induction in endothelial cells

Replicative senescence is caused by telomere shortening after each cell division or by telomeric DNA damage caused by reactive oxygen species. Recognition of unrepaired damage by gH2AX and the activation of the DNA damage response engage the p53/p21 pathway. Different types of cellular stresses such as oxidative, metabolic, oncogenic or genotoxic, cause upregulation of the tumour suppressor cyclin-dependent kinase inhibitor 2A ($p16^{INK4a}$) which keeps Rb protein (pRb) in a hypo-phosphorylated growth-inhibitory state. On the other hand, activation of p53 may have a permissive role in regulation of p16/Rb pathway. Most senescence triggers converge at the level of Rb, which is essential for initiating a cell cycle arrest and permanent senescence.

1.4 Molecular factors concocting endothelial senescence

Senescence represents an intriguing biological process of irreversible cell cycle arrest despite high metabolic vitality of cells, and is believed to have evolved as a barrier against cellular transformation [43,44]. A multitude of factors are identified as drivers of senescence. By virtue of its location, morphology and specialised function, the endothelium is most susceptible to factors such as oxidative and nitrosative stress, DNA and mitochondrial damage as well as disturbances in protein homeostasis.

1.4.1 Oxidative/nitrosative stress

Reactive oxygen species (ROS) and reactive nitrogen species (RNS) are generated as by-products of cellular metabolic or enzymatic reactions as well as during mitochondrial

oxidative phosphorylation [45]. They act as second messengers mediating vital endothelial functions including proliferation, migration and angiogenesis [46]. However, conditions under which the load of reactive species overshoots normal threshold are frequent and countered by anti-oxidant cell responses. Super-threshold ROS levels or sub-threshold anti-oxidant defences due to alterations in cellular metabolism and mitochondrial function are seen in virtually all cardiovascular diseases. ROS are known to trigger both induction and acceleration of senescence. They can induce DNA damage or telomere erosion/damage, which further activates damage responses [47] (Fig.4). Furthermore, ROS are believed to activate "senescence signals", for instance protein oxidation, which lead to the establishment of senescence [48] (Fig.4). Studies in endothelial cells have shown that manipulation of the redox environment by exposure to homocysteine, application of glutathione inhibitors or exposure to advanced glycation end products (AGE) accelerates senescence while application of the antioxidant vitamin C delays it [49-51]. Thus, oxidative stress can be considered as a major stimulus for endothelial senescence induction and development by acting at multiple cellular levels.

Nitric oxide (NO) is produced by two enzymes in the vascular endothelium: endothelial nitric oxide synthase (eNOS) under normal conditions or inducible nitric oxide synthase (iNOS) in cases of inflammation. NO is particularly important in the regulation of vasotonus but its abnormal production by iNOS can induce endothelial dysfunction. In addition, uncoupling of eNOS under conditions of oxidative stress promotes dysfunction via production of superoxide anion. The role of NO in senescence remains controversial but recent studies suggest that eNOS-derived NO may counteract senescence in the context of cellular stress through upregulation of Sirtuin 1 (SIRT-1) [52]. A plethora of studies have established that senescent endothelial cells have lower levels of eNOS expression and a reduction in NO bioavailability, which was attributed to an increase in mitochondrial-derived ROS [52]. High NO output from iNOS may lead to production of peroxynitrite, which can have deleterious biological actions by oxidizing intracellular signal transduction molecules thereby disturbing their function and mediating pathophysiological alterations [53,54].

1.4.2 Telomere attrition

Telomere shortening is by far the best studied driver of cellular senescence. Telomeres are cap structures of linear chromosome consisting of tandem TTAGGG repeats. Its attrition is

attributed to the “end replication problem”, whereby replicative polymerases lack a template strand to extend daughter strands at chromosomal ends. It is thought that erosion of telomeres beyond a critical limit after several cell divisions results in the loss of genetic information at terminal loci of chromosomes, leading to replicative senescence [55] (Fig.4). Telomerase, the key enzyme, which is part of the enzymatic machinery maintaining telomere caps, is expressed in many cell types of renewable tissues such as pluripotent stem and germ cells [56]. In fact telomerase deficiency has been shown to negatively impact cell function as it increases oxidative stress by reducing catalase activity which is a determinant of redox imbalance. In addition, telomerase overexpressing cells accumulate lower concentration of peroxides [57]. Endothelial cells possess telomerase activity when they proliferate although at lower levels than those found in stem cells or cancer cells [58]. Endothelial telomerase activity is amenable to regulation by factors including cell mitogens, nitric oxide, inflammatory mediators and oxidative stress [50]. Regulation of telomerase activity has been shown at multiple levels starting from transcription, phosphorylation of its catalytic subunit, redox-controlled changes in intracellular localization as well as its direct oxidative modification [50]. A role of telomerase decline in endothelial senescence as well as prevention of senescence by telomerase overexpression in endothelial cells has been reported [59].

1.4.3 Mitochondrial damage

Mitochondria, cellular power houses, are sites of active metabolic turnover in the cell. Since mitochondria comprise the electron transport chain (ETC) complexes and oxidative phosphorylation reactions of cellular respiration, mitochondrial DNA, not protected by histones, is in close proximity to ROS sources and vulnerable to oxidative DNA damage [60] one of the many causes of mitochondrial dysfunction in senescence. Endothelial cells are primarily dependent on glycolysis and to a lesser extent on mitochondrial respiration [61], which may protect them from oxidative damage. However, mitochondrial ETC dysfunction seems to be an integral part of endothelial senescence (Fig.4). Anomalies in biogenesis, mitochondrial mass, expression of ETC complexes, fission and fusion of mitochondria are known to affect endothelial cell function and contribute to senescence [62]. Complex IV and complex I of the ETC have been shown to malfunction in ageing, leading to further generation of undesirable ROS, which can drive telomere-dependent senescence [63]. In

endothelial cells, excessive mitogenic stimulation due to forced expression of activated oncogenes such as Akt [64], Ras [65], or Rac1 [66], is known to induce senescence [50]. Cellular transformation with oncogenic Ras, best studied for senescence induction [67], is known to increase mitochondria biogenesis, elevate ROS levels, and cause DNA replication stress leading to damage and senescence [68]. In fact, pro-atherogenic conditions, like hyperinsulinaemia, chronic inflammation, and hypercholesterolaemia, activate Akt- and Ras-mediated signalling in endothelial cells, and may mediate senescence [27,69]. Additionally, evidence that mitochondria are drivers of senescence comes from reports which document that cells with absence or depletion of mitochondria, while preserving energy levels through enhanced glycolysis, reduce a spectrum of senescence effectors and senescence-associated changes [70]. Thus, it has been proposed that mitochondrial dysfunction is a common denominator linking stress-dependent and telomere-dependent physiological ageing processes in cells [71].

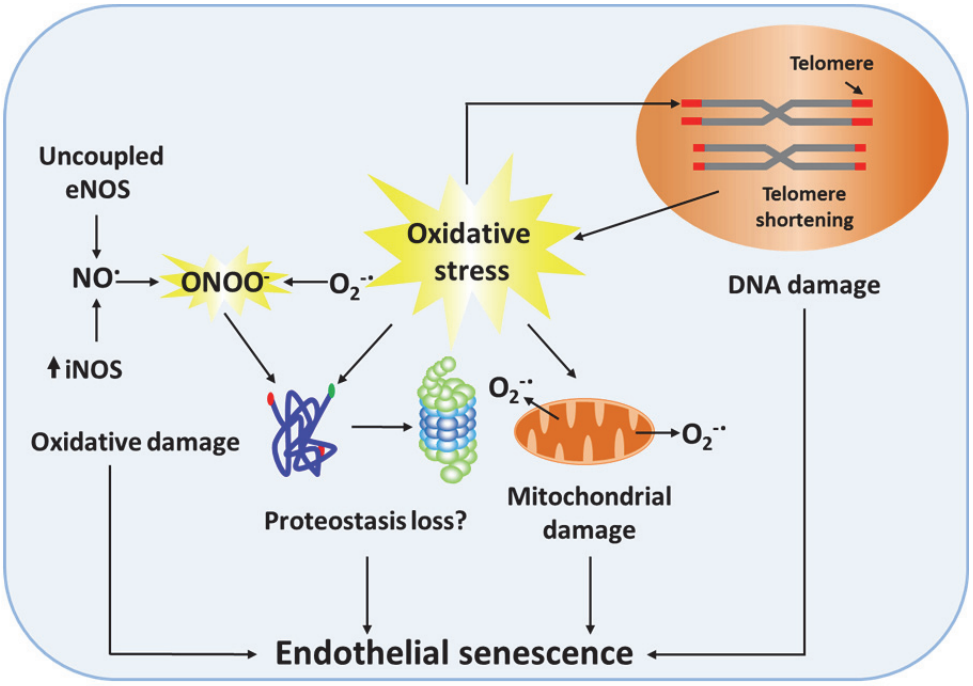

Figure 4: Molecular factors concocting endothelial senescence

Many factors contribute to senescence development starting from telomere shortening after each cell division which is associated with enhanced production of reactive oxygen species. A second factor is NO present in high concentrations as a result of eNOS uncoupling and upregulation of iNOS. Due to mitochondrial damage endothelial cells produce high levels of reactive species like superoxide anion. Superoxide in the presence of NO forms peroxynitrite, which is highly reactive and

can oxidize proteins resulting in loss of function. Highly modified proteins become unrecognized by the proteolytic system and cell suffers from proteotoxic stress.

1.4.4 Proteostasis loss

Protein homeostasis is indispensible to cellular health and longevity of organisms. Proteostasis entails the integration of diverse biological pathways that control the biogenesis, trafficking as well as degradation and recycling of proteins. Mammalian cells compartmentalise these functions to ensure protein quality by chaperone-assisted folding and unfolded protein response. In addition, they use complex mechanisms like the ubiquitin proteasome system (UPS) and autophagy to turnover proteins in order to regulate proteostasis [72]. Perturbations due to stress or ageing in any branch of the proteostasis network can elicit a breakdown of the entire network and manifest as numerous metabolic, cardiovascular or neurodegenerative disease. Toxic build-up of amyloid-β in Alzheimers' and the age pigment lipofuscin in the myocardium present evidence for loss of proteostasis with ageing [73]. Compromised protein homeostasis facilitates proteins to attain aberrant conformational structures and to generate misfolded aggregates, the persistence of which is believed to cause a myriad of cellular dysfunctions. Thus, gaining functional insight into the complex protein catabolic machinery, such as the proteasome, and understanding its relationship with endothelial senescence will aid conceptual advancement in the treatment of cardiovascular diseases.

1.5 Proteasome structure and function

Protein homeostasis is essential to cell survival and well-being [74]. In this context clearance of dysfunctional proteins, which have become resistant to folding due to protein modifications over time, becomes a challenge. To cope with it, eukaryotic cells have developed two major pathways: the UPS and autophagy [75]. While autophagy is primarily responsible for degradation of long-lived proteins and cellular organelles, the UPS is a very specialized and highly controlled protein shredder responsible for degradation of most cytosolic, nuclear and endoplasmatic reticulum proteins [75]. Even though largely distinct, the UPS and autophagy activities are carefully orchestrated through interfering elements and are critical for several aspects of cellular homeostasis.

The UPS is the major nonlysosomal protein degradation machinery in human cells and counts for a number of key biological regulatory mechanisms. The proteasome makes up 1% of total cell proteins. It diffuses freely within cytoplasm and nucleoplasm or is found associated with different structures [76].

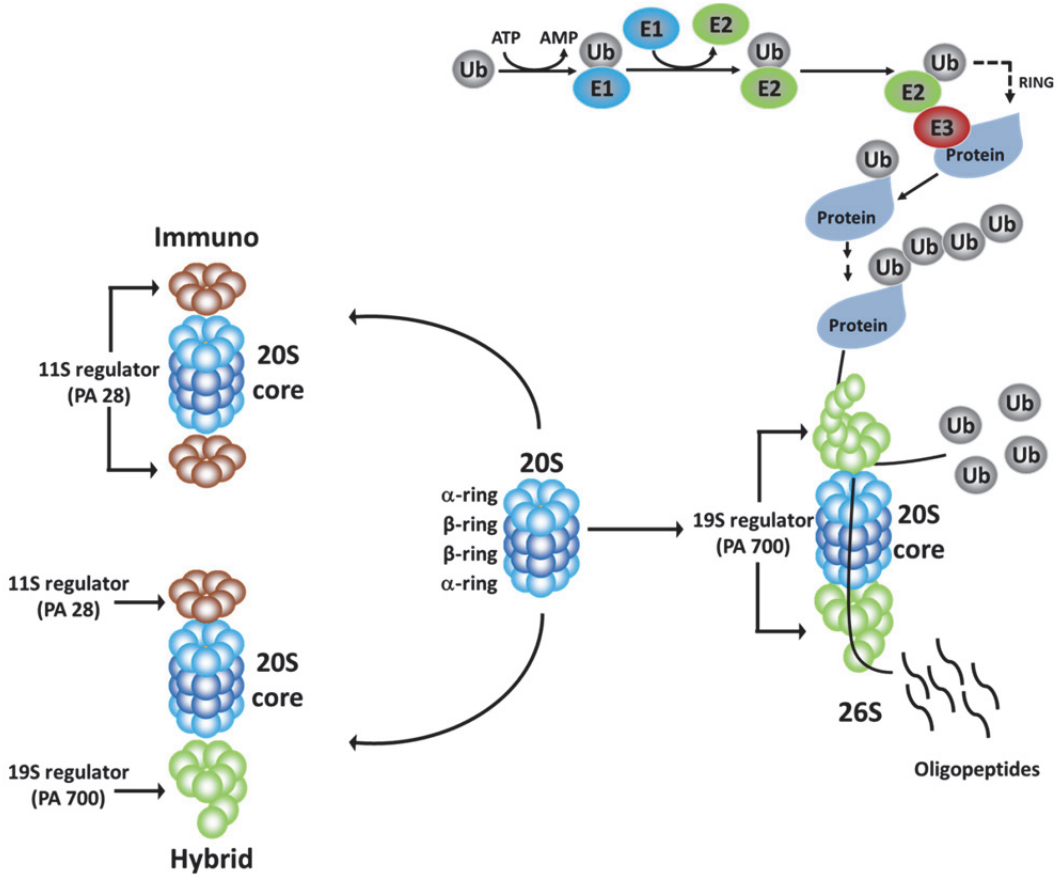

Figure 5: The ubiquitin proteasome system

Four kinds of proteasomes are known: the 20S proteasome, the 26S proteasome, the immunoproteasome and the hybrid proteasome. The 26S proteasome recognises substrates after they have been ubiquitinated.

In the cytosol, subpopulations of the proteasome are found associated with the external surface of the endoplasmic reticulum (ER), the cytoskeleton and the centrosome [77]. In the nucleus, the proteasome is found in subnuclear foci known as PML bodies. Several protease complexes are known such as the 20S and the 26S proteasme, the immunoproteasome and hybrid proteasome [78] (Fig. 5).

1.5.1 20S proteasome

The 20S proteasome builds up the core structure of all other functional forms of proteasomes and plays a crucial role in several cellular processes including half-life of proteins, protein quality control, gene expression, regulation of the cell cycle, DNA repair, stress and immune responses and degradation of oxidised proteins [79,80]. The 20S proteasome forms a barrel-like structure composed of two α rings forming the outer part of the barrel and two β rings arranged in the middle. Each of the α/β rings consists of 7α and 7β subunits ($\alpha_{1\text{-}7}/\beta_{1\text{-}7}$) [81]. The α-subunits are specialised in substrate recognition and binding of proteasome regulators. The β-subunits carry the proteolytic centers of the 20S core structure and degrade polypeptides and proteins introduced to them by α subunits. From 7 types of β subunits only three of them possess a threonine protease activity. The β1 subunit has a caspase-like activity (cleavage after acidic residues), the β2 subunit has a trypsin-like activity (cleavage after basic amino acids) and the β5 subunit has a chymotrypsin-like activity (cleavage after neutral amino acid) [82]. The specific catalytic activities are activated only after substrate proteins are recognised by α subunits. The 20S proteasome is known to degrade oxidised or damaged proteins in an ATP-independent manner [83,84] .

1.5.2 26S proteasome

The 26S proteasome is formed when the 20S proteasome assembles as a complex with two 19S proteasome regulators (also known as PA700) [81]. This results into formation of a huge complex of approximately 2 MDa. The 19S regulators form a base, which binds to the α-rings of the 20S core, and a peripheral lid for controlling entrance of polyubiquitinated substrate proteins. The base of the 19S regulator consists of six AAA-ATPase subunits, Rpt1–Rpt6, and four non-ATPase subunits, Rpn1, Rpn2, Rpn10, and Rpn13 [81,85,86]. The lid is composed of nine non-ATPase subunits including Rpn11. The base of the 19S regulatory particle is responsible for recognition and unfolding of ubiquitin-tagged substrates and its translocation to the α-subunits of the 20S core while the lid is responsible for deubiquitination. Protein unfolding and the opening of the proteasome gate are mediated by the six Rpt subunits in combination with Rpn1 and Rpn2 [87,88]. Rpn10 and Rpn 13 conduct recognition and binding of polyubiquitinated proteins while Rpn11 deubiquitinates proteins [88]. Degradation via the 26S proteasome is an ubiquitin-dependent process and is considered

the major system that mediates the degradation of damaged and short lived proteins [75,89]. The proteolysis process by the 26S proteasome requires not only the proteasome but also three important enzymes, which add ubiquitin onto substrate proteins. E1 enzymes activate the ubiquitin, E2 enzymes bind to the ubiquitin molecule and E3 enzymes transfer the ubiquitin molecule to the target protein [88,90,91] (Fig. 5). After being introduced to the proteasome and after proteolysis has taken place, free ubiquitin and oligopeptides are released.

1.5.3 Hybrid and immunoproteasomes

Two other forms of functional proteasomes are the hybrid proteasome and immunoproteasome. The hybrid proteasome forms when the 20S core binds two different regulatory particles: the 19S particle (PA 700) and the 11S particle (also known as PA28) [92]. The immunoproteasomes forms when the 20S core binds the 11S regulatory particles on both sides and at the same time normal β subunits (β_1, β_2, β_5) are replaced by inducible β-subunits (β_{1i}, β_{2i}, β_{5i}) [85]. Synthesis of the immunosubunits is induced upon stimulation with IFN-γ or TNF-α. The primary function of the immunoproteasome is related to MHC class 1 antigen presentation but recent studies have demonstrated other biological functions including regulation of proinflammatory cytokine production as well as differentiation and proliferation of T-cells [93,94]. Beside its immune functions, the immunoproteasome has other functions in non-immune cells such as protection from oxidative stress through degradation of oxidatively modified proteins and inhibition of protein aggregate formation [95,96]. Endogenous production of NO by iNOS seems to be important for basal regulation of the immunoproteasome since aortas of $iNOS^{-/-}$ mice reveal lower levels of β1i (also known as LMP2) and β5i (also known as LMP7) [97]. At the same time NO-mediated immunoproteasome signaling was shown to ameliorate transferrin-iron-mediated oxidative stress via the degradation of the transferring receptor [97].

1.6 Oxidative stress and protein modifications

Oxidative stress occurs as a result of ROS formation in the presence of poor anti-oxidative defense mechanisms. ROS are a large group of oxygen-containing molecules such as superoxide anion ($^{\cdot}O_2^-$), hydroxyl radicals ($^{\cdot}OH^-$), hydrogen peroxide, peroxynitrite ($ONOO^-$). The main source of ROS are the electron transport chain of the mitochondria and other

enzymes such as NAD(P)H oxidases, xanthine oxidase, cyclooxygenase and lipoxygenase [98]. To cope with oxidative stress cell have developed protective systems, which include glutathione, catalase and superoxide dismutase [99]. A loss in anti-oxidative mechanisms leads to chronic exposure of proteins, DNA and lipids to ROS. They can affect single amino acids with consequences for the structure of the whole protein thus facilitating protein aggregate formation. Some amino acid residues including cysteine, methionine, glutamine and the aromatic amino acids phenylalanine, tyrosine, histidine are more prone to oxidative modifications than others [100]. Direct oxidation of lysine, arginine, proline or threonine may lead to the formation of reactive ketones or aldehydes (protein carbonyls), which represent irreversible protein modifications and may serve as markers of oxidative stress [84,101]. Carbonylation can also occur as a result of interaction of proteins with lipid peroxidation products such as 4-hydroxy-2-nonenal (HNE), malondialdehyde (MDA), and advanced glycation end products (AGE) [102]. Another common marker of oxidative stress is formation of nitro-tyrosine modifications from the reaction of peroxynitrite with electron-rich-groups, such as sulfhydryls, iron-sulfur centers, zinc-thiolates and the active site sulfhydryl in tyrosine phosphatases [103]. Production of peroxynitrite can be instrumental in the development of many pathophysiological conditions in vivo since it affects signaling pathways and protein functions.

1.7 Protein aggregation

Protein modifications can affect three-dimensional structures of proteins, make their hydrophobic core more visible and prone to interact with other hydrophobic groups and thus promote aggregation [104]. Several reasons have been proved to contribute to this process starting from inherited genomic mutations (in case of neurodegenerative disease such as Alzheimers disease, Huntington's disease, Parkinson disease), mutations in quality control proteins like the heat shock family (HSP), defects in protein biogenesis including many translational errors, errors in post-translational modifications such as glycosylation, phosphorylation, ubiquitination and, finally, defects in proteolytic cleavage [105].

In addition to the above mentioned factors, chronic oxidative stress and UV-irradiation, which are known to accompany the ageing process, can serve as a major reason for aggregate formation [99]. Aggregation triggered by oxidative stress is a process happening

over time in a step-wise manner. When only moderate modifications occur, proteins are still active and functional but when oxidative stress persists and oxidation process advances, protein misfolding and loss of protein function occurs [106]. Depending on the degree of misfolding, the protein quality control decides whether the protein should be rescued by refolding or it should undergo degradation via the proteasome. If misfolded proteins are neither refolded nor degraded, oxidation goes on and proteins cross-link with others. In case of proteolytic insufficiency, be it due to the ageing process or other reasons, the amount of damaged proteins increases and therefore protein aggregation occurs [84].

1.8 Lipofuscin

Lipofuscin, also known as the age pigment is an extensively oxidized and cross-linked aggregate which contains oxidized proteins (30-58%), lipids (19-25%) and metals such as iron, copper, zinc, manganese and calcium (2%) [107]. Lipofuscin formation has been attributed to a decline in macroautophagy and activity of the UPS as a result of the ageing process [108-110]. It increases during the lifetime of a cell and negatively correlates with the life expectancy of postmitotic cells [111]. Being an active material with the ability to bind metals and grow in surface, it has toxic potentials through which it affects cells and tissue. Tissues with a high protein turnover such as the brain and heart have been shown to accumulate lipofuscin resulting in highly reactive surfaces which keeps protein oxidation on-going. An interesting observation from Höhn et al. revealed that lipofuscin alone can serve as an independent factor for preventing proteasome-mediated proteolysis [112], which is clearly correlated with the ageing process [113-115]. Lipofuscin is also accumulated in lysosomal storage disorders [116].

1.9 Proteasome inhibition as therapeutic approach

The expression levels of several key proteins involved in the control of inflammation, cell cycle regulation and gene expression are tightly controlled by the proteasome [117]. Accordingly, inhibition of the UPS affects a plethora of cellular processes [117,118] and may lead to cell cycle arrest and cell death in numerous cell types. UPS inhibition thus represents an attractive strategy for the therapy of hyperproliferative diseases such as multiple myeloma (Velcade/bortezomib) or vascular restenosis [119,120]. Beyond its antiproliferative and

proapoptotic effects, proteasome inhibition represents a novel approach for the treatment of inflammatory diseases including rheumatoid arthritis and reperfusion injuries, as several studies revealed their potent anti-inflammatory properties based on their ability to block activation of the inflammatory transcription factor nuclear factor kappa B (NFκB) [121]. In endothelial cells, non-toxic doses of proteasome inhibitors induced a dose-dependent transcriptional antioxidant response that conferred marked protection against H_2O_2-induced oxidative stress and improved endothelial function via upregulation of several antioxidant enzymes [122]. This effect was shown to be mediated by an Nrf2-dependent transcriptional activation of the anti-oxidant response element (ARE) on the promoter of superoxide dismutase 1 (SOD1) [123]. These data may suggest that nontoxic proteasome inhibition may open novel therapeutic avenues for the treatment of endothelial dysfunction in cardiovascular disorders. However, proteasome inhibitors can be grouped as poisons, that induce apoptosis, or as remedies, which modulate and improve cellular function. The effects are context-dependent and the right dose and cell type differentiate a poison from a remedy [124]. It is known that substantial, prolonged proteasome inhibition results in death of tumour cells and highly proliferative cells, while partial, short-term impairment of proteasome function primes a protective stress response in normal and quiescent cells. Given that a substantial amount of research has dissected the effects of proteasome inhibition in various disease settings, and proteasome inhibition is an approved therapy for some of them, the understanding of proteasome function in the context of endothelial dysfunction and senescence in particular, is still incomplete and will be addressed in this study.

2 Hypothesis and aims

Degradation of oxidized proteins or damaged organelles is an important part of cellular stress adaptation. Accordingly, the decline of proteasomal and lysosomal protein degradation systems and the resulting protein aggregate accumulation may affect the development of senescence and age-related cellular dysfunction. Since these processes may play an important role in the development of endothelial dysfunction and associated cardiovascular diseases the current project was aimed at characterising the role of proteasomal degradation in senescence and aged vascular endothelial cells.

We hypothesised that proteolytic insufficiency is linked to the development of senescence and investigated this relationship in *in vitro* models of oxidative and replicative stress as well as in endothelial cells prepared from aged mice.

In particular, the major experimental aims of the project were as follows:

1. To delineate senescence/ageing-associated cellular changes with a focus on proteasome expression and function

2. To characterise the effect of oxidative insult on expression and function of the ubiquitin proteasome system

3. To verify a causal relationship between proteolytic insufficiency and senescence development

3 Materials and methods

Table 1: Materials

Name	Vendor	Catalogue No.
5-Bromo-4-chloro-3-indolyl β-D-galactopyranoside (X-gal)	Sigma-Aldrich Chemie GmbH	B4252
2-Mercaptoethanol	Sigma-Aldrich Chemie GmbH	M3148
Acetic acid	Carl Roth GmbH & Co. KG	3738.5
Acrylamide 4K-solution 30 % Mix 29:1	AppliChem GmbH	A0951
Amersham ECL	GE Healthcare UK Limited, UK	NA931
Ammonium chloride	Sigma-Aldrich Chemie GmbH	A9434
Ammonium persulfate	AppliChem GmbH	A2941
AURION BSA-c (Bovine Serum Albumin)	Aurion Immuno Gold Reagents & Accessories	25509
Bio-Rad DC Protein Assay	Bio-Rad Laboratories Inc., Hercules, USA	500-0006
Bovine serum albumin Fraction V, pH 7,0 (BSA)	AppliChem GmbH	A1391
Bromphenolblue	Sigma-Aldrich Chemie GmbH	B0126
Calcium chloride	AppliChem GmbH	A4689,0250
Citric acid	Sigma-Aldrich Chemie GmbH	251275
Complete, EDTA-free Protease inhibitor cocktail tablets (PIC)	Roche Diagnostic GmbH	11836153001
Collagen	Sigma-Aldrich Chemie GmbH	C7661
Disodium hydrogen phosphate dehydrate	Carl Roth GmbH & Co. KG	T877.2
Dimethyl sulfoxide (DMSO)	Sigma-Aldrich Chemie GmbH	D2650
Dithiothreitol (DTT)	Sigma-Aldrich Chemie GmbH	D0632
Ethylenediaminetetraacetic acid (EDTA)	Sigma-Aldrich Chemie GmbH	E9884
Ethylene glycol tetraacetic acid (EGTA)	AppliChem GmbH	A0878,0025

Ethanol	Carl Roth GmbH & Co. KG	K928
FluoromountG	Southern Biotech, USA	OB100-01
Glucose	Sigma-Aldrich Chemie GmbH	G8270
Glutaraldehyde 25%	Sigma-Aldrich Chemie GmbH	G5882
Glycerol	Carl Roth GmbH & Co. KG	3783.2
Glycin	AppliChem GmbH	A1067
Goat Serum (Normal)	Dako Deutschland GmbH	X0907
HEPES	Sigma-Aldrich Chemie GmbH	H3375
Human Serum Albumin (HSA)	Bayer Vital GmbH	A9511
Hydrochloric acid 37 % (HCl)	Carl Roth GmbH & Co. KG	X942.1
Hydrogen peroxide (H_2O_2)	Sigma-Aldrich Chemie GmbH	H1009
Kodak GBX developer and replenisher	Sigma-Aldrich Chemie GmbH	P7042
Kodak GBX fixer and replenisher	Sigma-Aldrich Chemie GmbH	P7167
Magnesium chloride ($MgCl_2$)	Sigma-Aldrich Chemie GmbH	M8266
Magnesium sulfate	Sigma-Aldrich Chemie GmbH	M7506
Methanol	AppliChem GmbH	A3493
Oil red O	Sigma-Aldrich Chemie GmbH	O0625
Paraformaldehyde	AppliChem GmbH	A3813
Phenylmethylsulfonylfluoride (PMSF)	Sigma-Aldrich Chemie GmbH	78830
Potassium chloride (KCl)	Carl Roth GmbH & Co. KG	6781.1
Potassium hexacyanoferrate(II) trihydrate $K_4[Fe(CN)_6] * 3 H_2O$	Sigma-Aldrich Chemie GmbH	455989
Potassium hexacyano-ferrate (III) ($K_3[Fe(CN)_6]$)	Sigma-Aldrich Chemie GmbH	244023
Skimmed milk powder	AppliChem GmbH	A0830
Sodium chloride (NaCl)	Carl Roth GmbH & Co. KG	3957.2

Sodium dodecyl sulphate (SDS)	Sigma-Aldrich Chemie GmbH	71725
Sodium hydroxide (NaOH)	Sigma-Aldrich Chemie GmbH	9356.1
Sodium orthovanadate (Na_3VO_4)	Sigma-Aldrich Chemie GmbH	S6508
Sodium diphosphate tetrabasic ($Na_4P_2O_7$)	Sigma-Aldrich Chemie GmbH	P8010
Spectra Multicolor Protein Ladder (10-260 kDa)	Fermentas GmbH	26634
Sudan Black B	Sigma-Aldrich Chemie GmbH	S2380
Sulfuric acid	Sigma-Aldrich Chemie GmbH	339741
TEMED	AppliChem GmbH	A1148
Tris ultrapure	AppliChem GmbH	A1086,5000
Triton® X-100	Carl Roth GmbH & Co. KG	6683.1
Tween® 20	SERVA Electrophoresis GmbH	3747.0

Table 2: Cell Culture Media and Supplements

Name	Vendor	Catalogue No.
Ascorbic acid	Sigma-Aldrich Chemie GmbH	A4403
Human serum	Lonza, Walkersville Inc., USA	H4522
Medium 199 (M199)	Lonza, Ealkersville Inc., USA	12001-538
Ciprofloxacin Kabi	Fresenius Kabi Deutschland GmbH	3277624
Collagenase II	Worthington Biochemicals Corporation	LS004174
Dulbecco`s modified Eagle`s medium (DMEM/F12 1X)	Gibco® Life Technologies Corporation, UK	10564011
Dulbecco's modified Eagle medium (high glucose)	PPA Laboratories GmbH	11965092
Dynabeads	Dynal Biotech ASA	110.35
Endothelial mitogen (EM)	Biomedical Technologies Inc., USA	B-203
Fetal calf serum (FCS)	Cambrex Bio Science Verviers SPRL	B-4800
Gelatine	ICN Biomedicals GmbH	02901771
Heparin-sodium	Hoffmann-La Roche AG	

L-Glutamine	ICN Biomedicals GmbH, Germany	02194678
Penicillin/streptomycin	Sigma-Aldrich Chemie GmbH	P4333
Trypsin-EDTA (0.05 % / 0.02 %)	Sigma-Aldrich Chemie GmbH	59417C

Table 3: Commercial kits

Name	Vendor	Catalogue No.
DC ™ Protein assay kit II	BIO-RAD Laroratories GmbH	#500-0112
Glucose (GO) Assay kit	Sigma-Aldrich Chemie GmbH	#GAGO20
OxyBlot Protein Oxidation Detection kit	Merck Millipore Corporation	S7150

Table 4: Inhibitors and activators

Name	Vendor	Catalogue No.
DL-buthionine-[S,R]-sulfoximine (BSO)	Sigma-Aldrich Chemie GmbH	B2640
Bortezomib	Selleckchem	S1013
MG132	Sigma-Aldrich Chemie GmbH	M7449
Oleuropein	Sigma-Aldrich Chemie GmbH	12247

Table 5: Buffers and Solutions

Buffer / Solution	Preparation/Composition
Ammonium persulfate (APS)	dissolved freshly before usage: 0.5 g APS in 5 ml ddH2O

Blocking buffer for western blot	5 % milk (for most antibodies) or 5 % bovine serum albumin (BSA) (for detection of carbonylation, O-GlcNAc, nitrotyrosin), 0.1 % Tween®20 in TN buffer
Blocking buffer for immunofluorescence	0.2% BSA-C, 5% goat serum, 0.1% Triton
Blotting buffer (10x)	25 mM Tris base, 192 mM glycine, storing at 4°C, for usage dilute 1:10 + 10 % methanol
Bromophenol blue	30 mg bromophenol blue diluted in 1 ml phosphate buffered saline (PBS), storage at 4°C
Buffer for diluting primary antibodies	5 % BSA, 0.1 % Tween®20 in Tris/NaCl (TN) buffer, storage at 4°C
Buffer for diluting secondary antibodies	5 % milk or 5% BSA, diluted in 0.1 % Tween®20 in TN buffer
Electrode buffer (10x)	30.3 g/l Tris base, 144.2 g/l glycine, 10 g/l sodium dodecyl phosphate (SDS), stored at room temperature (RT), dilution 1:10 before usage
Fixing solution for SA-β-galactosidase assay	2% formaldehyde, 0.2% glutaraldehyde prepared in PBS, storage for 1 month at RT
Gelatine for coating culture dishes	0.2% dissolved in ddH2O at 56°C, sterile filtered, storage at 4°C
HEPES buffer	145 mM NaCl, 5 mM KCl, 1 mM MgSO4, 10mM HEPES, 10 mM glucose, pH =7.4, after sterile filtration storage at 4°C
3 x 26S incubation buffer for proteasome activity	0.45 mM Tris base, 0.089 mM KCl, 15 mM Mg(CH3COO)2 * 4H2O, 15 mM MgCl2 * 6 H2O, dissolved in ddH2O, pH=8.3, storage at -20°C
1 x 26S Incubation buffer for AMC standards	Mixture of 26.64 ml 3 x 26S Incubation buffer + 48 ml ddH2O + 5.28 ml DMSO
Krebs-Ringer-HEPES (KRH) buffer	50 mM HEPES, 137 mM NaCl, 4.7 mM KCl, 1.85 mM CaCl2, 1.3 mM MgSO4, pH = 7.4, storage at 4°C

Laemmli buffer (3 x)	9 % SDS, 15 % glycerol, 10 mM EDTA, 186 mM Tris base, pH = 6.8, storage at -20°C, addition of 6 % 2-mercaptoethanol, 0.03 % bromophenol blue before usage
Lysis buffer A for cytosolic fractionation	250 mM sucrose, 20 mM HEPES (pH 7.4), 10 mM KCl, 1.5 mM MgCl2, 1 mM EDTA, 1 mM EGTA, addition of 1 mM dithiothreitol (DTT), 0.2 M PMSF, PIC (10 µl/ml) before usage
Lysis buffer B for nuclear fractionation	50 mM Tris (pH= 8), 150 mM NaCl, fresh addition of 1 % NP-40 (dissolved in buffer B), 0,1 % SDS, 0,5 % deoxycholate, 10 % glycerol, 1 mM PMSF, 10 µl/ml PIC
Lysis buffer for proteasome activity	250 mM sucrose, 25 mM Hepes, 1 0mM MgCl2 * 6H2O, 1 mM EDTA dehydrate, 1 mM DTT prepared in ddH2O, pH=7.8
Lysis buffer for western blot	Washing buffer plus 1 % Triton® X-100, 0.1 % SDS, kept at 4°C, addition of 1 mM PMSF, 10 µl/ml PIC just before usage
Phenylmethylsulfonyl fluoride (PMSF)	200 mM stock solution, 1 mg PMSF dissolved in 28,7 µl DMSO
Phosphate-buffered saline (PBS)	145 mM NaCl, 2.7 mM KCl, 1.5 mM KH2PO4, 8 mM Na2HPO4 x 2 H2O, pH= 7.4, storage at 4 °C
Protease inhibitor cocktail (PIC)	1 tablet dissolved in 500 µl ddH2O, storage at -20°C
Protein standard for Lowry	10 mg BSA diluted in 10 ml NaCl, storage at 4°C
Reaction buffer for GSH/GSSG assay	1 M Tris, 0.5 M EDTA, 150 mM NADPH, 10 mM 5,5'-dithiobis-(2-nitrobenzoic acid) (DTNB)
Reagent mix for proteasome activity	Mixture of 33.3 µl of 3 x 26S incubation buffer + 0.2 µl 1M DTT + 66.5 µl ddH2O, prepared freshly on the day of assay
SDS stock solution (10 %)	10 g SDS dissolved in 100 ml ddH2O, storage at RT
Staining solution for SA-β-galactosidase	40 mM citric acid/Na phosphate buffer, 5 mM K4[Fe(CN)6] * 3 H2O, 5 mM K3[Fe(CN)6], 150 mM NaCl, 2 mM MgCl2, 1 mg/ml X-gal, prepared in ddH2O, pH=6

Solubilization buffer	0.4 % NaOH, 2 % Na2CO3, 1 % SDS, storage at RT
TN buffer (10x)	150 mM NaCl, 10 mM Tris base, pH =7.6, storage at 4°C, dilution 1:10 before usage
TN-T buffer	% Tween®20 in TN buffer
Tris-EDTA (pH 7.5)	50 mM Tris base, 4 mM EDTA, storage at 4°C
Tris-HCl buffer (pH 6.8)	1.25 M Tris base, pH=6.8, storage at 4°C
Tris-HCl buffer (pH 8.8)	1.875 M Tris base, pH=8.8, storage at 4°C
Washing buffer for lysis	50 mM Tris (pH = 7.4), 2 mM EDTA, 1 mM EGTA, 50 mM NaF, storage at 4°C, addition of 1 mM DTT, 10 mM Na4P2O7, 1 mM Na3VO4 just before usage

Table 6: Media Composition

Media / Supplement	Composition
Complete growth medium for HUVECs	M199 plus 17.5 % heat inactivated fetal calf serum (FCS), 2.5 % human serum (HS), 100 U/ml penicillin, 100 µg/ml streptomycin, 680 µM L-glutamine, 25 mg/ml heparin, 7.5 mg/ml endothelial mitogen, 5 µg/ml vitamin C freshly added; in primary cultures addition of 10 µg/ml ciprofloxacin
Lactate production medium (LPM)	M199 without phenol red, 2 % heat inactivated sterile FCS, 2 mM glutamine, sterile filtered and stored at 4°C
Minus medium for MLECs	DMEM/F12 plus 20 % heat inactivated FCS, 100 U/ml penicillin, 100 µg/ml streptomycin, 2 mM glutamine

Plus medium for MLECS	DMEM/F12 plus 20 % heat inactivated FCS, 100 U/ml penicillin, 100 µg/ml streptomycin, 2 mM glutamine, 25 µg/ml Heparin, 75 µg/ml endothelial mitogen
Stop medium for HUVECs	10 % FCS heat inactivated, 100 U/ml penicillin, 100 µg/ml streptomycin prepared in M199

Table 7: Primary antibodies

Antibody	Vendor	Catalogue No.	Application	Dilution
AMPK	Cell Signaling Technology, Inc.	2532	Western blotting	1:1000
Anti-phospho_Histone H2A.X (Ser 139) clone JBW301 FITC conjugate	Merck Millipore Corporation	FCMAB 16-202A	Flow cytometry	1:800
Anti-Proteasome 20S alpha 1+2+3+5+6+7	abcam®	ab22674	Western blotting	1:1000
Anti-Proteasome 20S LMP2	abcam®	ab42987	Western blotting	1:1000
Anti-Proteasome 20S LMP7	abcam®	ab180606	Western blotting	1:1000
Anti-PSMB5	abcam®	ab3330	Western blotting	1:2000
β-actin	Cell Signaling Technology, Inc.	4970	Western blotting	1:5000
β1 subunit	Santa Cruz Biotechnology, Inc.	sc-67345	Western blotting	1:1000
β2 subunit	Enzo	MCP165	Western blotting	1:1000
CD102	BD Biosciences	553326	Beads conjugation	1 : 25
CD31	BD Biosciences	550274	Flow cytometry	1:25
eNOS	BD Biosciences	610297	Western blotting	1:2000

iNOS	BD Biosciences	610599	Western blotting	1:2000
Nitro-tyrosine	Merck Millipore Corporation	AB5411	Western blotting	1:1000
O-GlcNAc	Covance, Inc	MMS-248R	Western blotting	1:1000
P-AMPK alpha (T172) (40H9) Rabbit mAb	Cell Signaling Technology, Inc.	#2535S	Western blotting	1:1000
p21 (F-5)	Santa Cruz Biotechnology, Inc.	sc-6246	Western blotting	1:1000
p53 (1C12) Mouse mAb	Cell Signaling Technology, Inc.	#2524S	Western blotting	1:1000
p-p53 (S15) Rabbit Ab	Cell Signaling Technology, Inc.	#9284S	Western blotting	1:1000
Proteasome 20S core subunits	Enzo	BML-PW8155	Western blotting	1:1000
Anti-ubiquitin	Cell Signaling Technology, Inc.	#3936	Western blotting	1:1000
Vinculin Antibody	Cell Signaling Technology, Inc.	#4650S	Western blotting	1:1000

Table 8: Secondary antibodies

Secondary antibody	Type	Dilution	Application	Manufacturer
Anti-rabbit IgG (H+L)	goat/ peroxidase	1:5000 or 1:10000	Western Blotting	Kirkegaard & Perry, Laboratories, Inc.
Anti-mouse IgM (µ)	goat/ peroxidase	1:5000	Western Blotting	Kirkegaard & Perry, Laboratories, Inc.
Goat anti-mouse AlexaFluor488	goat polyclonal	1:250	Immunofluorescence	Life Technologies

3.1 Methods

3.1.1 Preparation of endothelial cells

Primary endothelial cells deriving from two different sources have been employed in this study. For in-vitro-experiments, human umbilical vein endothelial cells (HUVECs) isolated from umbilical cords of healthy donors were used. For ex-vivo-experiments, microvascular lung endothelial cells (MLEC) were prepared from lungs of young or old wild-type mice.

3.1.2 Preparation of HUVECs

Human umbilical cords were transported in sterile containers and maintained at 4°C until endothelial cells were prepared. Umbilical cords were first surface-sterilised with 70% ethanol. Then, the umbilical veins were perfused with sterile buffer (3.1.5). Subsequently, endothelial cells were dissociated by applying 0.01% collagenase II dissolved in M199 into the vein and incubating it at 37 °C for 3 min in a water bath with gentle massaging. The medium containing dislodged cells was collected in a falcon tube with stop medium to block collagenase activity, and the suspension was centrifuged at 500 x g for 6 min. The obtained cell pellet was resuspended in stop medium and seeded in a 75 cm2 culture flask pre-coated with 0.2 % gelatine. Cells were incubated under standard growth conditions (37 °C, 5% CO2, 95% humidity). Once firmly adhered, HUVEC were washed twice with phosphate-buffered saline (PBS), pH–7.5, to remove tissue debris and supplied with fresh growth medium supplemented with 0.5% ciprofloxacin until the first passage. HUVECs were routinely passaged by trypsinisation (trypsin-EDTA, 0.005% / 0.002% at 37 °C for 3 min), centrifugation at 500 x g for 6 min, and reseeding at a density required for the experimental design. HUVEC of passage 2 (second subculture) were used for virtually all experiments with proteasome inhibitors (MG132 and bortezomib), and for the premature senescence model (H2O2 treatment).

3.1.3 Preparation of MLEC

MLECs used for *ex-vivo*-experiments were prepared from wild type mice at the age of 2 months, considered as young mice, or at the age of 24 months, considered as old mice. The procedure for endothelial cell isolation was as follows:

Animals were sacrificed by cervical dislocation and the whole body surface was immediately disinfected with 70% ethanol. Under aseptic condition mice lungs were excised and stored in ice-cold DMEM until processing of tissue. Sterile instruments such as scissors and tweezers were used for mincing to obtain a homogeneous mass. The minced tissue was collected in a falcon tube and incubated with 0.2% collagenase II in DMEM at 37 °C for 1 hour. During this period, every 10 min a gentle mixing was performed. Next, the digest was triturated 20 times using a blunt edge cannula and filtered through a 40 µM cell strainer, which prevented the undigested tissue particles to pass through. After this step, the cell strainer was washed with (-) medium (Table 6), which at the same time stopped collagenase II enzymatic activity. The soulution containing the digested tissue was then centrifuged at 500 x g for 10 min. The obtained cell pellet was resuspended in (+) medium (Table 6) and seeded on 75 cm^2 culture flasks, which had previously been pre-coated with 0.2% gelatin. One day after preparation, the culture flasks containing a mixture of cells from the whole lung tissue were washed briefly with 2% FCS/PBS and fresh (+) medium was added. Cells were cultured and just before confluence was reached, the first positive selection for endothelial cells using magnetic beads was performed. To this end, magnetic beads coupled to sheep anti-rat IgG (3 x 10^6 beads per 75 cm^2 flask) (Table 7) were washed three times with 2 % FCS/PBS and then conjugated to rat anti-mouse CD102 antibody (4.5 µg per 75 cm^2 flask). After an incubation time of 2 h at 4 °C on a rotator machine, conjugated beads were washed with 3 % FCS/PBS solution using a magnet (Dynabeads MPC-S; Dynal Biotech ASA). The anti-CD102-conjugated beads were then added to the mixed cultures and put for incubation at 4 °C for 1 hour. After binding of conjugated beads to endothelial cells, culture flasks were first washed with warm PBS and then rinsed with trypsin. Detachment of cells took place after allowing incubation with trypsin at 37 °C for 5 min. The enzymatic reaction was stopped using (-) medium and the cell solution was transferred into a 15 ml tube. Then, a second 15 ml tube was placed in a magnet and the suspension was pipetted into this tube on the side of contact between the tube and the magnet. This allowed only endothelial cells bound to magnetic beads to attach to the wall of the tube while other cells types not expressing CD102 were left in suspension. After 10 min of incubation, the solution containing bead-free cells was discarded and the tube containing endothelial cells was removed from the magnet. The tube wall was rinsed with (+) medium and cells were

resuspended and seeded into new culture flasks. A second selection procedure was performed after cells reached a confluent state. Then, endothelial cells were seeded according to the planned experiment. Fresh medium was provided daily to allow optimal growth. Cellular yield was approximately 5 -10 x 10^6 for each mouse. Culture purity was assessed by CD31 staining (a specific endothelial cell marker) using flow cytometry and varied from 85% - 95%.

3.1.4 Long-term treatments of HUVECs

3.1.4.1 Treatment of HUVECs with H_2O_2 – stress-induced senescence model

HUVECs of the second subculture were seeded to 30 mm culture dishes at a density of 2.2×10^5 cells. 48 hours post seeding, cells were stimulated with H_2O_2 in complete growth medium at a final concentration of 75 µM and 100 µM. H_2O_2 was readded daily in fresh growth medium for 8 days. After 8 days, cells were used for different analysis.

3.1.4.2 Culture of HUVECs for replicative senescence model

Generation of senescent endothelial cells required passaging of HUVECs in culture for a period of approximately 80 days equivalent to 20-22 passages and 15-17 population doublings. HUVECs were split at a ratio of 1:4 in early passages and as the cells growth slowed down during the late passages when features of senescence started to occur, at a ratio of 1:2. Passaging of cells was done when the endothelial monolayer was about 80 – 90 % confluent. Cumulative population doublings (cPDL) were calculated using the following equation: CPD = (log (A) – log (B))/log2 (A: number of cells at the end of one passage; B: number of cells that were seeded at the beginning of one passage). After roughly 20 passages almost 80 % of cells reached a senescent state and were ready to be used for experiments.

3.1.4.3 Treatment of HUVECs with proteasome inhibitors

In order to study the role of proteasome inhibition on endothelial cells senescence, two inhibitors, MG132 and bortezomib, were applied to second subcultures of HUVECs. Cells (2.2×10^5) were seeded on 30 mm culture dishes. 48 h after seeding, treatment of cells with 0.25 µM, 0.5 µM or 1 µM MG132 in complete growth medium was started and proceeded

for 4 consecutive days. Medium was changed every day and freshly prepared inhibitor was readded to the culture dish. Then, a period of 1 week in culture was given for the restoration of proteasome activity. The treatment of cells with bortezomib (10 nM or 20 nM) was performed in a similar way but was continued for only 2 days before the inhibitor-free recovery period of 1 week. Cell lysates for proteasome activity measurement and western blotting analyses were made at the end of treatment period for each proteasome inhibitor as well as after the recovery period in the absence of the inhibitors.

3.1.5 Characterization of endothelial cells by staining techniques

3.1.5.1 Senescence associated β–galactosidase (SA-β-gal) staining

For identifying senescent cells, SA-β-gal staining was performed. Staining of HUVECs was done on 30 mm dishes seeded at a rather low density of 1.6 x 10^5 cells per culture dish to avoid false positive results due to high cell confluence. MLECs stained for SA-β-gal were seeded at 8 x 10^4 cells per 30 mm dish. On the day of staining, growth medium was aspirated from each culture dish and cells were washed once with ice-cold PBS. Immediately thereafter, cells were fixed for 5 min at room temperature using 0.2 % formaldehyde/0.02 % glutaraldehyde. Fixed cells were washed again two times with PBS and finally, 1.5 ml staining solution (3.1.5) was added to each dish. Cells were left in a dry incubator at 37 °C overnight in case of HUVECs and for 48 hours in case of MLECs. While the staining solution was still on the culture dish, cells were checked under the microscope (10 x magnification) for the development of a blue colour. 10 pictures were taken in random fields and senescent cells were counted with the help of ImageJ software. Senescent cells were calculated as a percentage of blue positive SA-β-gal cells compared to the total number of cells in the respective fields.

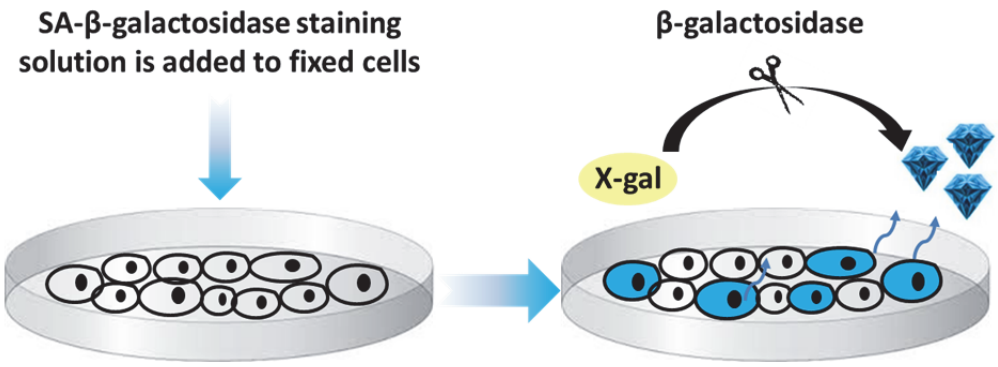

Figure 6: SA-β-Galactosidase Staining

Senescence-associated β-galactosidase (SA-β-gal), a lysosomal enzyme, becomes very abundant in senescence due to increased lysosome numbers per cell. Cells expressing high amounts of the β-galactosidase enzyme stain blue at the pH of 6.0, due to the cleavage of the chromogenic substrate 5-bromo-4-chloro-3-indolyl β D-galactopyranoside (X-gal).

3.1.5.2 Oil-Red-O staining

Oil-Red-O is a fat soluble dye used for staining of neutral triglycerides and lipids. Thus, it is suitable for observation of lipid droplet formation under certain conditions. The red-stained lipids can be visualised under light or fluorescent microscope. For this assay, HUVECs were seeded on coverslips in a 24-well-plate at a density of 3.5 x 10^4 cells per dish. The staining procedure started with washing the coverslips two times with Hepes/$CaCl_2$/HSA-buffer. Cells were then fixed for 20 min with 4 % paraformaldehyde and further washed three times with PBS. Then, cells were incubated with Oil-Red-O solution [0.5% (w/v) in 60% Propan-2-ol / H_2O (v/v)] for 30 min in the dark. At the end of incubation, the dye was aspirated and cells were washed 3 times with PBS. The coverslips were imbedded on slides and visualisation of staining was done under a light microscope. For the quantitative analysis of Oil-Red-O staining, parallel dishes were prepared and stained the same way. Only at the final step after staining with Oil-Red-O and washing with PBS, the dye was extracted using 250 µl of 100 % isopropanol for each dish. Culture dishes were left for 5 min with isopropanol under gentle shaking. Finally, the absorbance of the extract was measured at 510 nm in a CLARIOstar plate photometer.

3.1.5.3 Sudan Black Staining

The Sudan black staining was performed to detect lipofuscin, which is accumulating in senescent cells. Preparation of Sudan black solution was done by dissolving 0.7 g of Sudan black powder in 100 ml of 70 % ethanol in a dark glass bottle, which needs to be tightly closed to avoid evaporation of ethanol. The solution was stirred overnight at room temperature. Cells were seeded on coverslips in a 24-well-plate at a density of 3.5 x 10^4 cells per dish. On the day of staining, medium was aspirated and cells were washed two times with PBS and then fixed for two minutes in 70 % ethanol. 250 µl of Sudan staining solution was added to the coverslips and left to incubate for 5 min. The cells were then washed three times with PBS. The coverslips were carefully lifted, wiped on the edges and mounted in 40% Glycerol/TBS mounting medium on a slide. The lipofuscin staining was visualized under a light microscope.

3.1.6 Protein analytics

3.1.6.1 Western blotting

For sample preparation, culture dishes were brought on ice and cells were washed two times with cold wash-lysis buffer. Lysis buffer (60 µl for 30 mm dishes, 80 µl for 60 mm dishes, 200 µl for 90 mm dishes) was added to the cells and left for 15 min. Cells were then scraped from the culture dish and the lysates were transferred to eppendorf tubes standing on ice. At this step, two aliquots of lysate were taken for protein determination while half volume of 3x Laemmli buffer was added to the remaining lysate. Samples were boiled for 5 min at 95 °C to allow protein denaturation. Lysates were stored at -20°C until processing for western blotting. The protein concentration was analyzed spectrophotometrically by applying the Lowry method using an Uvikon 930 spectrophotometer (Tresser Instruments).
SDS-PAGE of proteins was performed using 20-50 µg proteins and applying a water-cooled system. Separated proteins were then transferred by the BioRad Trans-Blot tank transfer system onto polyvinylidene fluoride membranes. The membranes were blocked either with 5 % non-fat dry milk or 5 % BSA diluted in TN-tween buffer for 1 hour at room temperature. Incubation with primary antibody was performed overnight at 4 °C. The next day, membranes were washed and incubation with secondary antibody was performed for 1 hour at room temperature. Thereafter, membranes were washed again and visualisation of

peroxidase-coupled secondary antibody was done using a chemiluminescence kit and autoradiography films described in materials and methods. In case of reusing the same membrane for another antibody, the membranes were stripped using stripping buffer for 35 min at 56 °C under soft agitation. To document experimental results, all films were scanned and quantification of blots was performed using ImageJ software.

3.1.6.2 Subcellular fractionation of proteins

For fractionation of cytosolic and nuclear proteins, HUVECS were seeded on 90 mm dishes at a density of 10^6 cells and lysates were prepared 48 h post seeding. Culture dishes were placed on ice and washed twice with cold PBS. 300 µl of buffer A (Table 5) were added on each dish and incubated for 30 min. Cells were scraped and transferred to eppendorf tubes standing on ice. The lysates were homogenized using a 25G needle and centrifuged at 700 x g, 6 min, 4°C. The sediment of this centrifugation contains nuclear proteins. The supernatant (cytosol + membranes) was transferred to ultracentrifuge tubes and centrifuged at 50.000 x g and 4°C, for 60 min. After ultracentrifugation, the supernatant containing cytosolic proteins was concentrated by centrifugation at 14000 x g for 3 min at 4°C through an ultra-15 centrifugal filter provided by Amicon. The concentrate was shaken softly, filtered and recentrifugated. The final sample was then transferred to a new tube and 2 times 2 µl were taken for protein determination while the rest was boiled in Laemmli-buffer for 5 min at 95 °C.

The pellet obtained after the first centrifugation was washed three times with 500 µl of cold buffer A including centrifugations at 700 x g for 10 min at 4°C. The remaining pellet containing nuclear proteins was then lysed in 60 µl of lysis buffer B (Table X). Lysates were sonicated with 10 strokes and incubated on ice for 15 min. After 15 min, lysates were centrifugated again at 1700 x g for 5 min at 4°C. The supernatant was transferred into new eppendorf tubes and 2 times 2µl of lysate were taken for protein determination. To the rest of lysate 3x Laemmli buffer was added and samples were boiled for 5 min at 95 °C. Samples were frozen at -20 °C until western blotting analyses of proteins was performed.

3.1.6.3 Protein carbonylation assay

For determining carbonylated proteins under certain conditions we made use of the OxyBlot protein oxidation kit S71500. The principle of this assay is based on derivatising carbonyl

groups at protein side chains with 2,4-dinitrophenylhydrazine (DNPH). The generated 2,4,-dinitrophenyl adducts can then be detected by antibodies specific to the attached DNP moiety of the proteins in western blots. Lysates for detecting protein carbonyls were prepared in a similar way as lysates for western blotting with some distinctions. First, growth medium was aspirated from each culture dish and cells were washed 2 times with wash buffer (Table 5). Dishes kept on ice were then lysed in 40 µl (in case of 30 mm dishes) or 60 µl (in case of 60 mm dishes) of complete lysis buffer (Table 5). After 15 min incubation on ice, lysates were transferred into eppendorf tubes and centrifuged at 700 x g for 6 min at 4 °C. The supernatants were then transferred into new eppendorf tubes on ice. At this stage, 2 times 2 µl of lysate was taken for protein determination. Before preparing samples for loading on gel electrophoresis, protein concentration of all samples was adjusted. Total amount of proteins used for this assay varied from 15 µg – 20 µg. For each sample, 10 µl of total lysate volume was transferred into a new eppendorf tube and 10 µl of 12 % SDS was added. Next, 20 µl of derivatisation solution was pipetted to each sample. After incubation for 15 min at room temperature, addition of 15 µl neutralization solution stopped the derivatisation reaction. Samples were separated in 12 % gels or gradient gels followed by western blotting. Finally, PVDF membranes were blocked in 5 % BSA for 1 hour at room temperature and then washed three times with TN-T buffer for 5 min. Blocked membranes were incubated overnight at 4 °C with a primary antibody specific to DNP moiety of the proteins. The next day, after several washing steps with TN-T buffer the PVDF membrane was incubated with goat anti-rabbit IgG for 1 hour at room temperature and immunodetection of proteins was done as described below.

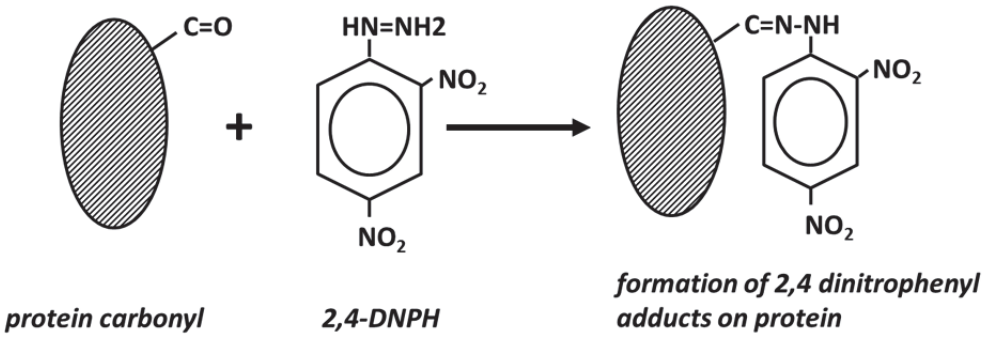

Figure 7: Derivatization of protein carbonyl groups with 2,4-dinitrophenyl hydrazine

The carbonyl groups at the protein side chains are derivatised with 2,4-dinitrophenylhydrazine (DNPH). The generated 2,4,-dinitrophenyl adducts DNP-derivatised protein samples can be detected in western blots with specific antibodies after separation by polyacrylamide gel electrophoresis.

3.1.6.4 Immunofluorescence staining of 20S core proteasome

MLECs seeded on coverslips, which had been coated before with 0.2 % gelatine, were washed two times with HEPES-buffered solution and fixed with 4 % paraformaldehyde at room temperature. Fixed cells were washed two times with PBS and permeabilized using 0.1 % Triton in PBS for 5 min. Afterwards, cells were blocked for 30 min in blocking solution (0.2 % BSA-c and 5 % goat serum in PBS with 0.1 % Triton). The incubation with primary antibody anti-rabbit 20S core (Enzo PW8155-0100) was done for 1 h at room temperature. After two washings, samples were incubated in the dark with fluorophore-conjugated secondary antibody goat anti-mouse AlexaFluor488 for 30 min at room temperature. Cell nuclei were then stained with 4',6-diamidino-2-phenylindole (DAPI, 1 µg/ml in PBS) for 10 min and coverslips were embedded on slides with Fluoromout. Slides were stored at 4 °C until analysis with a fluorescent microscope.

3.1.6.5 Detection of CD31 by flow cytometry

CD31 is a 130 kDa adhesion molecule commonly used as a surface marker of endothelial cells. We verified and confirmed the purity of MLEC isolates (young/old mice) and the identity of late passage HUVECs (senescent cultures) by monitoring CD31 staining via flow cytometry. Briefly, cells in culture dishes were PBS-washed and fixed on ice in 0.5 % paraformaldehyde for 2-3 minutes. This fixation step maintains the CD31 antigen structure and allows trypsinisation without loosing the surface antigen. The cell suspension was further washed twice in PBS including centrifugation steps at 500 x g for 6 min. Resuspended cells were then blocked in 0.2 % BSA-c/PBS for 30 minutes at room temperature followed by incubation with the primary antibody rat anti-mouse CD31 (BD Pharmingen, # 550274) for 30 min. Thereafter, cells were washed and incubated for 30 minutes with Cy5-conjugated goat anti-rat IgG diluted in 0.2% BSA-c/PBS as secondary antibody (Millipore, # AP136S). Following a final wash, cells were resuspended in PBS and analysed by flow cytometry using the BD FACS canto instrument equipped with Arg and

He/Ne laser sets. For most experiments, about 2-4 x 10^4 cells were used and analyzed using FlowJo software.

3.1.7 Proteasome activity assay

3.1.7.1 Lysis procedure for proteasome activity assay

For determination of proteasome activity, HUVECs were seeded on 60 mm dishes at a density of 3.6 x 105 cells and MLECs at 1.6 x 105 cells per dish. On the day of lysis, cell culture dishes were placed on a plate warmer at 37 °C. Cells were washed two times with 2 ml Hepes/Ca and 500 µl trypsin-EDTA was added for 5 min. Trypsin enzymatic reaction was stopped by addition of 1 ml of stop medium to the culture dish. Then, the cell suspension was collected in 2 ml eppendorf tubes placed on ice and centrifuged at 600 x g for 5 min at 4°C. The cell pellet was resuspended in 1.5 ml Hepes/Ca. A second round of centrifugation was performed at 500 x g for 5 min at 4 °C. After aspiration of the supernatant, the cell pellet was lysed in 80 µl lysis buffer (3.1.5). The lysate was further triturated 20 times with a 20G needle and subjected to 3 rounds of freezing in liquid nitrogen and thawing in a water bath at 37 °C. Subsequently, the lysates were centrifuged at 14000 x g for 10 min at 4°C. Supernatants were transferred into new eppendorf tubes and 2 times 2 µl lysate was taken from the lysate for protein determination.

3.1.7.2 Measurement of proteasome activity

For determining proteasome activity, 3 different peptide substrates were used, which were all tagged to 7-amino-4-methylcoumarin (AMC). Each substrate is specific for a distinct proteasome activity. In the presence of a proteasome activity, these substrates release free highly fluorescent AMC, which can be measured in a fluorescent plate reader at $\lambda_{ex}360/\lambda_{em}460$. AMC standards (10 µM, 5 µM, 2 µM, 1 µM, 0.5 µM, 0.25 µM, 0.1 µM and 0 µM) were prepared in a final volume of 120 µl of 1 x 26S incubation buffer (Table 5) and used for a standard curve for calculating proteasome activity of samples. For the samples of one experiment, protein concentration was adjusted to the concentration of the sample with the lowest concentration in a total volume of 10 µl. Protein concentration used for proteasome activity varied from 15 µg – 25 µg proteins per 10 µl in different experiments. Double determination for each sample was performed. On the day of the assay, 10 µl of

sample lysate with adjusted protein content was transferred to a well of a 96 well plate. Then, 100 µl of freshly prepared reagent mix was added (Table 5) and the plate was gently agitated for 2 min. Thereafter, samples were incubated for 10 min at room temperature. Subsequently, the plate was brought to a dark room where 10 µl of substrate was added to each well except the wells containing the standards. The plate was agitated gently to allow mixing of the substrate and covered with aluminium foil to protect samples from light. After incubation for 30 min at 37 °C, measurement of fluorescence was performed in a fluorescent plate reader at $\lambda_{ex}360/\lambda_{em}460$. Using the AMC standards, a linear regression equation was set up to calculate specific proteasome activities. Activity was calculated as nmol AMC substrate / mg protein * min. Results were presented as mean ± standard error of mean (SEM) of independent experiments.

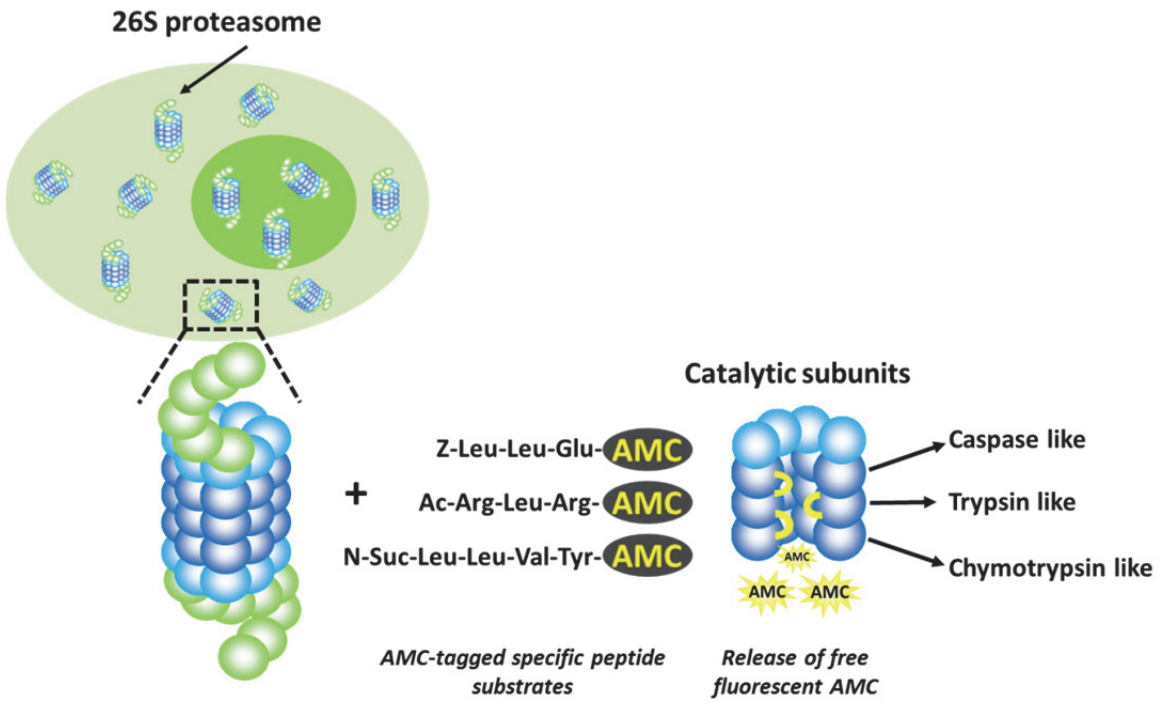

Figure 8: Principle for determining Caspase-like, Trypsin like and Chymotrypsin like activity

Proteasome activity is measured by adding AMC-tagged substrates (specific for each activity) to cell lysates prepared for proteasome activity. In the presence of proteolytic activities substrates release free and highly fluorescent AMC. Fluorescence intensity can be measured and is proportional to proteasome activities.

3.1.8 Detection of metabolites

3.1.8.1 Glutathione (GSH) assay

GSH / GSSG is an antioxidative defense system, which cells use to counteract oxidative stress situations. For determining GSH levels in HUVECs the colorimetric 5, 5'-dithiobis-(2-nitrobenzoic acid) (DTNB) GSH reductase assay was used. This assay is based on the reduction of GSSG by NADPH in the presence of glutathione reductase. In addition, the colorless substance 5, 5'-dithiobis-(2-nitrobenzoic acid) (DTNB) reacts with the formed GSH to the colored product 2-nitro-5-thiobenzoate (TNB). The regeneration of GSH by glutathione reductase allows recycling of the reaction. The TNB formation is proportional to the number of reaction cycles and to the GSH concentration of the sample.

Young and senescent HUVECs seeded on 60 mm dishes were cultured for 3 days. 24 hours before sample preparation, the medium was renewed. Buthionine sulfoximine (BSO) at a final concentration of 100 µM was added to one culture dish 12 hours before cell lysis as a positive control. All samples were washed two times with PBS and scraped from the culture dish using 90 µl of 0.01N hydrochloric acid (HCl). Immediately after, cells were frozen and stored at -80°C. In parallel, identically treated samples were processed for protein determination. To this end, culture dishes were washed three times with 1 ml of ice-cold HEPES buffer and 2 ml solubilization (Table 5) buffer was added to each dish. 50 µl aliquots were taken two times for protein determination.

GSH analysis was performed at the Institute of Nutritional Science in Jena at the laboratory of Prof. Dr. Oliver Klotz. To obtain GSSG standards, a 10 mM GSSG solution was prepared in 0.01 N HCl and diluted to obtain the following GSSG (µM) concentrations : 1000, 300, 100, 30, 10, 3, 1, 0.3, 0.2, 0. On the day of the assay, frozen lysates were thawed on ice and then centrifuged for 10 min at 15000 x g at 4 °C. 80 µl of the supernatant were transferred into a new eppendorf tube and 27.2 µl of 20% 5-sulfosalicylic acid (SSA) were added to allow precipitation of proteins. Each sample was incubated for 5 min on ice and then centrifuged for 5 min at 15000 x g at 4 °C. The supernatant was frozen at -2ß°C until the analysis took place. On the day of the assay, 40 µl of each sample and standards were mixed with 360 µl of reaction buffer (Table 5). From this mixture 100 µl were transferred to a well of a 96 well plate and 20 µl of glutathione reductase at a final concentration of 2 U/ml were added. For

each sample, triplicate determination was performed. Using a CLARIOstar microplate photometer (software Omega Control), TNB formation was measured at 410 nm over 12 min every 30 seconds. Analysis of total GSH amounts in HUVECs was done by calculating the values of TNB formation in the linear range according to the GSSG calibration curve. Obtained values were multiplied by two as two GSH molecules correspond to one GSSG molecule. Each value was further normalized to the corresponding protein amounts obtained from identical parallel dishes. Results were presented as mean ± SEM of three independent experiments.

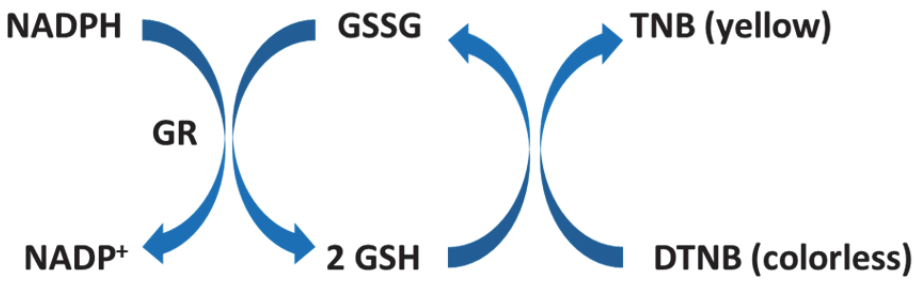

Figure 9: Principle of glutathione measurement using the DTNB glutathione reductase assay

GSSG is reduced by glutathione reductase (GR) in the presence of NADPH as a cofactor. The formed GSH reacts with the colorless DTNB to form yellow TNB and GSSG. The recovery of GSSG by GR allows the reaction to continue. *DTNB, 5,5 i-dithiobis-2-nitrobenzoic acid; TNB, 2-nitro-5-thiobenzoate; GSH, glutathione; GSSG, GSH disulfide; GR, GSH reductase; NADPH, nicotinamide adenine dinucleotide phosphate; NAD+, nicotinamide adenine dinucleotide.*

3.1.8.2 Glucose consumption

To study whether endothelial cell metabolism was altered during senescence, glucose consumption was analyzed. HUVECs were seeded in 30 mm dishes and cultured for three days. Then, culture dishes were washed two times with lactate production medium (LPM) without phenol red containing 2% FCS and 2 mM glutamine and each culture dish was supplied with 1 ml of this medium. A separate dish without cells was prepared to incubate 1 ml of LPM at 37°C (LPM control). After 24 hours, the medium was collected into an eppendorf tube and stored at -20°C until the day of measurement. Cells were then washed two times with PBS, trypsinized and counted in a Neubauer chamber to allow normalization

of the obtained glucose values against cell numbers. Measurements for glucose consumption were done by using a Glucose (GO) Assay Kit (Table 3). This assay is based on two biochemical reactions during which glucose is oxidized to gluconic acid and hydrogen peroxide (H_2O_2) and a second reaction during which H_2O_2 oxidizes the colorless o-dianisidine into a yellow product. In addition, sulfuric acid (H_2SO_4) converts this product to a stable pink-colored dye, whose intensity is proportional to the initial concentration of glucose in the medium.

On the day of the assay, control LPM as well as LPM from different samples was centrifuged at 14,000 x g for 5 min at room temperature. From the supernatant 5 µl were taken and diluted 1:20 in ddH2O. If very high glucose values were observed, samples were further diluted to 1:40. Glucose standards were prepared according to datasheet provided in the kit. 0 µl, 2 µl, 4 µl, 6 µl, 8 µl of glucose standards were taken and then filled up to 100 µl using ddH2O. The assay reagent containing o-dianisidine and glucose oxidase/peroxidase was prepared just before the experiment. 200 µl of this reagent were added to each standard and sample and incubated for 30 min at 37 °C under soft agitation. Addition of 200 µl of 12 N H_2SO_4 stopped the reaction. 100 µl of the reaction mixture were transferred into a well of a 96-well plate and absorbance was measured at 540 nm using the absorbance reader Sunrise™ (TECAN). Glucose determination was performed in triplicates. In order to calculate glucose amounts in the medium of each sample, a linear regression equation was set up by using glucose standards. Glucose consumption was calculated as the difference between the amount of glucose in the LPM control dish without cells and the glucose level in each experimental sample. Obtained values were normalized to the respective cell numbers. Results were presented as mean ± standard error of the mean (SEM) of three independent experiments.

3.1.9 Flow Cytometry

3.1.9.1 DNA damage estimation

DNA strand breaks were estimated by flow cytometry measurement of γH2AX (DNA damage marker) positive cells in at least 2 x 10^5 events. Briefly, untreated cells or cells treated with bortezomib were harvested by trypsinisation, washed in 1 x PBS /1 % BSA, fixed in 4% PFA for 15 min at room temperature and then in ice-cold 70% ethanol and stored frozen at -

20°C. For flow cytometry, cells were permeabilised in 1 x PBS/1 % BSA/0.5 % Triton-X 100 for 30 min at room temperature, blocked with 5 % serum in 1 x PBS /1 % BSA for 1 h and stained with γH2AX-FITC (1:800, Millipore FCMAB16-202A) for 2 hours. Then samples were treated with RNase A for 15 min at 37°C with agitation and stained with 100 µg/ml propidium iodide for DNA content. Samples were subjected to flow cytometry on a FACS Canto (BD Biosciences) and acquired data were analysed using FlowJo software. Samples were pre-gated for cells (FSC-A vs SSC-A) and singlets (FSC-A vs FSC-W dot plots) and singlets were used to plot DNA content on x- Axis vs γH2AX-FITC intensity on Y-Axis.

3.1.9.2 Size and granularity measurement

The relative differences in cell size and granularity was estimated by recording the forward (FSC) and side scatter (SSC) parameters in live, trypsinized PBS suspensions of young and senescent cells at identical voltage and instrument settings. Median values of FCS and SSC histograms were considered a measure of size and granularity of cells. BD FACS Canto II instrument was used for measurement and FlowJo software was used for data analysis.

3.1.9.3 Autofluorescence analysis

Spontaneous fluorescence increase in senescent cells relative to background fluorescence signals from young cells was recorded across multiple detection sets including: Alexa fluor 488, Alexa fluor 647, PE-A, PE-Cy5, PE-Cy7 on the FACS Canto II instrument. Median fluorescence was used for autofluorescence evaluation.

3.1.10 Statistical analysis

Information regarding number of subjects used for each experiment as well as the statistical test applied is given respectively in the figure legends. Paired two-tailed Student's t-test and one-way or two-way repeated measurements ANOVA was used for significance calculation after variance analysis with Holm-Sidak correction for multiple comparisons. $p<0.05$ was considered significant. Data in the figures are represented as mean ± SEM of independent experiments performed with cells from different endothelial cultures.

4 Results

4.1 The effect of replicative senescence on expression and function of the proteasome

4.1.1 Characterisation of replicative senescence in endothelial cells

In order to investigate the effect of senescence on proteasome expression and function, a model of replicative senescence was established using primary HUVECs. These cells were passaged until they stopped proliferation, which occurred after 15-17 cumulative population doublings, i.e. after about 20 passages (Fig. 10).

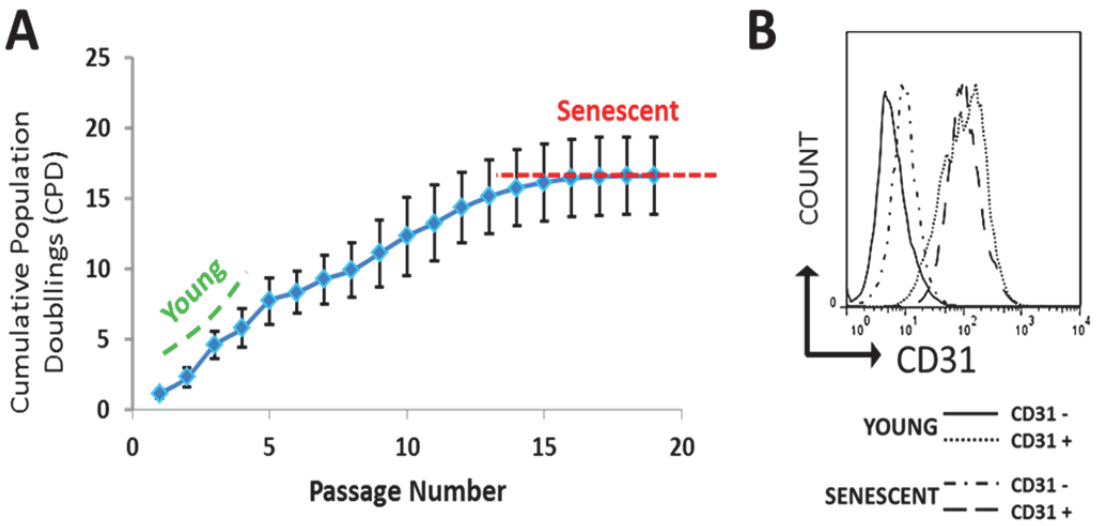

Figure 10: HUVECs undergo replicative senescence in vitro

A) Cumulative population doublings calculated as previously described (3.1.4.2), expressed as an average of 3 batches of HUVECs passaged to replicative senescence *in vitro.* Mean values ± S.E.M. **B)** Representative histogram of flow cytometric detection of the endothelial lineage marker CD31.

Under these conditions, HUVEC developed signs of senescence but kept their endothelial cell identity as shown by the presence of the endothelial marker CD31 (Fig. 10). Over 80% of all cells stained positive for the marker senescence-associated β-galactosidase (SA-β-gal) (Fig. 11). In contrast, almost no SA-β-gal was detected in young endothelial cells (CPD 3-5).

Senescence was confirmed by detection of morphological alterations in size (1.5-fold increase) and granularity (2-fold increase) as measured by flow cytometry (Fig. 11)

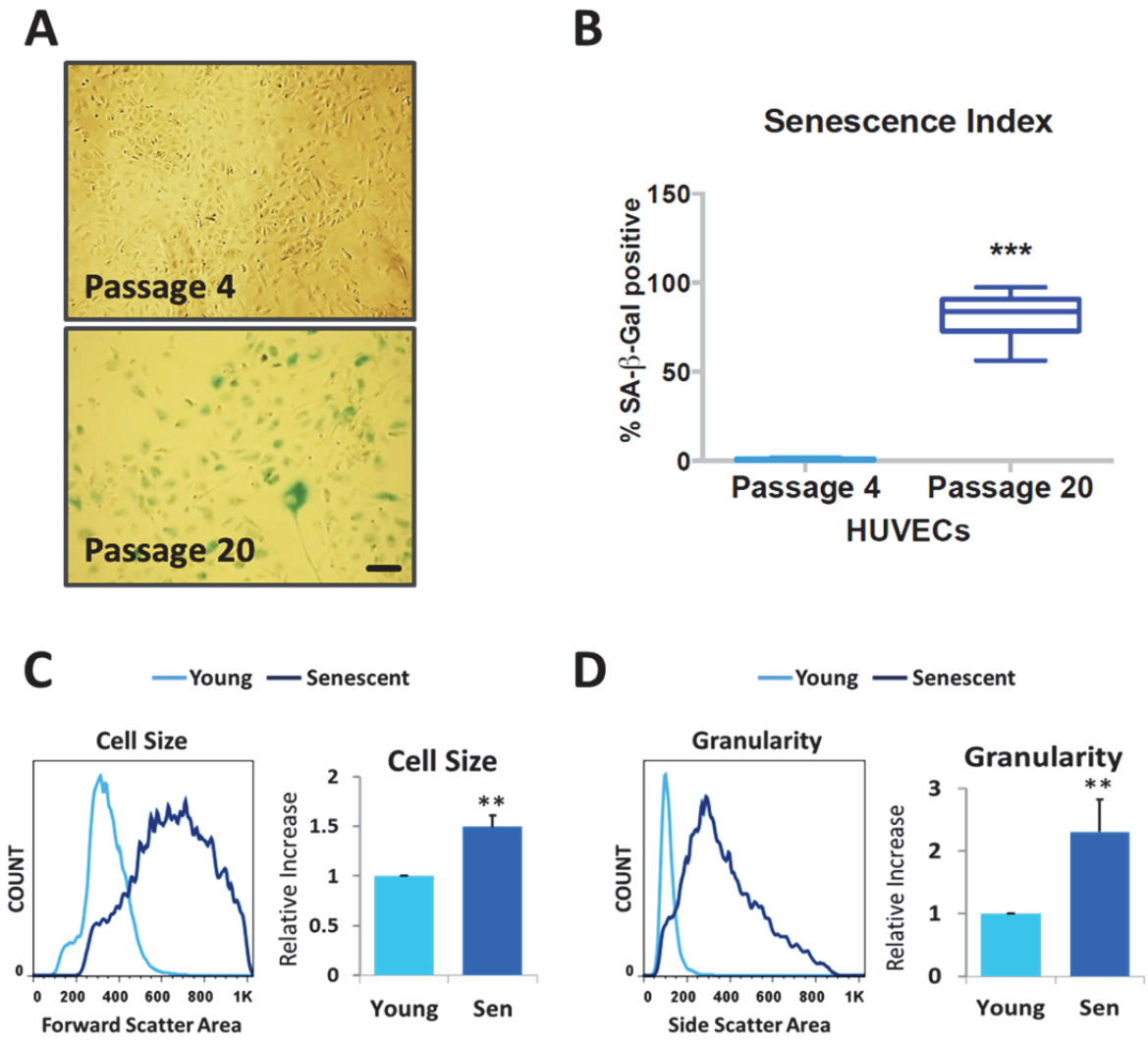

Figure 11: Replicatively senescent HUVECs are morphologically distinct

A) Representative light microscopic images of SA-β-Gal staining in young or replicatively senescent HUVECs. Scale bar = 20μm. **B)** Quantification of SA-β-gal-stained young and senescent HUVECs. Mean values ± S.E.M. *** $p<0.001$. Representative flow cytometry histograms of **C)** forward scatter values plotted against cell counts (left) and relative cell sizes (right) and **D)** Side scatter values plotted against cell counts (left) and relative cell granularity determined from median scatter values (n=3) of young or senescent HUVECs. Mean values ± S.E.M. ** $p<0.01$.

Immunoblot analysis revealed upregulation of several molecular markers of senescence such as the tumour suppressor p53 and its transcriptional target, the cell cycle inhibitor p21, activation of AMPK as well as S6 kinase phosphorylation. (Fig. 12, A, B). Senescent HUVECs

were characterized by a decreased eNOS expression and upregulation of iNOS (Fig. 12, C, D), both of which are alterations implicated in endothelial dysfunction.

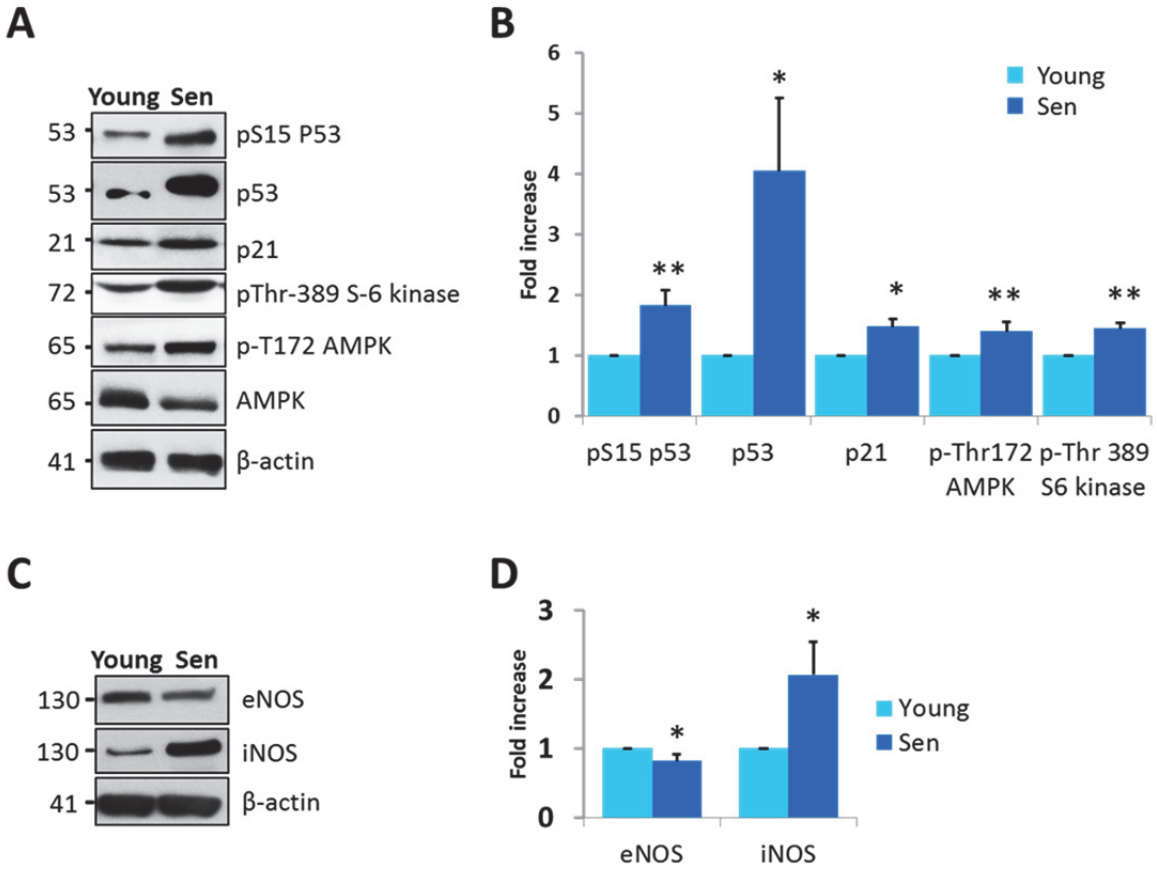

Figure 12: In vitro aged HUVECs reveal molecular signatures of senescence and dysfunction

A) Representative immunoblot (1 of n=3) for the senescence markers p53 and p21 as well phosphorylation of S6 kinase and AMPK in young or replicatively senescent (late passage) HUVECs. **B)** Quantification of pS15 p53, p53, p21, pTr172 AMPK, p-Thr 389 S6-kinase. Mean values ± S.E.M. * p<0.05 ** p<0.001. **C)** Representative immunoblot (1 of n=3) for expression analysis of enzymes eNOS and iNOS in young or replicatively exhausted HUVECs. **D)** Quantification of eNOS and iNOS. Mean values ± S.E.M. * p<0.05

4.1.2 Oxidative stress and metabolic alteration in senescent endothelial cells

The development of senescence is suggested to involve increased generation of reactive oxygen and nitrogen species and subsequent oxidative stress-induced protein modifications. In line with this, we observed decreased levels of reduced glutathione (GSH) in senescent cells compared to young endothelial cells (Fig. 13). The glutamyl cysteine synthase inhibitor

buthionine sulfoximine (BSO), known to inhibit synthesis of GSH, was used as a negative control for the GSH assay.

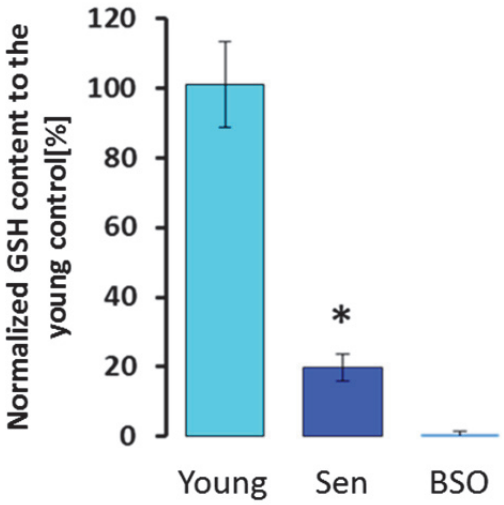

Figure 13: Senescent HUVECs reveal diminished antioxidant GSH levels

A) GSH levels estimated by the DTNB GSH reductase activity in young and senescent HUVECs as well as BSO (100 µM, 12h) as a control. BSO depletes GSH levels by inhibiting its *de novo* synthesis. Results are expressed relative to the GSH amount of the young HUVECs (100%). Mean values ± S.E.M. Non-parametric two-tailed student T-test was used for statistical significance. n=3 * $p<0.05$.

We next attempted to identify and characterise the extent of protein modifications in replicatively aged HUVECs. We first applied the *OxyBlot* Protein Oxidation Detection Kit to identify protein carbonylation, the most prominent form of oxidative modification. As shown in (Fig. 14, A) we observed an overall increase in the amount of protein carbonyl derivatives in senescent HUVECs when compared to young cells confirming increased oxidative stress in the former. Based on the identified induction of the enzyme iNOS (Fig. 14, B) in senescent cells, which presumably results in higher nitric oxide levels, we next probed for protein nitration with a specific antibody against nitrotyrosine. As expected, a higher nitration of several protein bands was observed in senescent cells (Fig. 14, C). Furthermore, we were able to show increased O-GlcNAcylation of serine/threonine protein residues in senescent cells compared to young control cells using a specific antibody against O-GlcNAcylated proteins.

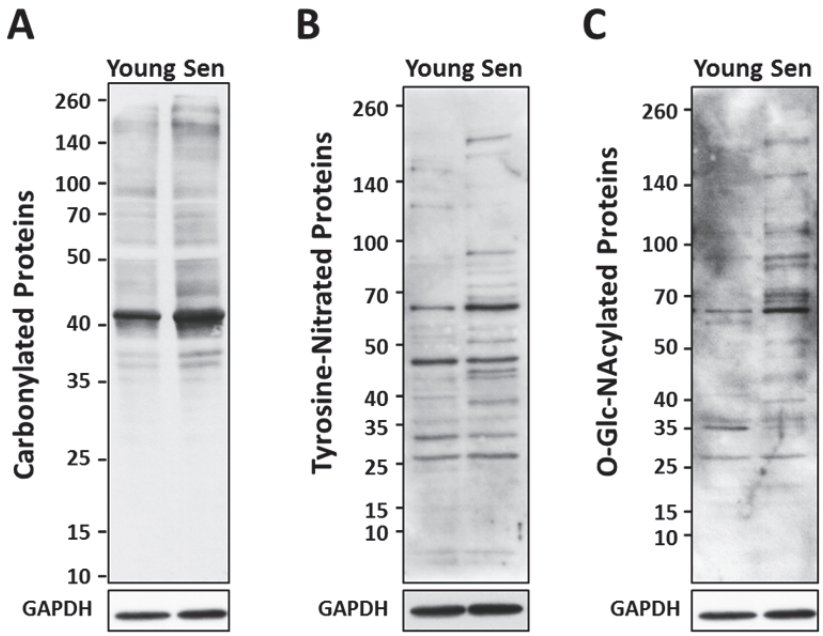

Figure 14: Senescent HUVECs host a range of protein modifications

Representative immunoblots (1 of n=3) showing senescence associated modifications of cellular proteins detected by immunoblot analysis for A) Carbonylated proteins, B) Tyrosine-nitrated proteins and C) O-GlcNACylated proteins.

This finding suggests an increased activity of the hexosamine biosynthetic pathway (HBP), which delivers the substrate for this protein modification. Since the activation of the HBP is triggered by glucose we compared glucose consumption between senescent and young cells. Fig. 15 shows that senescent cells consume considerably higher amounts of glucose suggesting a link between high glucose consumption, high flux through the HBP and protein glycosylation.

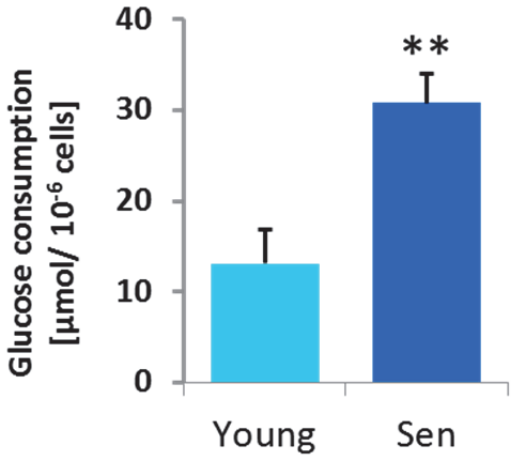

Figure 15: Senescent HUVECs have higher energy (glucose) demand

Glucose consumption estimated by the GO colorimetric assay kit (Sigma), in young and senescent HUVECs maintained in LPM media under standard conditions after 24 hrs in culture. Data represents mean of 3 independent experiments (n=3) and error bars indicate standard error of mean (S.E.M.). ** p<0.05.

4.1.3 Senescent cells accumulate lipid droplets

To understand whether the increased cytoplasmic granularity is related to increased storage of intracellular fat, we performed oil red-O staining. Absorbance measurement at 570 nm showed a significantly increased accumulation of lipid-containing vesicular structures in senescent HUVECs (Fig. 16) compared to young cells. These structures are likely to represent lipid droplets, which are made up of lipid esters encapsulated by a monolayer of phospholipids and insulated from the hydrophilic cytosol by structural proteins called perilipins [125]. They may derive from the surplus glucose consumed by senescent HUVECs or from disturbances in fatty acid metabolism.

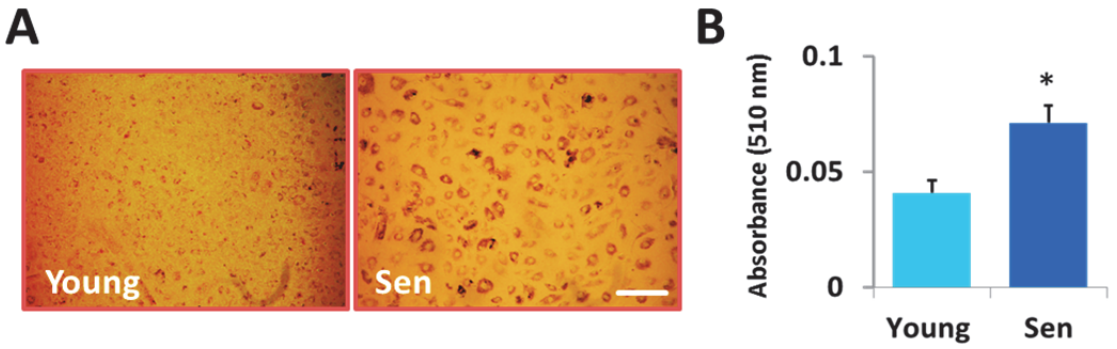

Figure 16: Senescent HUVECs have elevated lipid storage compartments

A) Representative (1 of n=3) light microscopic images of Oil- Red-O-stained young and senescent HUVECs under basal conditions. Scale bar = 10μm. **B)** Quantification of Oil- Red-O-stained young and senescent HUVECs. Mean values ± S.E.M. * p<0.05.

4.1.4 Expression and activity of the proteasome in senescent endothelial cells

In order to gain insight into a possible failure of the proteasomal system in replicative senescence, we performed western blot analysis of the proteasome subunits α, β1, β2, β5 and of the 20S core. We observed an appreciable reduction in the expression of β2 and β5 subunits, while the other subunits remained unaltered (Fig. 17).

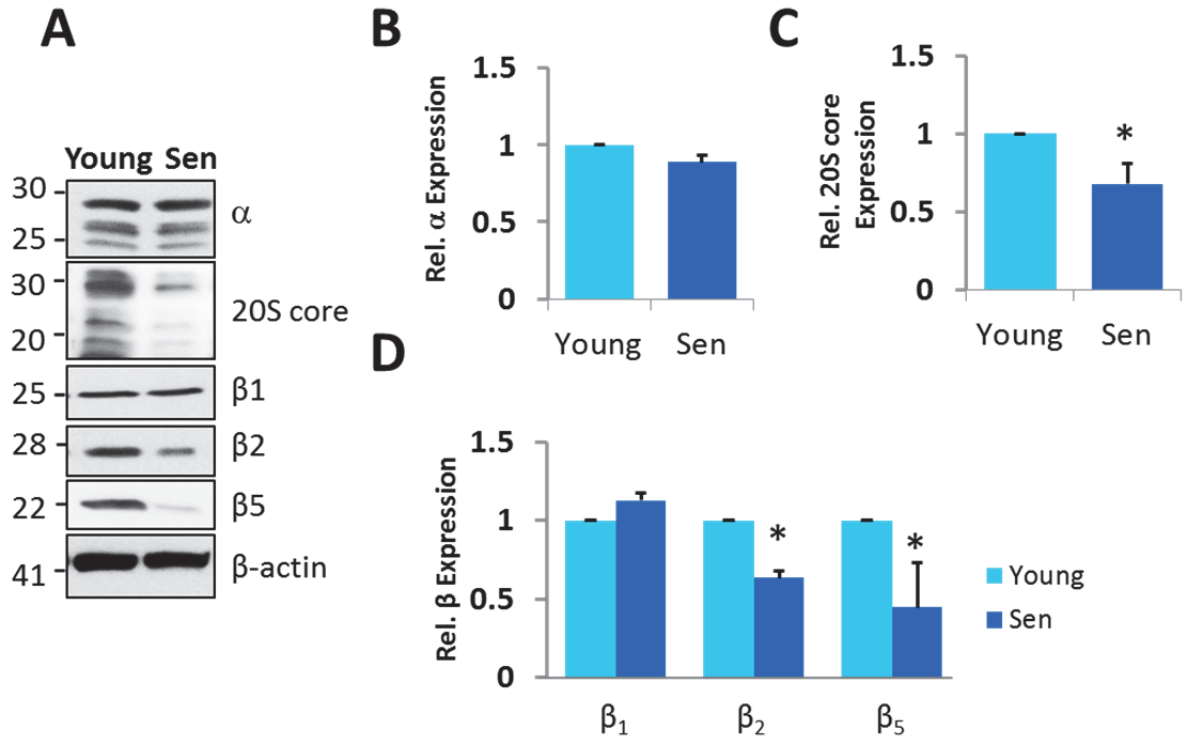

Figure 17: Senescent HUVECs display repressed 20S proteasome subunit expression levels

A) Representative immunoblots (1 of n=4) showing senescence-associated alterations of cellular proteins detected by immunoblot analysis for 20S core and subunits α, β1, β2, β5 and β-actin. **B)** Quantification for α subunit **C)** Quantification for 20S core **D)** Quantification for β1, β2, β5 subunits. Mean values ± S.E.M. * $p<0.05$.

We wondered if this loss of expression of certain subunits had functional consequences. Using defined fluorogenic peptide substrates for specific subunits we determined the major hydrolysing activities of the proteasome in young and senescent HUVECs. Expression loss led to a concomitant and significant decline of the trypsin-like and chymotrypsin-like activities (Fig. 18), while the caspase-like activity remained intact.

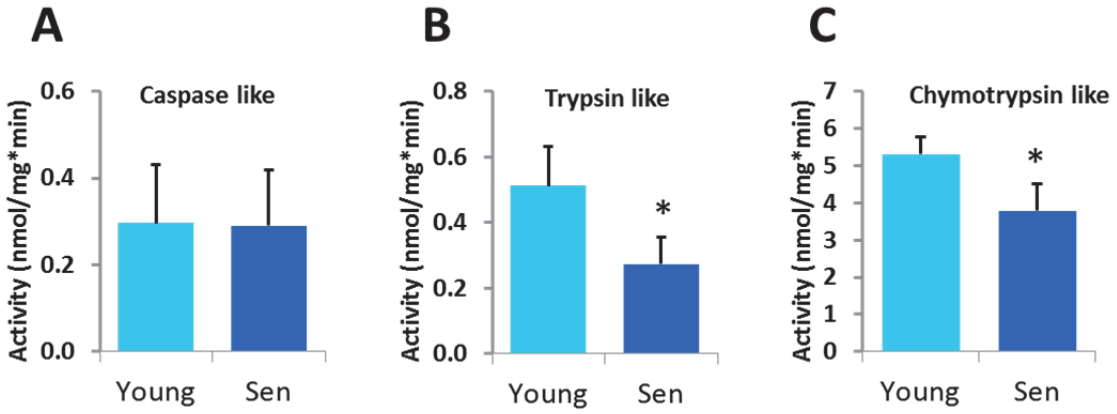

Figure 18: Low expression correlates with low proteasome activity in senescent HUVECs

Absolute activities of the three major catalytic subunits of the 20S core proteasome in young and senescent HUVECs, namely **A)** Caspase-like, **B)** Trypsin-like, and **C)** Chymotrypsin-like. Values are mean of 3 independent experiments (n=3) and error bars are S.E.M. Non-parametric one-way ANOVA was used for statistical analysis of significance. * $p<0.05$.

3.1.5. Expression of the immunoproteasome in senescent endothelial cells

Coincidentally with the decrease of the β2 and β5 subunits of the constitutive proteasome, we observed an induction of the immunoproteasome subunit LMP2, but not LMP7 in senescent cells compared to young cells (Fig. 19). Although the biological function of the immunoproteasome in non-immune cells remains largely unknown, literary reports speculate its involvement in the regulation of pro-inflammatory cytokines production, self-antigen tolerance and prevention of autoimmune conditions, activation of NF_KB pathway and management of oxidative stress. [126]

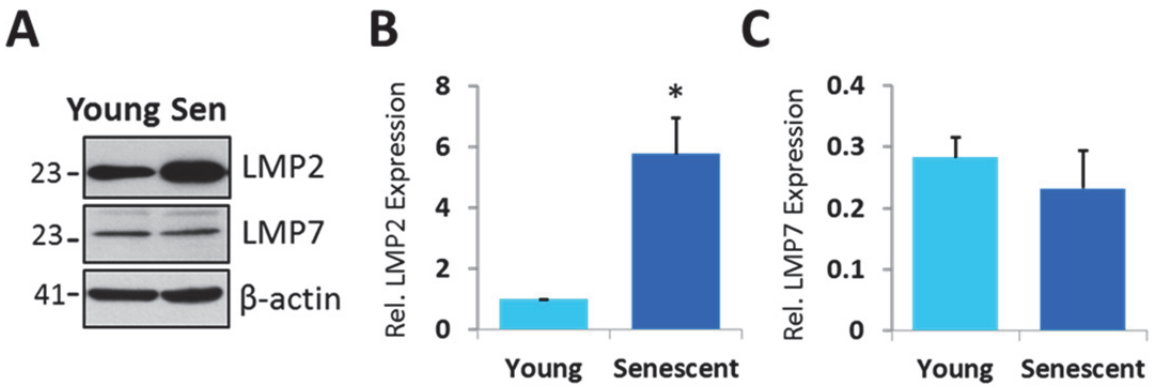

Figure 19: Immunoproteasome component LMP2 is upregulated in senescent HUVEC

A) Representative immunoblots (1 of n=3) showing senescence-associated upregulation of the LMP2 immunoproteasome subunit and no alteration of the LMP7 subunit **B)** Quantification for LMP2 expression **C)** Quantification for LMP7 expression. Mean values ± S.E.M. Non-parametric one-way ANOVA was used for statistical analysis of significance. * $p<0.05$.

4.1.5 Lipofuscin accumulation in senescent endothelial cells

A decline of proteolytic systems is suggested to lead to the emergence of a family of oxidatively modified protein byproducts that converge on lipofuscin formation in the

lysosomes of aged cells. In line with this, lipofuscin accumulation was also shown in senescent HUVECs. We recorded visible, perinuclear and cytoplasmatic lipofuscin aggregates (blue granules) in replicatively exhausted HUVEC employing the lipophilic Sudan Black Staining (Fig. 20, A). In addition, lipofuscin was identified via its autofluorescence using fluorescent confocal microscopy as well as flow cytometric recording on multiple channels (Fig. 20. B, C, D).

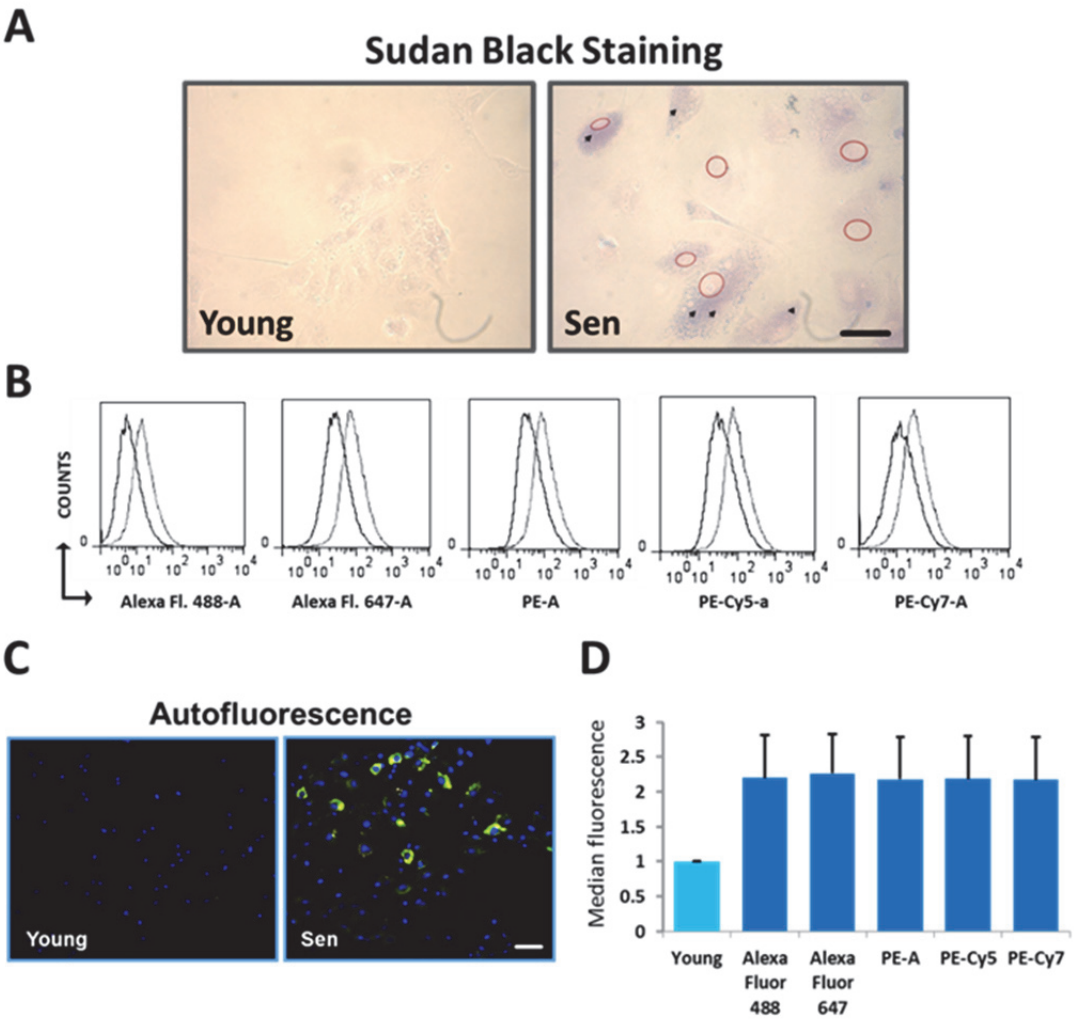

Figure 20: Protein oxidation products contribute to lipofuscin formation

A) Representative light microscopic images of Sudan black staining for the complex ageing pigment Lipofuscin, in young and senescent HUVECs. Scale bar = 10µm. **B)** Flow cytometry histograms indicating autofluorescence or spontaneous increase in fluorescent intensity of senescent cells, measured across several detector sets at pre-set excitation parameters. **C)** Representative fluorescent confocal microscopic images of young and senescent HUVECs, for visualising autofluorescence due to lipofuscin. Scale bar = 20µm. **D)** Quantification of median fluorescent intensities from B. Data represent an average of 2 experiments. Mean values ± S.D.

4.1.6 Stability of the proteasome content in the nucleus during endothelial senescence

Since there is emerging evidence that the ubiquitin proteasome system plays a major role in the nucleus by controlling initial steps of gene expression, DNA repair and quality control, we investigated the subcellular distribution of the proteasome in senescent endothelial cells. As depicted in Fig. 21, the decline in expression of the β5 and β2 subunits appears to be confined to the cytosol, while the nuclear proteasome was unaffected.

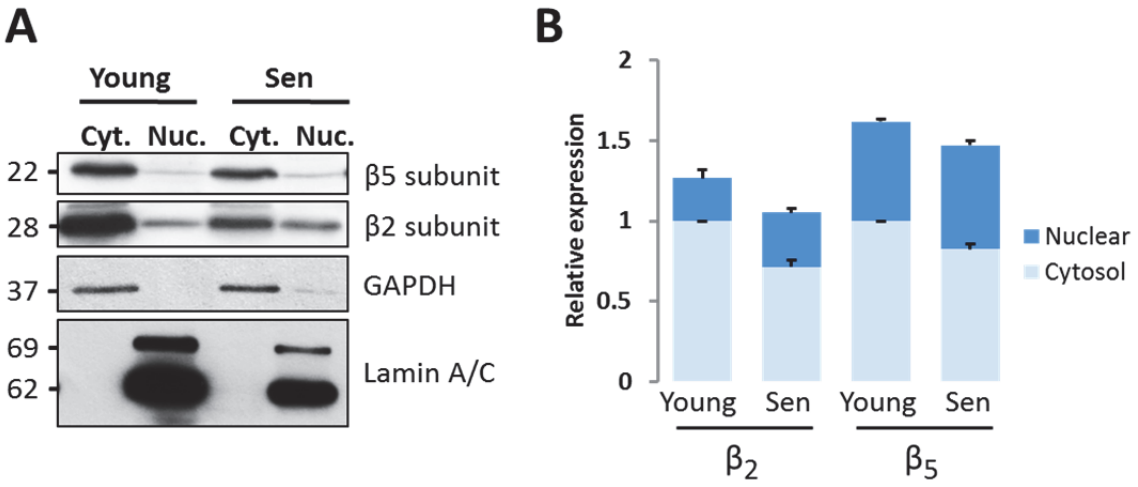

Figure 21: Cytoplasmic, but not nuclear proteasome distribution is affected in senescence

Representative immunoblot (1 of n=2) for nucleo-cytoplasmic distribution of proteasomal β2 and β5 subunits. GAPHD and Lamin A/C serve as markers for cytoplasmic and nuclear fractions ,respectively. **B)** Quantification for nuclear and cytosolic fraction of β5 and β2 subunits normalized to young cytoplasmic fraction. Error bars = S.E.M.

4.1.7 Oleuropein application improves proteasome activity in senescent cells

Oleuropein, a polyphenolic natural extract, has been reported to enhance proteasome activities *in vitro* in human embryonic fibroblast possibly via conformational changes of proteasome [127]. In a pilot experiment we could confirm these data in HUVEC, which encouraged us to test this compound in senescent endothelial cells. As shown in Fig. 22, treatment of HUVEC with 200 µM oleuropein led to a slight elevation of chymotrypsin-like activity, which was comparable between young and senescent cells (28% and 24%, respectively). In the same experimental setting, trypsin-like activity was enhanced by 60% and 21% in young and senescent cells, respectively. Caspase-like activity was not affected.

Of note, the increase of chymotrypsin- and trypsin-like proteasomal activities by oleuropein almost restored the senescence-induced decreases indicating a possible therapeutic approach for normalization of disturbed proteasomal function.

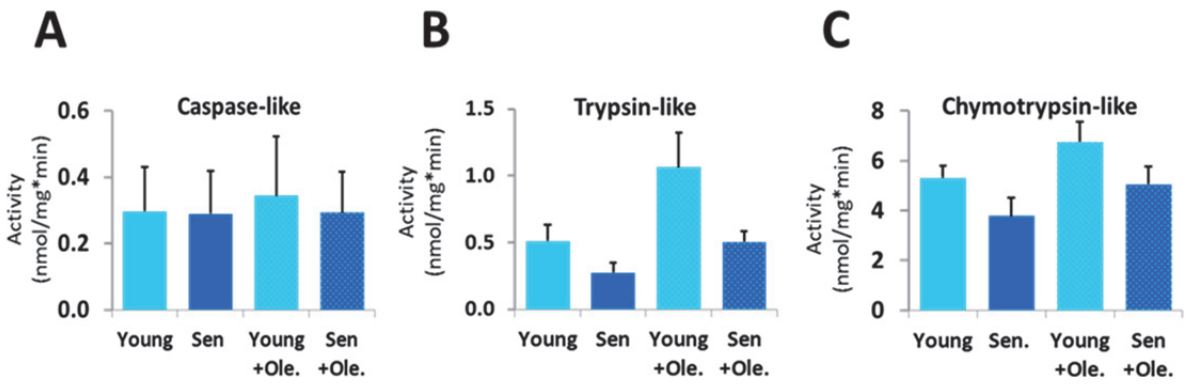

Figure 22: Oleuropein application improves proteasome activity in senescent cells

Absolute activities of the three major catalytic subunits of the 20S core proteasome in young and senescent HUVECs untreated or treated with 200µM Oleuropein for 24 hours. **A)** Caspase-like, **B)** Trypsin-like, and **C)** Chymotrypsin-like. Values are mean of 3 independent experiments (n=3) and error bars are S.E.M. Non-parametric one-way ANOVA was used for statistical analysis of significance.

4.2 The effect of chronological ageing on expression and function of the proteasome

4.2.1 Characterisation of endothelial cells prepared from aged mice

We now wished to verify our *in vitro* findings on proteasome dysfunction in senescent cells in chronologically aged endothelial cells. To this end we established cultures of murine lung endothelial cells (MLEC) isolated from the lungs of young (4–6 months) and old (24–26 months) mice. Purity of isolated cultures was ascertained by flow cytometric detection of CD31 endothelial marker expression. Over 90% of cells had endothelial identity (Fig. 23, A, B). Under identical settings, we investigated senescence markers in MLECs *ex vivo*. While cells from young animals were almost free (< 0.5%) of SA-β-gal-positive cells, about 5% of those derived from aged animals were positive for SA-β-gal (Fig. 24, A, B). Despite the meagre percentage of SA-β-gal-positive MLEC, a 4-fold increase in p53 activity and over 10-

fold induction of p21 were detected in immunoblots from aged cells compared to cells prepared from young mice (Fig. 24, C, D, E).

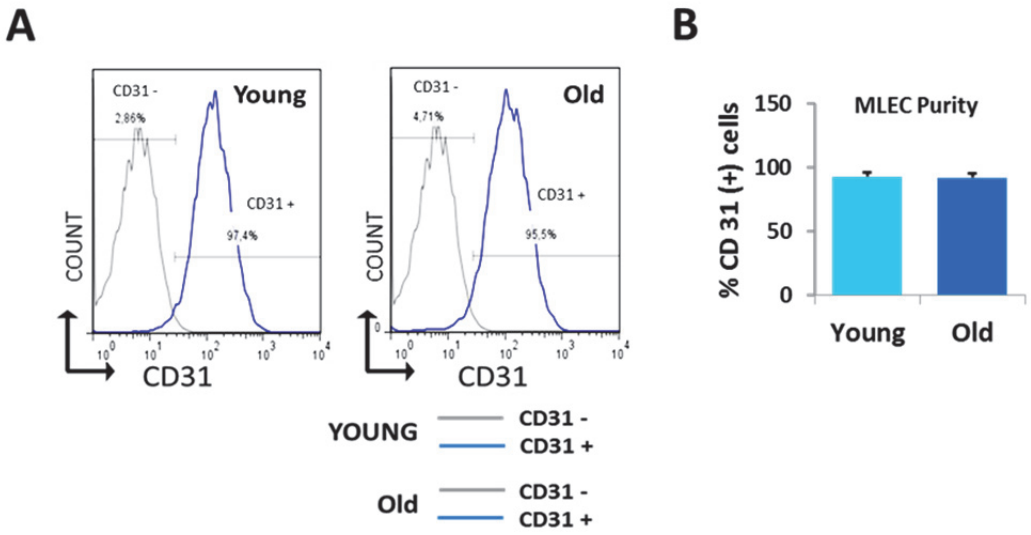

Figure 23: Purity of endothelial cells explanted from mouse lungs

A) Purity of magnetic-sorted mouse lung endothelial cells (MLECs) determined by flow cytometry for the endothelial differentiation marker CD31 A) Representative histogram of CD31 staining **B)** quantification of A with MLEC samples from 10 young and 10 old mice. Mean values ± S.E.M.

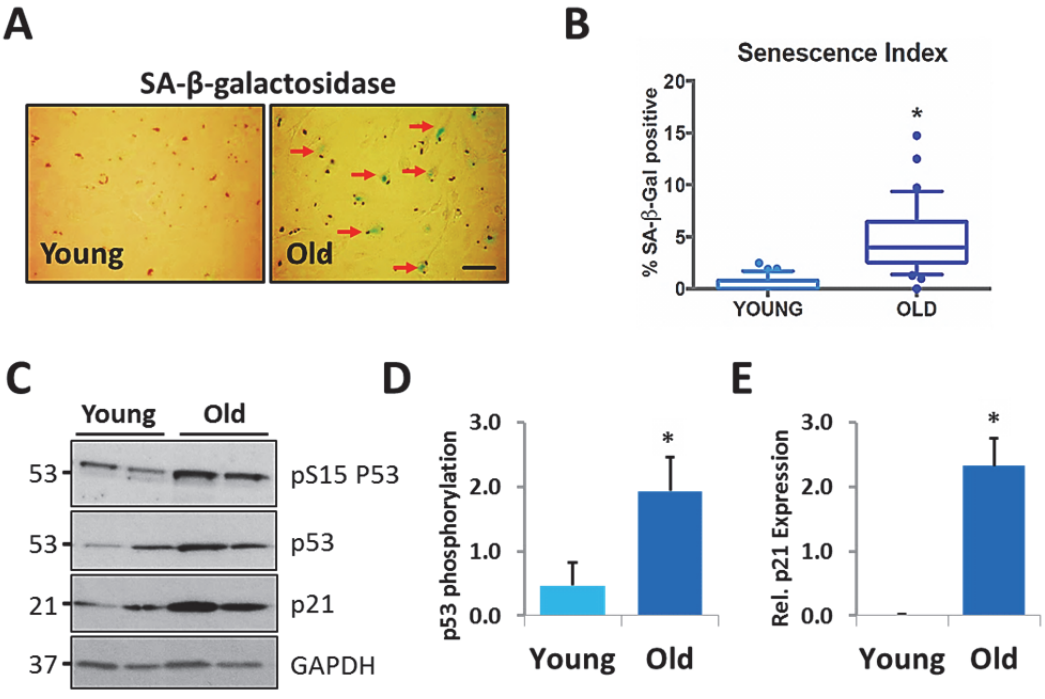

Figure 24: MLECs from old mice evidence endothelial senescence *in vivo*

A) Representative light microscopic images, and **B)** quantification of SA-β-Gal staining of MLECs from young and old mice. Scale Bar = 20µm. Mean SA-β-Gal positive cell counts taken from 5 images each, from cells from 7 young and 7 old mice. **C)** Immunoblots of basal and phosphorylated p53, as well as p21 relative expression in MLECs from 3 young and 3 old mice. **D)** Quantification of p53 phosphorylation and **E)** Quantification of relative p21 expression. Mean values ± S.E.M. * $p < 0.05$.

In parallel, we found an overall increase in protein carbonylation (Fig. 25, A, B) and a marked upregulation of iNOS indicating endothelial dysfunction (Fig.25, C, D).

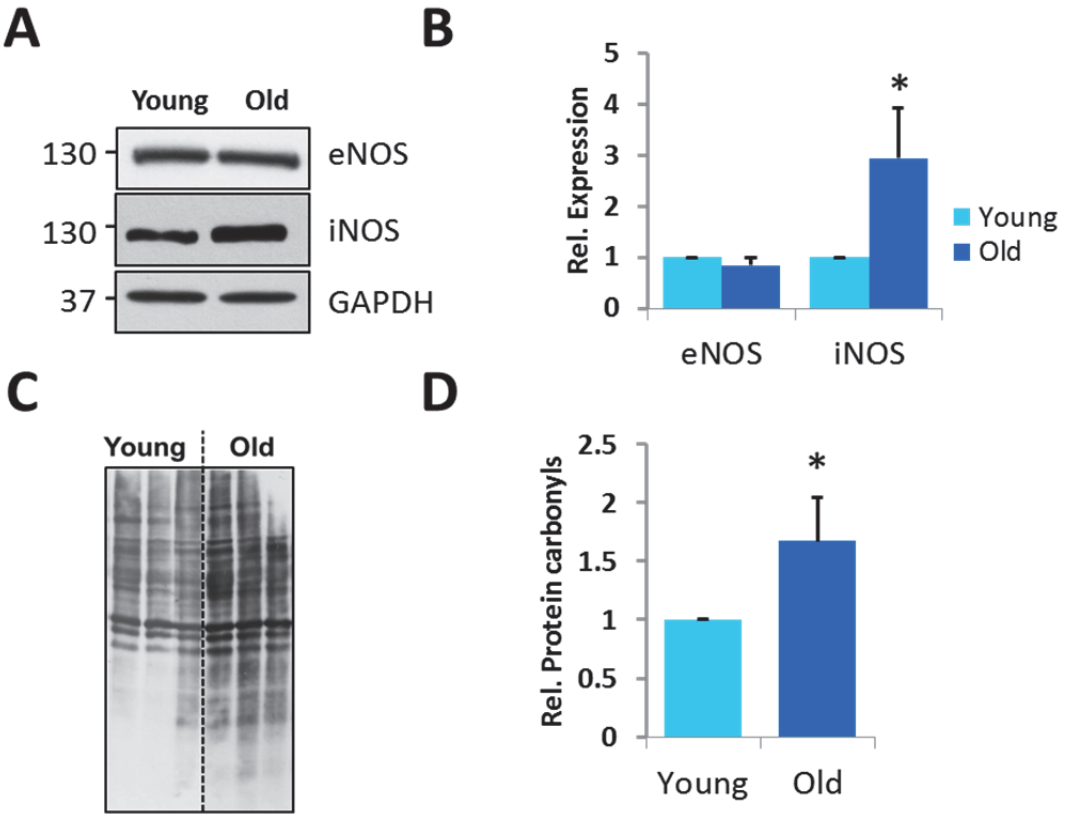

Figure 25: MLECS from old mice reveal signs of endothelial dysfunction

A) Representative immunoblots (1 of n=3) of eNOS , iNOS and GAPDH showing unaltered eNOS expression and an upregulation of iNOS in MLECS from young and old mice **B)** Densitometry of eNOS and iNOS expression. **C)** Representative immunoblot depicting carbonylated proteins detected by the OxyBlot method in endothelial lysates from 4 young and 4 old mice. **D)** Densitometry of eNOS and iNOS expression.

4.2.2 Proteasome expression and activity in chronologically aged endothelial cells

Of note, we also observed reduced levels of the 20S core (Fig. 26) and proteasomal subunits β5 and β2 (Fig. 27) in endothelial cells from aged mice similar to what we had seen in our HUVEC model of replicative senescence, and a decrease of the chymotrypsin-like activity while trypsin-like and caspase-like acivities were not altered (Fig. 28). Furthermore, a selective upregulation of LMP2 (β1i) immunoproteasome subunit was observed (Fig 27). Through these findings, we provide evidence that the aged endothelium acquires a dysfunctional phenotype with reduced proteolytic capacity thereby confirming data obtained in the *in vitro* model of replicative senescence.

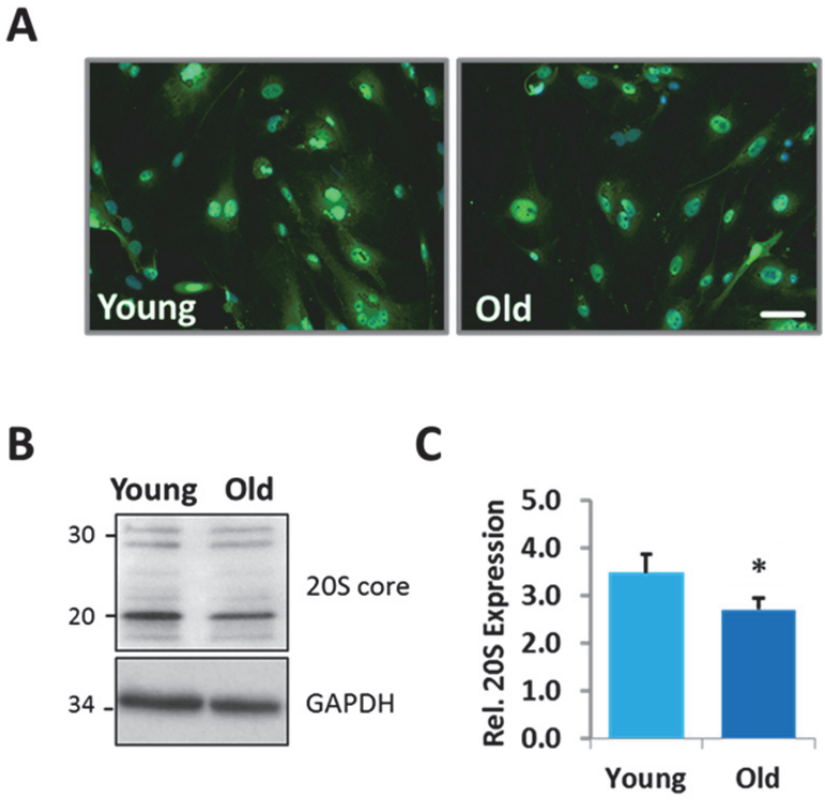

Figure 26: Chronologic age of mice affects 20S core proteasome expression

A) Representative images of immunofluorescent staining for the 20S core proteasome from young and old mice. Scale Bar = 20µm. **B)** Immunoblot of the same samples as in A, and **C)** Densitometry for expression of the 20S core from 4 independent MLEC samples. Mean values ± S.E.M. Non-parametric two-tailed T-test was used for statistical significance. * $p < 0.05$.

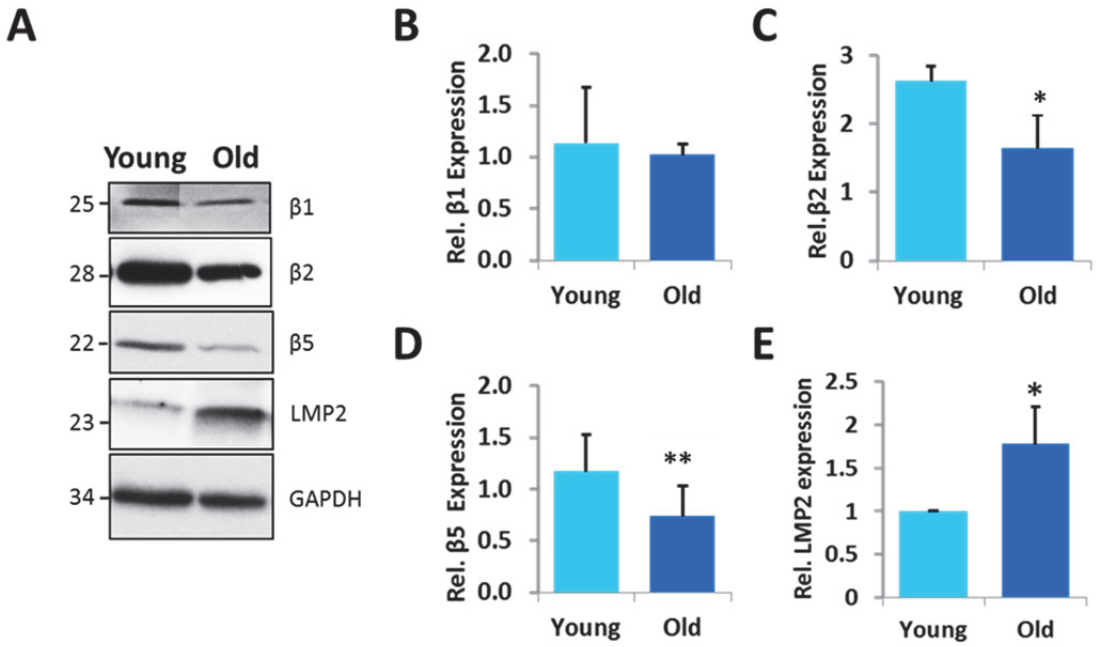

Figure 27: Chronologic age of mice affects proteasome subunit β5 and β2 and LMP2 immunoproteasome expression

A) Immunoblot of MLEC lysates from 5 young and 5 old mice showing age-associated alterations of the proteasome subunits: β1, β2, β5, LMP2 and GAPDH. **B)** Quantification for β1 subunit **C)** Quantification for β2 subunit **D)** Quantification for β5 subunit **E)** Quantification for LMP2 subunit Mean values ± S.E.M. Non-parametric two-tailed student T-test was used for statistical significance. * p<0.05.

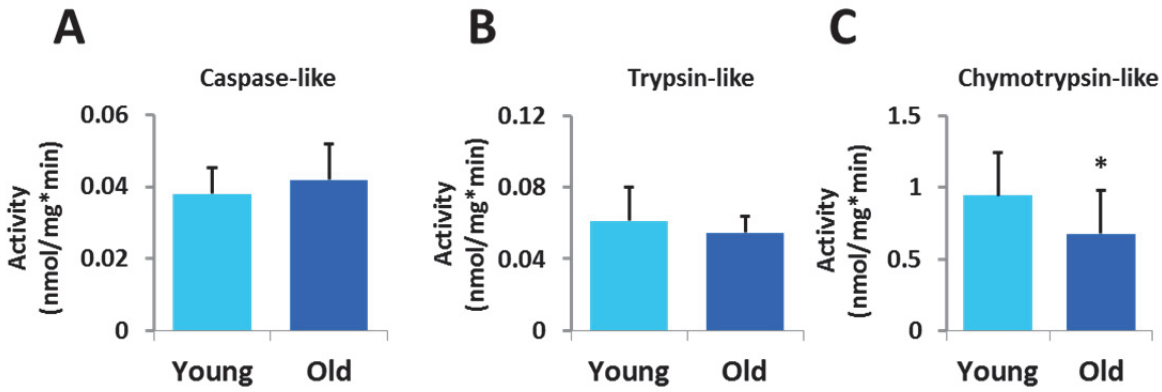

Figure 28: Proteasome activity declines in endothelial cells of old mice

Absolute activities **A)** Caspase-like **B)** Trypsin-like **C)** Chymotrypsin-like in endothelial cell lysates from 10 young and 10 old mice. Mean values ± S.E.M. Non-parametric two-tailed student T-test was used for statistical significance. * p<0.05.

4.2.3 Effect of oleuropein on proteasome activity in chronologically aged cells

As described in chapter 4.1.7 oleuropein is able to activate the chymotrypsin- and trypsin-like activities of the proteasome. Here, we tested whether this was also seen in endothelial cells from aged mice. We applied oleruopein to MLECs from young and old mice at a concentration of 200 µM for 24h. This treatment enhanced chymotrypsin-like activity in young cells by 25% and in aged endothelial by 18% (Fig. 29). These results indicate that that the diminished proteasome activity in aged cells could be improved by application of proteasome activators despite a decreased expression of proteasomal subunits.

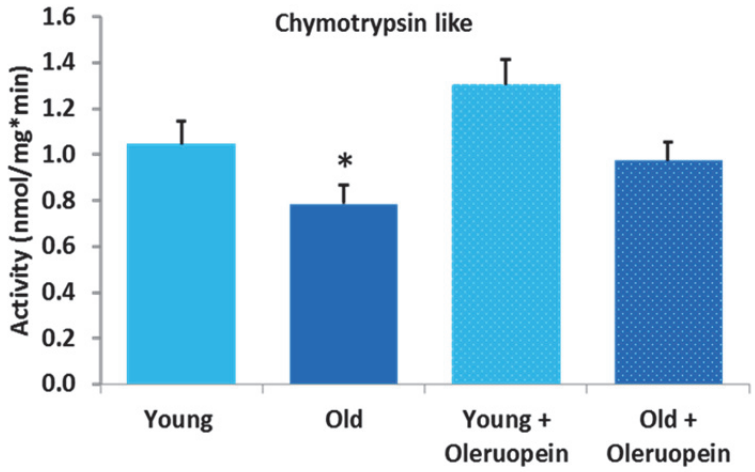

Figure 29: Oleuropein application improves chymotrypsin-like activity in MLECs from old mice

Chymotrypsin-like activity in MLECs under basal conditions and upon treatment with the proteasome activator oleuropein at a final concentration of 200µM for 24h. Data represent an average of 4 experiments. Mean values ± S.E.M. * $p<0.05$.

4.3 Chronic oxidative stress induces senescence

In an attempt to understand how cellular proteostasis is influenced by chronic oxidative stress, we treated young HUVECs with 75 µM or 100 µM H_2O_2 daily for 8 consecutive days. Oxidative stress in HUVECs was verified by a significant increase in the amount of protein carbonyls (Fig. 30, A), which represent a signature of oxidative stress. In addition, a downregulation of eNOS expression was detected (Fig. 30, C, D) after treatment with H_2O_2

indicating the development of endothelial dysfunction by chronic oxidative stress. The expression of iNOS remained unchanged (Fig. 30, C, D)

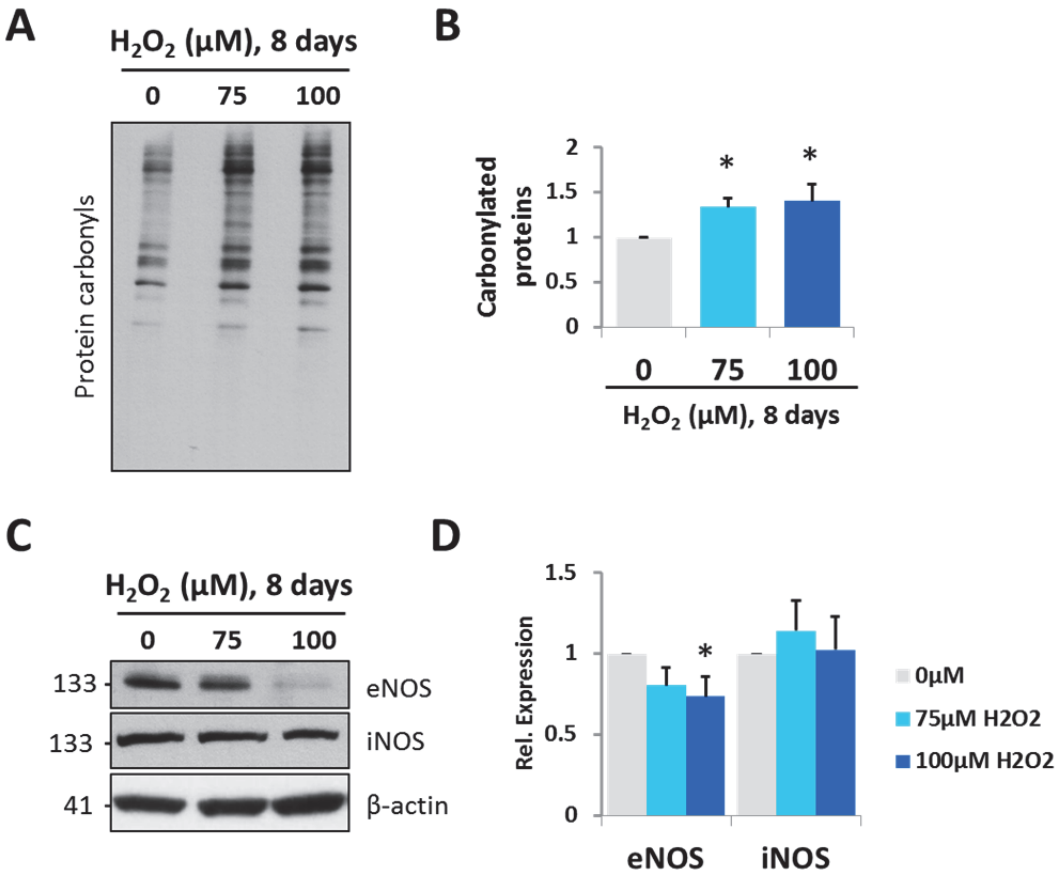

Figure 30: Chronic hydrogen peroxide exposure induces oxidative protein modification and a decrease of eNOS expression

A) Representative immunoblot out of 3 experiments depicting carbonylated proteins as detected by the OxyBlot method in untreated HUVECs or HUVECs treated daily with 75 or 100 µM H_2O_2 for 8 days. **B)** Densitometry analysis of protein carboyls shown in A. **C)** Representative immunoblot out of 3 experiments from HUVEC treated as in A) and probed for the expression of eNOS and iNOS. **D)** Densitometry for eNOS and iNOS relative expression of immunoblot in C. Mean values ± S.E.M. * $p<0.05$.

Of note, we observed that chronic H_2O_2 treatment induced endothelial cell senescence in a time- and dose-dependent manner as revealed by SA-β-gal staining. A striking increase in senescent cells by ~30% and ~45% was seen in HUVECs treated for 8 days with 75µM or 100µM H_2O_2, respectively, compared to untreated controls (Fig. 31, A, B). Western analysis of lysates from HUVEC samples treated alike showed that the development of senescence

was associated with an activation of the classical p53/p21 cell cycle arrest pathway. Both, the expression and phosphorylation of p53 as well as the expression of its CDK inhibitor target gene p21 were enhanced (Fig. 31, C, D, E) indicating the importance of this pathway in mediating premature senescence in endothelial cells exposed to sustained oxidative environment.

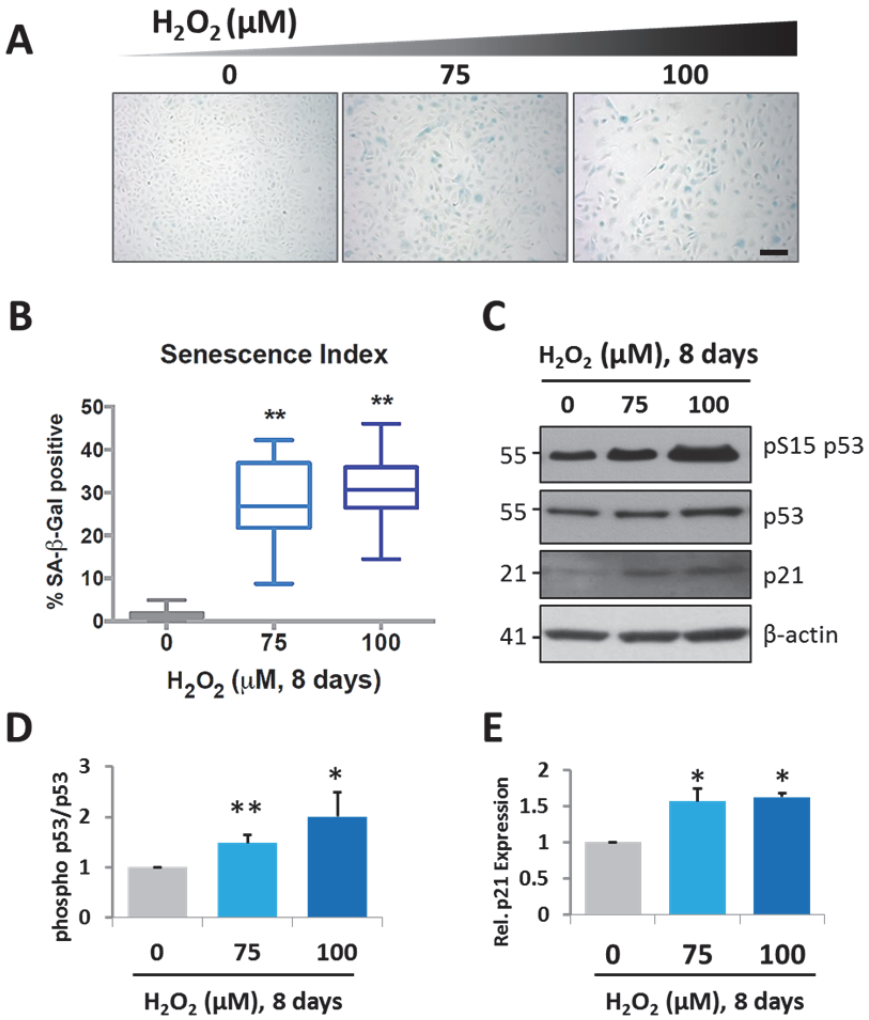

Figure 31: Oxidative stress causes premature endothelial senescence

A) Representative light microscopic images of SA-β-Gal-stained HUVECs following chronic administration of 75µM and 100µM H_2O_2 for 8 days, along with untreated control. Scale bar = 10µm **B)** Quantification of SA-B-Gal-positive senescent HUVECs treated as in A. 10 microscopic fields per treatment dish were evaluated, and data expressed as percentage of senescent cells compared to total cell number. Data represent mean ± SEM of 3 independent experiments,* $p<0.05$ compared to untreated controls. **C)** Representative western blot analysis of the senescence effector signaling pathway (p53 – p21) in lysates from samples treated as in A. **D)** Densitometry of immunoblot in C depicting phosphorylation of p53. **E)** Densitometry of immunoblot in C for relative expression of p21. Mean values ± S.E.M. *$p<0.05$, **$p<0.01$.

4.3.1 Chronic oxidative stress affects the activity of the 20S proteasome

To verify a potential effect of oxidative stress on proteolysis we measured specific proteasome activities corresponding to the respective subunits of the 20S proteasome (caspase-, trypsin-, and chymotrypsin-like activities for β1, β2, and β5 subunits, respectively). We found significantly reduced trypsin- and chymotrypsin-like activities but no alteration in the caspase-like activity (Fig. 32 C, D, E). In line with the reduction of the proteolytic capacity, a concomitant increase in the amount of ubiquitin-tagged proteins after chronic H_2O_2 treatment was detected as depicted in Fig. 32, A, B.

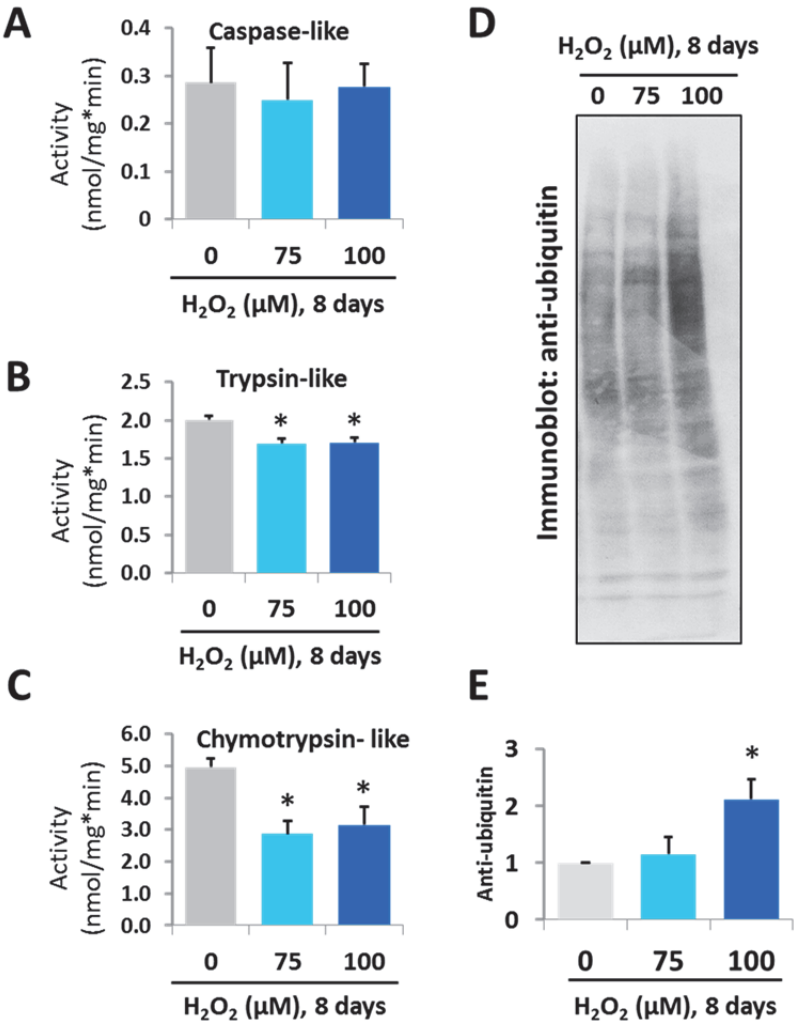

Figure 32: Oxidative stress inhibits proteasome function

A) Absolute activities of the three major catalytic functions of the 20S core proteasome in HUVEC following chronic oxidative stress induction with 75 or 100 µM H_2O_2 for 8 days, **A)** Caspase-like, **B)** Trypsin-like, and **C)** Chymotrypsin-like activities. **D)** Representative immunoblot for the detection of

ubiquitinated proteins (1 of n=3) in HUVECs treated with 75 µM or 100 µM H_2O_2 for 8 days. **E)** Densitometry of ubiquitin immunoblot. Values are means ± S.E.M. of 3 independent experiments.
* p<0.05 *versus* untreated control samples.

Next, we characterised the expression of subunits β1, β2 and β5 of the 20S core proteasome and the α regulatory subunits by western blot analysis of lysates from control and H_2O_2-treated HUVECs. We observed unaltered expression levels of the subunits (α, β1, β2, β5) examined after 8 days of chronic treatment with H_2O_2 (Fig. 33, A, B). We extended our analysis to the specialized subtype of the UPS, the immunoproteasome. However, no alteration in the expression of subunits LMP2/ β1i and LMP7/ β5i (Fig 33, C, D) was seen. Together, these results suggest that a functional deficiency of the 20S core proteasome may contribute to premature senescence development in oxidatively stressed HUVECs although a causal relationship cannot be concluded from the data described in this chapter.

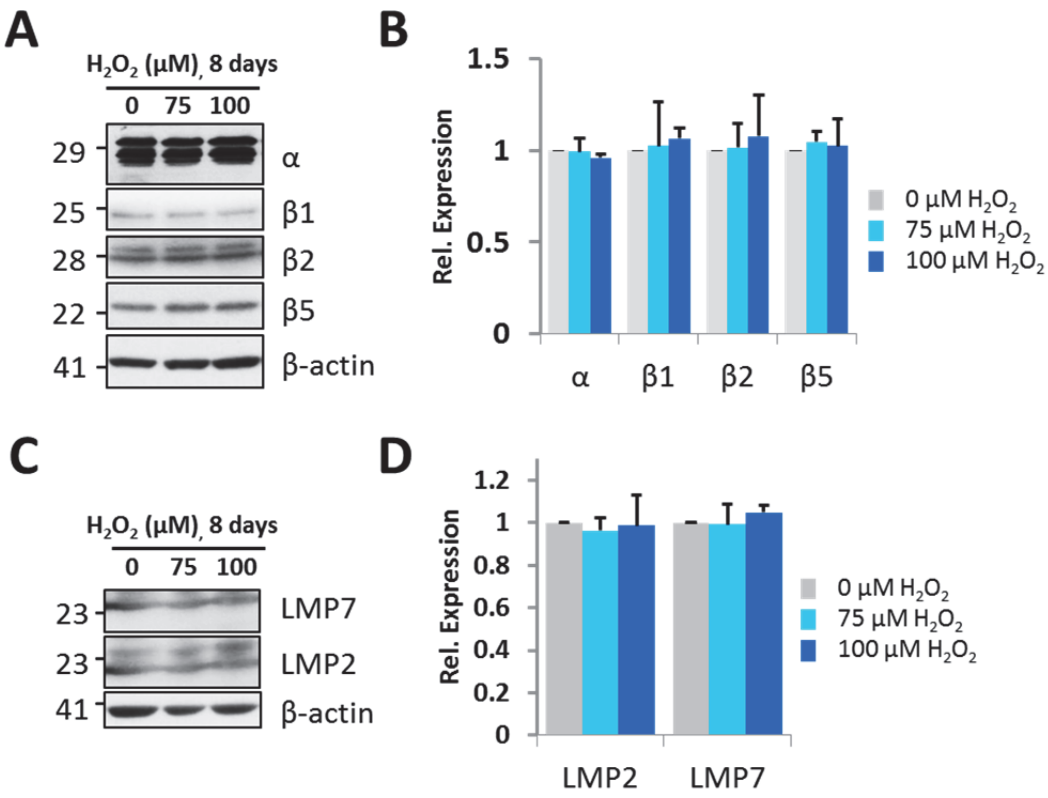

Figure 33: Oxidative stress does not alter proteasome expression

A) Representative immunoblot for the detection of different 20S proteasome subunits α, β1, β2, β5 (1 of n=3) in HUVECs treated with 75 µM or 100 µM H_2O_2 for 8 days. **B)** Densitometry analysis of immunoblot in A. **C)** Expression of LMP2 and LMP7 subunits of the immunoproteasome in HUVEC treated as in A. **D)** Densitometry analysis of immunoblot in C. Mean values ± S.E.M.

4.4 Transient inhibition of the proteasome on the development of senescence

In the previous sections, we have shown that proteasomal dysfunction is a hallmark of both replicative and premature senescence and occurs in chronologically aged cells. To clarify a causal relationship between these processes we investigated the effect of proteasomal inhibition in early passage HUVECs on the development of premature senescence.

4.5 Transient inhibition of proteasome activity by MG132

We first performed experiments with MG132, a reversible proteasome inhibitor, which is known to primarily inhibit chymotrypsin-like activity. HUVEC in full growth medium were treated with 250nM, 500nM or 1µM MG132 every 24 hours for 4 consecutive days. As seen in Fig. 34, A, this treatment led to a dose-dependent decrease of chymotrypsin-like activity, which was accompanied by an increased accumulation of ubiquinated proteins (Fig. 34, B). When HUVEC were allowed to recover for one week in the absence of the inhibitor, chymotrypsin-like activity was restored and the amount of ubiquitinated proteins returned to normal (Fig. 34, B).

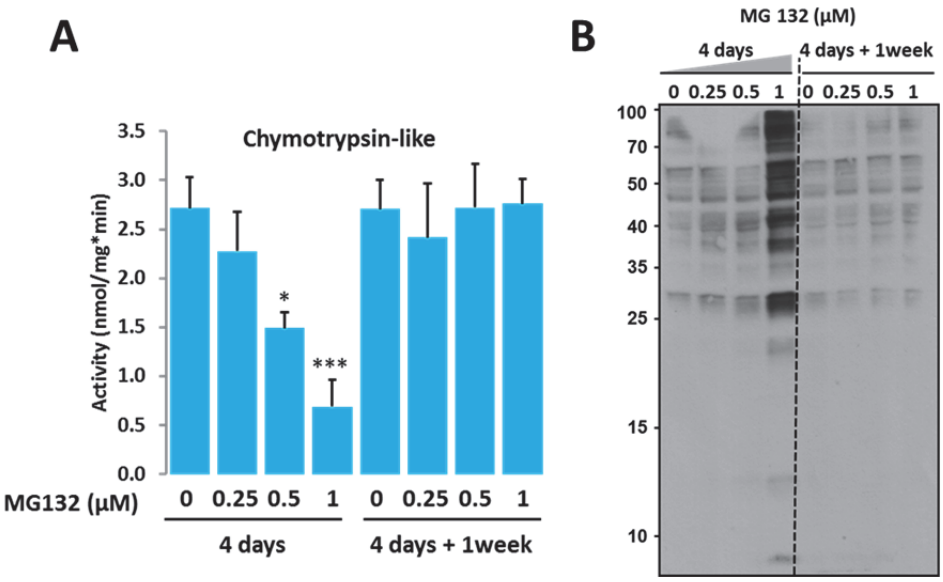

Figure 34: MG132 inhibition of proteasome activity is restored in the absence of the inhibitor

A) Chymotrypsin-like activity in early passage HUVECs treated with 250nM, 500nM or 1µM of MG132 or DMSO (control) for 4 days and after 1 week of recovery in the absence of the inhibitor

(4days + 1 week recovery). Data represent mean ± S.E.M., n=3. **B)** Representative immunoblot (1 of n=2) showing accumulation of ubiquitinated proteins in HUVEC upon MG132 treatment as in A) and clearance of ubiquitinated proteins after inhibitor removal. * p<0.05 . ** * p<0.001.

4.6 Transient inhibition of the proteasome by MG132 leads to irreversible accumulation of carbonylated proteins

We further analysed the status of carbonylated proteins in HUVEC treated with MG132. After 4 days of incubation with 250nM, 500nM or 1µM MG132 a dose-dependent accumulation of carbonylated proteins as opposed to control cells was observed. This status remained after the removal of the inhibitor and the restoration of the proteasomal activity (Fig. 35).

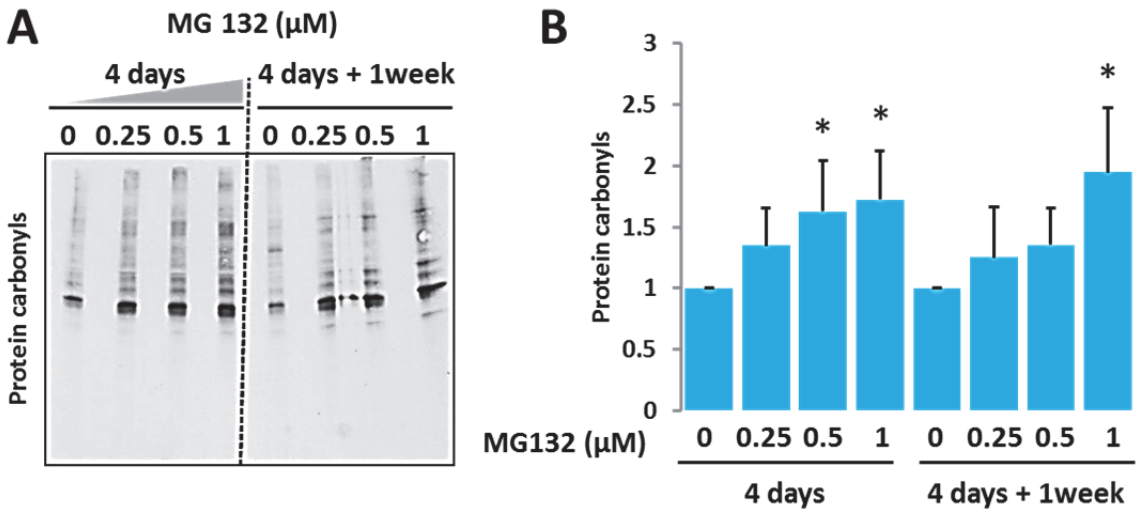

Figure 35: Transient inhibition of proteasome with MG 132 leads to accumulation of carbonylated proteins

A) Representative immunoblot (1 of n=3) for the detection of carbonylated proteins in early passage HUVECs treated with 250nM, 500nM or 1µM of MG132 or DMSO (control) for 4 days and after 1 week of recovery in the absence of the inhibitor applying the OxyBlot method. **B)** Densitometry analysis of three independent experiments. Mean values ± S.E.M. *p<0.05.

4.7 Transient inhibition of proteasome activity by MG132 induces premature senescence

Next, we examined whether cells transiently treated with MG132 develop characteristics of senescence. Of note, HUVEC incubated with this compound and then allowed to recover for one week in its absence established senescence markers despite the restoration of proteasome activity. Treatment of HUVEC with 0.5 µM or 1 µM MG132 resulted in ~30% SA-β-Gal-stained cells (Fig. 36, A, B). In addition, elevated expression and phosphorylation of p53 and elevated levels of p21, a cyclin-dependent kinase inhibitor, were detected suggesting the involvement of this pathway in senescence development (Fig. 36, C, D, E).

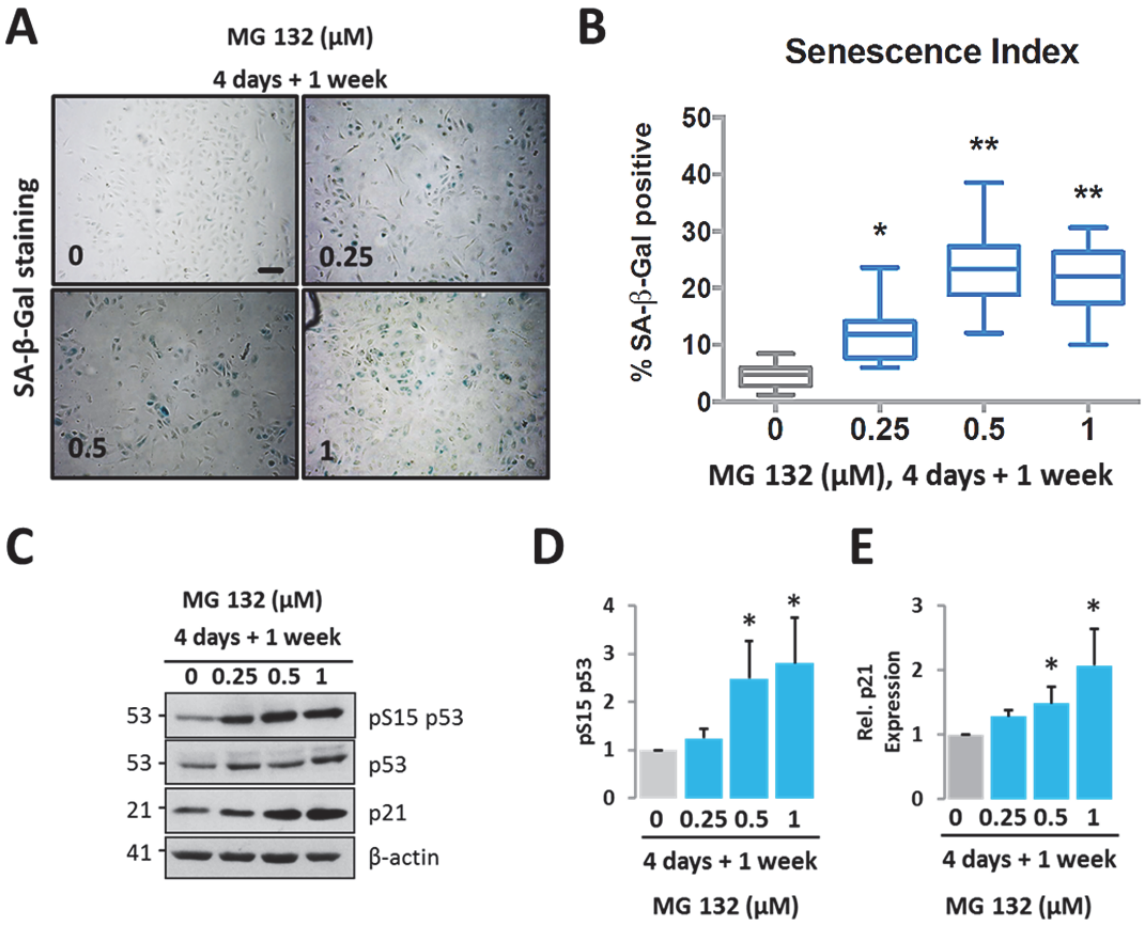

Figure 36: Transient inhibition of proteasome activity with MG132 induces premature senescence in early passage HUVECs

A) Representative light microscopic images of SA-β-Gal-stained HUVECs following chronic administration of 0,25µM 0.5µM and 1µM MG132 for 4 days and an inhibitor-free period of 1 week, along with untreated control (n=3). Scale bar = 10µm. **B)** Quantification of SA-β-Gal positive (blue) senescent HUVECs treated as in A). 10 microscopic fields were evaluated and data expressed as

percentage of senescent cells compared to total cell number per field. Data represent mean ± S.E.M. of 3 independent experiments,*p<0.05 compared to untreated controls **C)** Representative western blot analysis of the senescence effector signalling pathway (p53 – p21) in lysates from samples treated as in A. **D)** Densitometry analysis of immunoblot for p53 phosphorylation as shown in C. **E)** Densitometry analysis for the relative expression of p21 immunoblot shown in C. **D,E)** Mean values ± S.E.M., n= 3.

4.7.1 Transient inhibition of proteasome activity by bortezomib

In order to understand whether senescence development caused by MG132 was a general effect of proteasome inhibition, we performed experiments with bortezomib, another proteasome inhibitor. For these experiments an incubation time of 48 h was chosen, which was sufficient to obtain significant reduction of proteasome activity. HUVEC in full growth medium were treated with 10 nM or 20 nM bortezomib every 24 hours for 2 consecutive days and then allowed to recover in the absence of the inhibitor for one week. The proportion of cells and particles in the sub-G1 phase was negligible in all conditions (less than 5% cell death with both doses of bortezomib (data not shown). As shown in Fig. 37, a dose-dependent decrease of chymotrypsin-like activity was seen after 2 days treatment, which was completely restored, when cells were grown in inhibitor-free medium for another week (Fig. 37).

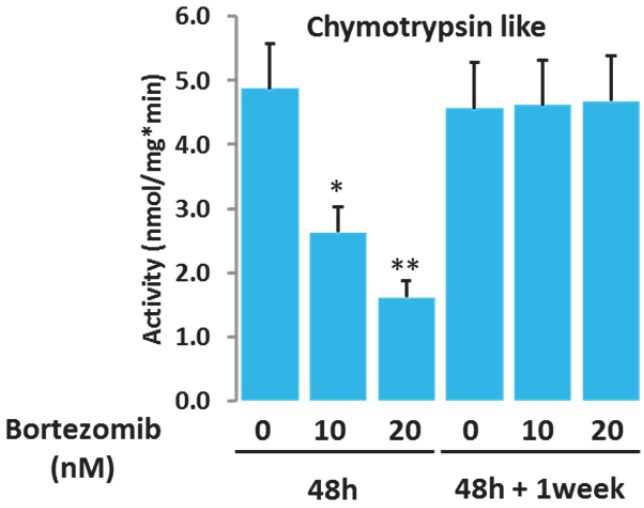

Figure 37: Bortezomib inhibition of proteasome activity is restored in the absence of the inhibitor

Chymotrypsin-like activity in early passage HUVECs untreated or treated with 10nM or 20nM Bortezomib for two days and an inhibitor-free period of one week. Data represent mean ± S.E.M., n=3. * p<0.05, ** p<0.01.

4.7.2 Proteasome inhibition by bortezomib leads to premature senescence

Similar to what we had seen in MG132-treated HUVEC, we observed that HUVECs, which had undergone transient proteasome inhibition by bortezomib, revealed features of premature senescence. HUVECs treated for 48h with 10nM and 20nM bortezomib and kept in culture for an additional week in the absence of the inhibitor showed approximately 25% senescent cells as detected by SA-β-galactosidase staining (Fig. 38, A, B). In parallel, an enhanced p53 expression and phosphorylation as well as p21 upregulation were detected suggesting that the p53/p21 axis belonged to the responsible pathways of senescence (Fig 38, C, D, E).

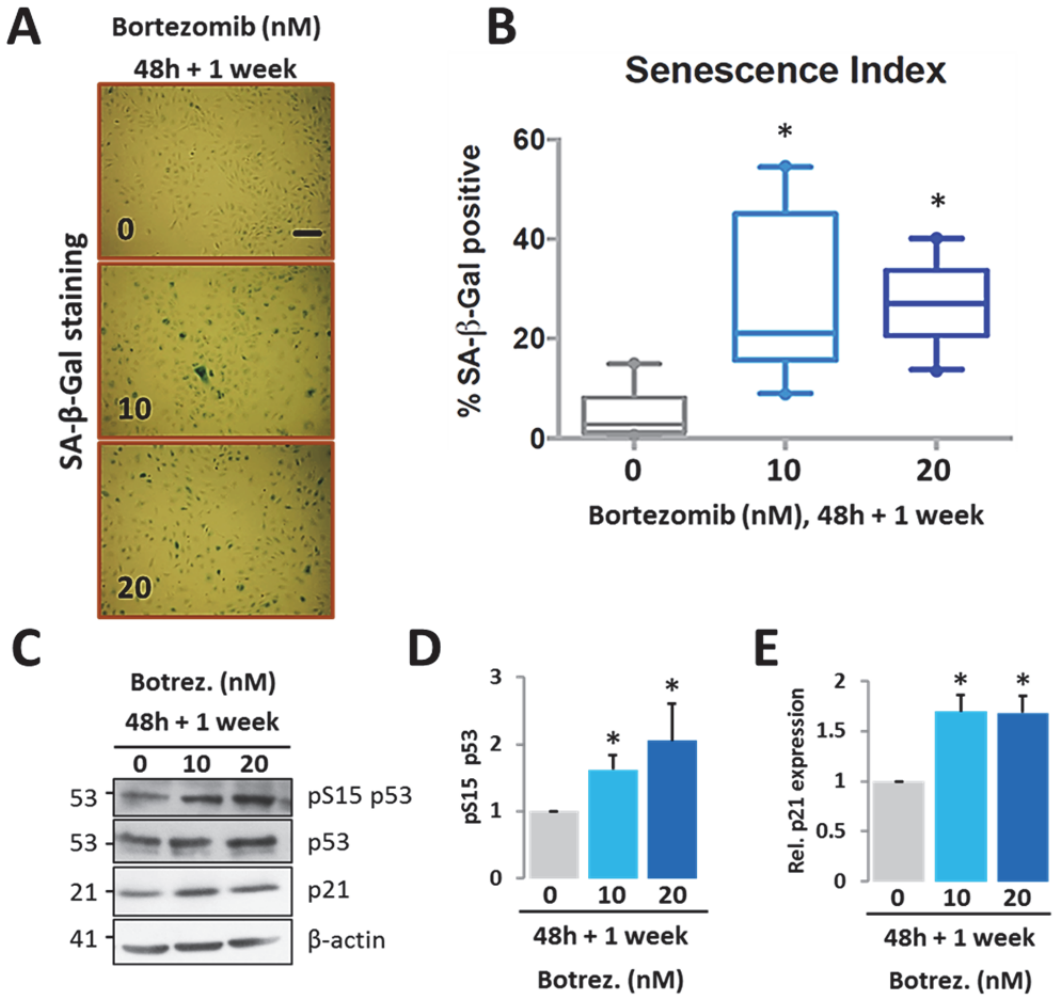

Figure 38: Transient inhibition of proteasome by bortezomib induces premature senescence in early passage HUVECs

A) Representative light microscopic images of SA-β-Gal-stained HUVECs treated with 10nM and 20nM Bortezomib for 48h and an additional inhibitor-free period of one week (48h + 1 week), along with untreated control. Scale bar = 10µm (n=4) **B)** Quantification of SA-β-Gal-positive (blue) senescent HUVECs treated as in A. 10 microscopic fields per treatment dish were evaluated and data expressed as percentage senescent cells compared to total cell number per field. Data represent mean ± S.E.M. from 4 independent experiments. *p<0.05 versus untreated controls. **C)** Representative western analysis of the senescence effector signalling pathway (p53 – p21) in lysates from samples treated as in A. Densitometry analysis of **D)** p53 phosphorylation **E)** relative p21 expression from three independent experiments in lysates from samples treated as in A. Mean values ± S.E.M., n=3.

4.7.3 Proteasome inhibition with bortezomib mediates cell cycle arrest via upstream DNA damage signalling

Despite the well documented accumulation of p53 upon proteasome inhibition, there is little evidence on how exactly proteasome inhibitors activate p53 and lead to a cell cycle arrest. In an attempt to explore possible mechanisms and factors by which proteasome inhibition renders young HUVECs senescent we performed direct flow cytometry measurement of Ser139-phosphorylated Histone H2A variant X (γH2AX), a marker of DNA double strand breaks, following acute (10nM - 20nM, 48h) bortezomib treatment. As depicted in Fig. 39, we observed elevated levels of DNA damage (20%) 48h after bortezomib treatment. This may explain phosphorylation of p53 at Ser 15 following proteasome inhibition, which is possibly triggered by DNA damage response signalling pathways. This in turn may further stabilize p53 and contribute to the observed induction of p21 and development of a senescence-like arrest.

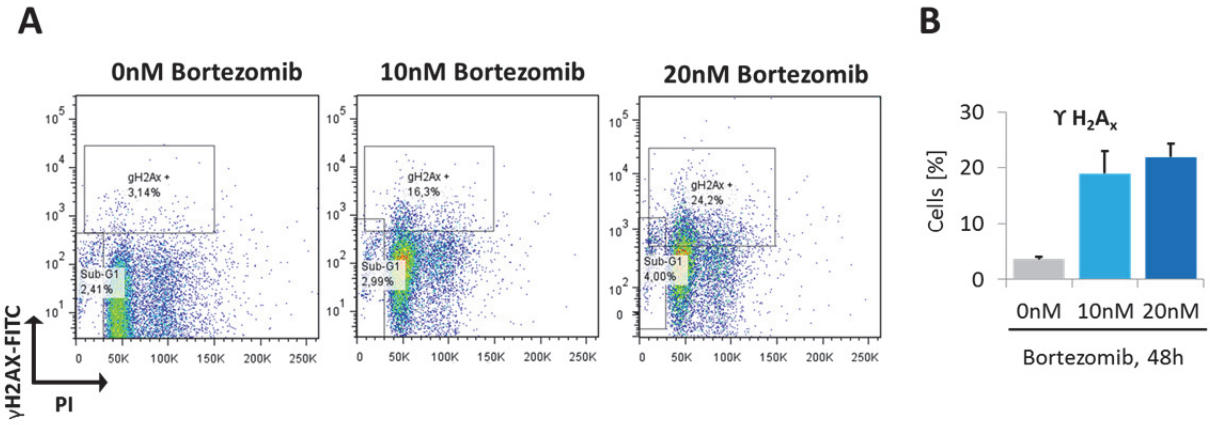

Figure 39: DNA damage follows acute treatment with bortezomib

A) Representative (n=2) flow cytometry dot plots for direct measurement of DNA strand break marker γH2AX (Y-axes) plotted against DNA content (X-axes), without and with 10-20 nM bortezomib treatment for 48h. **B)** Quantification of percentage γH2AX positive cells in samples treated as in A. Mean values ± S.E.M.

Together, these data confirm that transient proteasome inhibition triggers not only enhanced p53 levels but also elevated oxidative stress leading to oxidatively modified proteins and manifestation of DNA damage/response signaling, which together mediate a senescence-like phenotype, implying a causal link of proteasome inhibition and senescence development.

5 Discussion

This thesis was aimed at examining the role of ubiquitin proteasome system in endothelial senescence *in vitro* and in endothelial ageing *in vivo*. In order to accomplish these aims, proteasome function was analysed in primary endothelial cells subjected to long-term culture until replicative exhaustion or chronic oxidative damage. Additionally, mice lung endothelial cells from young and aged mice were used to reveal a possible role of the ubiquitin proteasome system in the physiological ageing process. Our data show that in all three models, i.e. replicative senescence, premature stress-induced senescence and chronological ageing proteasomal activities were reduced. Moreover, we could show a causative link between proteasomal decline and the development of senescence by employing proteasomal inhibitors, namely MG132 and bortezomib, the latter being a clinically approved therapeutic agent.

5.1 Molecular signatures of replicative senescence in HUVECs

In order to investigate proteasome function in replicative senescence we employed a model based on continuous culturing of HUVECs until loss of proliferative capability. Critical telomere shortening is believed to be the most important trigger for this type of senescence[128]. We observed growth arrest after 15-17 cumulative population doublings associated with activation of the p53/p21 pathway known to mediate cellular senescence upon telomere attrition [129] and with a positive SA-β-gal staining in more than 80% of cells.

Replicative senescent HUVECs, unlike young HUVECs, appeared to be morphologically heterogeneous, with a vast variability not only in the degree of SA-β-galactosidase activity but also with regard to their size and granularity despite maintenance of endothelial identity (CD31 positivity). In line with this, literature points out that senescent cells can assume diverse morphological traits [130]. The elevated granularity of senescent cells may indicate cytoplasmic inclusions such as lipofuscin or misfolded aggregates, whereas the larger size may be due to ongoing cell growth while proliferative capacity is slowed down. Along this line we have observed an activation of protein S6 kinase 1 reflecting mTORC1 activation although mTORC1 inhibition may also occur as a consequence of p53 activation [131].

Replicative senescent endothelial cells were characterized by the occurrence of oxidative stress. This was verified by elevated levels of protein carbonyls as well as by a significant

decline in cellular GSH levels. Protein carbonylation may be attributed to enhanced ROS formation but also to a decline in the antioxidant defence system, diminished clearance of oxidized proteins, or even to an increased susceptibility of proteins to oxidative attack. How protein carbonylation affects cellular function is still a matter of debate but the degree at which it occurs certainly dictates beneficial versus detrimental cellular outcome. While mild carbonylation could be considered beneficial as it marks proteins for proteolysis, heavy carbonylation of proteins tends to result in high molecular-weight-aggregates that escape degradation [132-134]. The glutathione redox-cycle plays a predominant role as an anti-oxidant defence system against peroxide-induced oxidative stress in endothelial cells [135]. Our observation of GSH depletion complies with the finding of Kurz *et al*. emphasizing that glutathione homeostasis is important for endothelial cells and its perturbation enhances oxidative stress, which is a mechanism leading to endothelial senescence and pathogenesis of vascular disease [135].

Oxidative stress is known to induce or accelerate the development of cellular senescence. In endothelial cells, an association between oxidative stress, accelerated telomere shortening and senescence has been suggested [136,137]. Oxidative stress may arise from mitochondrial dysfunction and, indeed, literature evidence points to reduced mitochondrial ROS buffering capacity as a key event in endothelial senescence [138]. For instance, downregulation of the mitochondrial antioxidant MnSOD results in diminished capacity of ROS buffering of mitochondria [27,139] and could contribute to oxidative stress in senescence. In addition, factors including disturbed mitochondrial biogenesis, reduced mitochondrial mass, altered expression of components of the electron transport chain and others may lead to excessive formation of superoxide and H_2O_2, which are major determinants for oxidative damage during endothelial senescence [47,138,140,141]. Accordingly, deficiency of the mitochondrial ETC complex IV has been shown to play a role in senescence [142].

Replicative senescent endothelial cells revealed a marked upregulation of iNOS and a downregulation of eNOS [27,132-135,139]. This observation confirms what has been previously reported in the literature [28,143-145] and may be considered as one of the major causative factors of endothelial dysfunction observed in senescence. A reduced eNOS expression leads to a decrease of tightly controlled formation of NO, which is a vasodilative and anti-inflammatory key signalling molecule. iNOS induction, on the other hand, promotes oxidative stress and further diminishs NO production by eNOS. Experimental evidence from

Katusic *et al.* showed that iNOS upregulation leads to S-nitrosylation of arginase 1, which increases its ability to compete with eNOS for L-arginine and ultimately results in an impairment of NO biosynthesis. Reduced L-arginine concentration in turn promotes uncoupling of eNOS and formation of superoxide anion and peroxynitrite thus having deleterious effects on endothelial function [146]. Along this line, we recorded nitrotyrosine modification of proteins in senescent HUVECs, which is a marker for peroxynitrite formation. Nitration of proteins could directly affect protein function or in long term add to the process of protein aggregation known to be associated with senescence.

Senescence is a complex phenotype with extensive metabolic restructuring [147]. We hence looked at glucose consumption and key signalling molecules regulating glucose metabolism. We saw that senescent HUVECs exhibit enhanced phosphorylation of AMPK pointing to an increased energy demand [148]. Comparing young and senescent HUVECs, we observed an increase in glucose consumption in senescent HUVECs. This may not only feed glycolytic ATP synthesis but also contribute to an increased glucose flux through pathways branching off from glycolysis. One of these is the hexosamine biosynthetic pathway with the end product UDP-*N*-acetylglucosamine, which acts as a donor for adding N-acetylglucosamine to serine/threonine residues of proteins. This post-translational modification is known as O-GlcNAcylation. In line with the suggestion of higher glycolytic fluxes in senescence, we recorded higher *O*-GlcNAcylation of proteins in senescent cells. Contrary to our observation, a recent study using primary peritoneal mesothelial cells did not show significant alteration of global *O*-GlcNAcylation but suggested a change in the dynamics of this process during senescence [149]. *O*-GlcNAcylation is known to modulate key biological processes such as transcription, signal transduction and cytoskeletal reorganisation. According to a recent study the proteasome may also be regulated by this process [149]. Modification of the Rpt2 ATP-ase in the mammalian proteasome 19S cap has been shown to decrease the function of the proteasome. This may suggest that an altered metabolism during senescence may affect proteasome function through O-GlcNAcylation of specific regulatory and core proteasome subunits.

We saw a significant increase in Oil red-O-positive lipid droplets in senescent HUVECs as compared to young HUVECs [150]. Lipid accumulation may contribute to the inflammatory status and endoplasmic reticulum stress in senescent endothelial cells and may indicate disturbances in lipophagy, the degradation of lipids by autophagic processes [151]. An

interesting aspect is that lipid droplets have been shown to accommodate a special isoform of O-GlcNAcase (which removes O-GlcNAc from targeted proteins), which is a key regulator of the proteasome and is involved in lipid droplet surface remodelling [152].

Collectively, endothelial cells undergoing replicative senescence exhibit enhanced oxidative stress, an inflammatory state with an eNOS/iNOS imbalance and lipid accumulation as well as metabolic alterations, which are all characteristics of endothelial dysfunction.

5.2 Premature senescence of endothelial cells

While replicative senescence is associated with attrition of telomeres, stress-induced premature senescence seems to be independent from telomere length. It can be initiated by various conditions including oxidative stress or oncogenic stimuli and is thought to include the p16-pRb pathway through the mediation of the p38-MAPK signalling cascade. Oxidative stress can also lead to the activation of p53 thereby stimulating the p53-p21-pRb pathway to initiate premature senescence. Our data show that chronic application of H_2O_2 to HUVECs rendered young endothelial cells senescent and dysfunctional. After 8 days of treatment with H_2O_2 we found 40-50 % SA-β-gal-positive cells associated with increased activation of the p53/p21 pathway and a downregulation of eNOS. Oxidative stress was verified by showing increased carbonylation of proteins. Endothelial cells exhibit a slow replication rate *in vivo* but are prone to local oxidative stress environments such as atherosclerotic plaques. Thus, endothelial cells are probably more susceptible to stress-induced senescence rather than to replicative senescence [28]. Premature senescence may play a role in vascular ageing and age-related vascular diseases. In line with this, proatherogenic and proinflammatory factors like oxidized LDL or TNFα have been implicated in ageing of endothelial cells [153,154] and senescent cells were detected *in vivo* [52].

5.3 Constitutive proteasome function is impaired in replicative and premature senescence of endothelial cells

The ubiquitin proteasome system is of major importance in the degradation of oxidized and misfolded proteins [155]. Its expression is tissue specific and under developmental control. In vertebrates, the constitutive proteasome (20S) is ubiquitously expressed [90,156] while the

inducible immunoproteasome is expressed mostly in lymphoid tissues [93,157] and also in non-immune cell-types in response to oxidative and inflammatory cues. Impaired proteasome function has been reported during senescence and ageing in several tissues [96,158-161] resulting in protein aggregate formation [162-165] and tissue damage due to proteotoxic stress [96,158,159,166].

Our analysis of replicative and premature senescence in endothelial cells revealed that proteasome function, specifically chymotrypsin- and trypsin-like activities, were reduced in both types of senescence. However, while in replicative senescence a decline of activities was paralleled by reduced expression of proteasomal subunits, in premature senescence no changes in proteasome expression was seen. In replicative senescent HUVECs, a loss of the total 20S core, the β5 subunit and to a lesser extent the β2 subunit of the constitutive proteasome was observed, which is in line with previous reports in other cell types [166-168] and correlates with decline in chymotrypsin-like and trypsin-like activities. The observed decline in expression levels of β5 and β2 subunits was restricted to the cytoplasm and does apparently not involve the nuclear proteasome, an observation previously detected in human fibroblasts [169]. In this study, the nuclear proteasomal system was only marginally affected by the senescence process although a malfunction of the nuclear proteasome was detected. It remains to be elucidated, why the nuclear proteasome, which critically affects vital nuclear processes [152,170-172], is more resistant against alterations in senescence.

The question of how the expression of proteasomal subunits is downregulated during senescence also remains to be clarified. Previously, a study in fibroblasts revealed a decreased synthesis and assembly of proteasomal subunits in senescence [167], which may also occur in endothelial cells. The expression of proteasome subunits has been shown to be under the control of the redox response transcription factor NF-E2 related factor 2 (NRf2) [127,173]. Nrf2 activation either by oxidants or dietary Nrf2 inducers leads to enhanced proteasome expression and protects cells from oxidative stress [174]. For instance, dithiolethione-3-H-1,2-dithiole-3-thione (D3T) application led to upregulation of several proteasomal subunits in the liver of wild type mice while no effect was observed in livers of Nrf2 knockout mice [174,175]. Similarly, application of the dietary activator sulphoraphane promoted Nrf2 binding on the promoter of the β5 proteasome subunit gene and increased its RNA expression in wild type but not Nrf2-deficient mice [174,175]. Since it is known that Nrf2 declines during senescence [127] its input on proteasome regulation in response to oxidative

stress may decrease although it is not known whether this may affect basal expression of proteasomal subunits. Nrf2, however, is not the only transcription factor for proteasome subunits and the β5 subunit has been shown to be under transcriptional control of the JAK-STAT signalling member STAT3 [176].

The importance of declined proteolytic capacity in senescence was also demonstrated by the fact that overexpression of the β5 subunit leads to extended life span in fibroblasts *in vitro* [177], as well as to alleviation of senescence biomarkers such as SA-β-Gal and p21 [177]. β5 overexpression resulted in the upregulation of other β-type proteasome subunits in several cell types implying a common regulatory loop [167,177,178]. Future studies including conditional knockout mice are expected to strengthen the causal relationship between proteolytic decline and senescence/ageing.

During replicative senescence loss of specific subunit is definitely the major factor for the loss in proteasome activity but this does not exclude other factors. Proteasome modifications such as carbonylation, glutathionylation, glycation and modifications with lipid peroxidation products may directly modulate proteasome activity [155,179]. It is still not clear at what level and through which detailed mechanisms these modifications act, but it seems that the 26S proteasome is more susceptible to oxidants than the 20S proteasome [180-182]. In addition, lipofuscin, the "age-pigment", which was also detected in replicative senescent endothelial cells in our study, does not only reflect a possible failure of the protein degradation machineries, but may also reduce proteasomal activities. Recent studies claim that the hydrophobicity of lipofuscin promotes its ability to occlude proteasome entry sites [112], thus operating in a cycle to aggravate ageing phenotypes.

Our data suggest that the decline of proteasomal activities in cells undergoing premature senescence in response to chronic H_2O_2 may be due to oxidative protein modifications. We observed inhibition of two major catalytic activities, the trypsin-like and chymotrypsin-like activities, while the expression of the respective catalytic subunits remained unchanged. In contrast, caspase-like activity was not altered [183]. Why the various subunit activities are differentially inhibited by oxidation, is not fully understood, but it may be attributed to the differential susceptibility to oxidisable moieties of the subunits [179,184-186]. Contrary to our observation, short exposure to H_2O_2 was shown to increase expression of proteasome and immunoproteasome subunits and to enhance proteasomal activity by activation of the transcription factor Nrf2 [173]. In this study, however, one hour of oxidant incubation was

used while we applied H_2O_2 for 8 days. However, when we added sub-lethal concentrations of H_2O_2 to endothelial cells for 30 min, we detected an increase of ubiquitinylated proteins suggesting that even at shorter incubation times the proteasome activity was inhibited. Our findings obtained after long-term exposure to oxidative stress are in accordance with a report from Thomas *et al.* [187]. These authors showed that low levels of H_2O_2 induce NO-dependent proteasome activity in endothelial cells while higher concentrations of H_2O_2 lead to decreased proteasome activity and accumulation of modified proteins.

The fact that Nrf2 inducers trigger proteasome expression also in senescent cells [127] opens a new direction to manipulation of senescent phenotypes. In general, pharmacological approaches to activate the proteasome would be an attractive strategy to delay cellular senescence. So far, drug-like small molecules that can activate or enhance proteasome activity are rare and are not well studied. An exception are oleuropein and betulinic acid that can activate the proteasome at low micromolar concentrations. Oleuropein is a natural product isolated from *Olea europaea* [188], which acts most likely through structural changes of the 20S-gated channel conformation. It was shown to enhance all three proteasome activities and delay replicative senescence of human embryonic fibroblasts. Accordingly, we observed a moderately elevated chymotrypsin-like activity in both, replicative senescent HUVEC and endothelial cells prepared from aged mice after an acute treatment with oleuropein. These are preliminary data, which need to be statistically confirmed. They let us suggest, however, that chronic administration of oleuropein starting at an earlier stage may delay the onset and progression of senescence and may have beneficial effects on the overall vascular function. In line with this, Micucci *et al.* investigated the antioxidant and cytoprotective effects of oleuropein in cultured primary vascular endothelial cells (HUVECs) and found that it reduced intracellular ROS formation and improved cell viability following oxidative stress in a dose-dependent manner [189].

5.4 Immunoproteasome expression in endothelial senescence

Our data show an upregulation of the immunoproteasome subunit LMP2 in replicative senescent HUVECs and in MLECs obtained from aged mice. In contrast, no changes in LMP2 or LMP7 expression were seen during premature senescence of HUVECs. The increased LMP2 expression in senescent endothelial cells was not associated with a decrease of caspase-like activity as it has been reported in the previous studies [190]. In line with our

results, Meiners *et al.* reported a similar increase in LMP2 expression in whole lung tissues from old mice free from immune infiltration by macrophages [191]. The gene coding for LMP2 is under the control of the transcription factors STAT1 and IRF-1 [160,192], which are mediators of growth signals as well as of signals of infection and inflammation. While immune cells constitutively express immunoproteasomes, an age-related increase in immunoproteasome subunits has been recorded in brain [193] and muscle [194] tissue, mostly reflecting a state of inflammation and cellular stress during ageing. Particularly in endothelial cells, an upregulation of LMP2 is considered to be a defense mechanism, being induced by nitric oxide (NO) via a cGMP/cAMP-mediated mechanism [97]. The NO-dependent upregulation of immunoproteasome protects endothelial cells from transferrin iron-induced oxidative stress by regulating the level of the transferrin receptor [195]. While NO is crucial for vasodilation, NO-induced changes in the relative activities of constitutive and immunoproteasome might also contribute to pathological consequences such as in autoimmune disorders [196]. Alternatively, LMP2 upregulation is speculated to be an undesirable outcome of autocrine inflammatory mediators belonging to the SASP which is a peculiarity of only replicative senescent cells. In contrast to our data, Stratford *et al.* demonstrated a slight downregulation of immunoproteasome expression in human fibroblast and loss of responsiveness to IFN-γ [192]. Together, increased oxidative stress during ageing and the role of immunoproteasome in the clearance of oxidized proteins and damaged proteins implies that upregulation of the immunoproteasome subunits may be a need-based cellular response for degrading oxidized proteins in senescence. While other studies [173,197] have shown that immunoproteasome expression is increased after H_2O_2 stress, we did not find a difference in the expression of LMP2 or LMP7 in premature senescent HUVECs caused by chronic treatment with H_2O_2. This discrepancy could be related to the doses of H_2O_2 as well as time of treatments and argue for a defined and tissue specific effect of immunoproteasome upon H_2O_2 stress.

5.5 Organismal ageing is associated with proteasomal decline in endothelial cells

An important part of this study was to verify the *in vitro* observations on endothelial senescence and proteolytic decline in *in vivo/ex vivo* models. To this end we prepared

endothelial cells from young (4-6 months) and old (24-26 months) mice and characterized them *ex vivo* with respect to senescence parameters and the expression and activity of the proteasome. MLECs revealed an increase in SA-β-gal-positive cells in old mice compared to cultures from young mice, which was, however, much lower (5%) than that seen in replicative or premature senescence models. This may be due to senescent cell immunoclearance *in vivo* [198,199] and/or loss of senescent cells during endothelial cell preparation. In spite of this, we recorded increased activation of the p53/p21 pathway, which is known to trigger senescence and ageing, and verified enhanced oxidative stress by an overall increase of carbonylated proteins as well as an enhanced iNOS expression. Importantly, the investigation of chronologically aged endothelial cells confirmed the decline of proteasome expression and activities observed in the *in vitro* model of replicative senescence. We found reduced expression levels of the total 20S core proteins and of β5 and β2 subunits as well as a decrease of chymotrypsin-like activity in aged cells indicating that proteolytic insufficiency may contribute to ageing of endothelial cells *in vivo*. Along this line, Minamino *et. al.,* demonstrated the presence of senescent vascular endothelial cells in atherosclerotic regions of human coronary arteries. Furthermore, they show that loss of telomere function induces endothelial dysfunction in aged arteries whereas inhibition of telomere shortening by hTERT overexpression suppresses senescence-associated dysfunction [28].

Very recently, several independent studies have investigated the benefits of selective elimination of senescent cells, both by genetic and pharmacological approaches. The latter appear to ameliorate various age-related symptoms including spine degeneration, osteoporosis and to improve cardiovascular function in old mice [200,201]. p16ink4a and p21 are by far the best markers of cellular senescence [29]. Baker *et al.* showed that naturally occurring p16Ink4a-positive cells shorten healthy lifespan of mice [202] and oppositely, their life-long clearance delays ageing-associated disorders in adipose tissue, skeletal muscle and eye [201]. Furthermore, late-life clearance attenuated progression of already established age-related disorders [201]. This concept of reducing the burden of senescence by selective ablation was extended by Zhu *et al.* They demonstrate the feasibility and efficacy of a newly discovered class of cytotoxic drugs called senolytics on alleviating symptoms of frailty in old mice by improving cardiac function, carotid vascular reactivity and exercise capacity, which in turn led to an overall extension in health span [200,203].

5.6 Transient proteasome inhibition and the role of p53 pathway in stress-induced premature senescence of young endothelial cells

In the final part of this study we asked whether the observed decline of the proteasome in replicative senescence and chronologically aged cells was causally related to senescence. Of note, in both situations an increased oxidative stress was observed and accordingly, we could show that oxidative stress led to proteasomal decline and premature senescence. We employed two different proteasome inhibitors, MG132 and bortezomib. Both reversibly inhibit the chymotrypsin-like activity of the constitutive proteasome, which was confirmed in our study. The partial inhibition of the proteasome was paralleled by accumulation of ubiquitinylated proteins and increased oxidative stress as evidenced by protein carbonylation. Drug withdrawal for one week resulted in nearly complete recovery of both proteasome activity and clearance of ubiquitinated proteins. However, signatures of oxidative modification of proteins, i.e. protein carbonyls were detectable even after the recovery period. In addition, a senescent phenotype developed, which was verified by an enhanced proportion of SA-β-gal-positive cells and by an activation of the p53/p21 pathway. Thus, these data suggest a causal link between proteasomal decline and the acquirement of a senescent phenotype.

Our data are consistent with a previous report by Chondriogiani *et. al.*, [204, 167] have shown the development of senescence in primary fibroblasts after irreversible inhibition of the proteasome by epoxomicin. In their study, however, an inhibition of the proteasome was maintained during the whole observation period. The mechanisms underlying premature senescence induced by proteasome inhibition may be manifold. Proteasome inhibition enhances not only protein but also DNA and RNA oxidation [205], alters mitochondrial homeostasis and turnover [206] and leads to increased endoplasmic reticulum stress [207]. In addition, the degradation of key signaling molecules is partially and temporarily restricted and this may result in cell cycle deregulation and other cellular effects. Chondrogianni *et al.* found that premature senescence induced by proteasome inhibitors was dependent on a functional p53 [204] while oxidative stress may influence the late outcome.

p53 is an established player in cellular DNA damage response and plays a key role in cellular senescence [208]. It has been proposed that telomere attrition leads to the activation of the DNA damage response pathway followed by p53-dependent cell cycle arrest and replicative

senescence [209]. The role of p53 in senescence is further supported by the several lines of observations in human diploid fibroblasts (HDFs), the most commonly used cellular model to study *in vitro* ageing. Firstly, functional p53 inactivation rescues cells from senescence arrest. Secondly, the $p21^{Cip1/waf1}$ gene encoding the cyclin-dependent kinase inhibitor p21 is transcriptionally controlled by p53 and overexpressed in senescent cells. Third, γ-irradiation of human diploid fibroblasts resulted in a prolonged p53-dependent G1 cell cycle arrest reminiscent of senescence, and fourth, DNA binding and transcriptional p53 activities markedly increase with cellular age [208]. It has also been shown that oxidative stress-mediated p53 activation protects cells from proteotoxic stress [210].

Little is known about how cellular ageing affects the ability of cells to respond to genetic insult. Senescent fibroblasts are known to be resistant to diverse apoptotic stimuli [211,212], and instead undergo a delayed, necrotic mode of cell death in response to cellular damage [208]. This apoptosis resistance has been attributed in part to the inability of senescent cells to stabilize p53 following DNA damage and also due to specific, senescence-associated post-translational p53 modifications [208,213]. Interestingly, exogenous overexpression, or accumulation and stabilization of p53 with proteasome inhibitors in old fibroblasts restored their ability to undergo apoptosis [208].

Although p53 has been linked to premature senescence after proteasome inhibition, a mechanistic link as to how p53 is activated under these conditions remained elusive. We demonstrate in endothelial cells, the accumulation of DNA strand breaks following acute/partial proteasome inhibition, and suggest that this is likely an indirect phenomenon, due to exhaustion of intracellular free ubiquitin pools translating into DNA repair deficiencies. More precisely, we have observed an elevated level of DNA damage (20%) by flow cytometric measurement of Ser139-phosphorylated Histone H2A variant X (γH2AX) following acute (10nM - 20nM, for 48h) bortezomib treatment. Ubiquitinated histone H_2A is known to play a major role in DNA damage and transcriptional responses by way of chromatin modifications. The observed DNA damage upon proteasome inhibition may be an indirect manifestation due to depletion of intracellular ubiquitin pools (proteasome inhibition and poor ubiquitin recycling) and diminished Ub-H_2A levels, translating into double strand break repair deficiencies. It is conceivable that upstream DNA damage response signalling converges at the level of p53.

At this stage it is clear that proteasome inhibition by bortezomib leads to manifestation of

DNA strand breaks that contribute to the p53-mediated cell cycle arrest. Based on our findings, we propose that p53 stabilisation by upstream DNA damage signalling due to proteasome inhibitor-induced DNA damage may represent a novel, additional link to establishment of p53-mediated stress-induced endothelial senescence.

6 Conclusions

Data obtained in this study reveal a central role of ubiquitin proteasome system in maintaining endothelial function and show its dysregulation during ageing and senescence

1. We have established several models to investigate replicative and premature endothelial cell senescence *in vitro*. We show that continuously passaged HUVECs develop features of senescence and dysfunction after about 15-17 cumulative population doublings and that premature senescence occurs after chronic oxidative stress. Endothelial cells isolated from old mice confirmed senescence *in vivo*.
2. We show that a decline of the proteasomal system is associated with both, stress-induced and replicative senescence. We show for the first time that replicative senescence in endothelial cells *in vitro* as well as chronological ageing *in vivo* is characterized by selective loss of the proteasome subunits β2 and β5 and a subsequent inhibition of the trypsin-like and chymotrypsin-like activities.
3. We demonstrate that proteasome inhibition is causally linked to endothelial senescence. Proteasomal decline leads to manifestation of DNA damage, which is at least in part responsible for the long-term cell cycle arrest in senescence development mediated by p53.
4. We have obtained preliminary data showing that oleuropein, a phenolic olive oil extract, was able to enhance proteasome activity in young and senescent endothelial cells.

In summary, these findings underlie the necessity to maintain proteostasis to extend cellular health span and opens avenues for preventing cardiovascular senescence and ageing by compensating for the loss proteasome expression/activity.

7 Acknowledgements

I am very grateful to my supervisor Prof. Dr. Regine Heller for her continuous support throughout the years of my PhD. Your discussions, ideas, and feedback have been absolutely invaluable. Thank you for selecting me through the Summer School of Molecular Medicine and for guiding my path and leading me through the discipline of vascular biology. You catalysed my motivation and desire for science.

I would like to thank Prof. Dr. Tilman Grune for his support and for offering his scientific expertise.

Furthermore I would like to thank the DAAD for offering me a three years scholarship for continuing my PhD studies.

I would like to thank all members of the research group of Prof. Dr. Regine Heller and all members at the Institute of Molecular Biomedicine for sharing their experience, offering a friendly working environment and giving me a wonderful time in Jena.

Special thanks go to all my friends in Jena and Albania. I feel blessed that I have you in my life. I owe you so much!

Thank you mom and dad for all you have sacrificed and done for all the years of my education. Thank you Anisa for your support and love and keeping me a motivated sister. Thank you Indrit for your enormous support, encouragement and believing in me. For me you all are the salt of the earth and undoubtedly I could not have done this without you.

8 References

1 Epstein, R. J. *Biomolecular evolution*. 21-22 (Cambridge University Press, 2003).

2 Sharan, R. *et al.* Conserved patterns of protein interaction in multiple species. *Proc Natl Acad Sci U S A* **102**, 1974-1979, doi:10.1073/pnas.0409522102 (2005).

3 Vijg, J. & Suh, Y. Genome instability and aging. *Annu Rev Physiol* **75**, 645-668, doi:10.1146/annurev-physiol-030212-183715 (2013).

4 Khalyavkin, A. V. & Krutko, V. N. Aging is a simple deprivation syndrome driven by a quasi-programmed preventable and reversible drift of control system set points due to inappropriate organism-environment interaction. *Biochemistry (Mosc)* **79**, 1133-1135, doi:10.1134/S0006297914100150 (2014).

5 Cleaver, O. & Melton, D. A. Endothelial signaling during development. *Nat Med* **9**, 661 - 668 (2003).

6 Tennant, M. & McGeachie, J. K. BLOOD VESSEL STRUCTURE AND FUNCTION: A BRIEF UPDATE ON RECENT ADVANCES. *Australian and New Zealand Journal of Surgery* **60**, 747-753, doi:10.1111/j.1445-2197.1990.tb07468.x (1990).

7 Subbotin, V. M. Neovascularization of coronary tunica intima (DIT) is the cause of coronary atherosclerosis. Lipoproteins invade coronary intima via neovascularization from adventitial vasa vasorum, but not from the arterial lumen: a hypothesis. *Theoretical Biology and Medical Modelling* **9**, 1-22, doi:10.1186/1742-4682-9-11 (2012).

8 van Hinsbergh, V. W. Endothelium--role in regulation of coagulation and inflammation. *Semin Immunopathol* **34**, 93-106, doi:10.1007/s00281-011-0285-5 (2012).

9 Bonetti, P. O. Endothelial Dysfunction: A Marker of Atherosclerotic Risk. *Arteriosclerosis, Thrombosis, and Vascular Biology* **23**, 168-175, doi:10.1161/01.atv.0000051384.43104.fc (2002).

10 Garlanda, C. & Dejana, E. Heterogeneity of Endothelial Cells: Specific Markers. *Arteriosclerosis, Thrombosis, and Vascular Biology* **17**, 1193-1202, doi:10.1161/01.atv.17.7.1193 (1997).

11 Seals, D. R., Jablonski, K. L. & Donato, A. J. Aging and vascular endothelial function in humans. *Clin Sci (Lond)* **120**, 357-375, doi:10.1042/CS20100476 (2011).

12 Ungvari, Z., Kaley, G., de Cabo, R., Sonntag, W. E. & Csiszar, A. Mechanisms of vascular aging: new perspectives. *J Gerontol A Biol Sci Med Sci* **65**, 1028-1041, doi:10.1093/gerona/glq113 (2010).

13 Tosato, M., Zamboni, V., Ferrini, A. & Cesari, M. The aging process and potential interventions to extend life expectancy. *Clinical Interventions in Aging* **2**, 401–412 (2007).

14 Becker, T. & Haferkamp, S. Molecular Mechanisms of Cellular Senescence. doi:10.5772/54120 (2013).

15 Storer, M. *et al.* Senescence is a developmental mechanism that contributes to embryonic growth and patterning. *Cell* **155**, 1119-1130, doi:10.1016/j.cell.2013.10.041 (2013).

16 Perez-Garijo, A. & Steller, H. The benefits of aging: cellular senescence in normal development. *EMBO J* **33**, 99-100, doi:10.1002/embj.201387401 (2014).

17 Santulli, G. Epidemiology of Cardiovascular Disease in the 21st Century: Updated Numbers and Updated Facts. *JOURNAL OF CARDIOVASCULAR DISEASE* **1**, (2013).

18 Hayflick, L. The limited in vitro lifetime of human diploid cell strains. . *Experimental Cell Research* **37**, 614 - 636 (1965).

19 Burton, D. G. Cellular senescence, ageing and disease. *Age (Dordr)* **31**, 1-9, doi:10.1007/s11357-008-9075-y (2009).

20 Chan, R. S. & Woo, J. Prevention of overweight and obesity: how effective is the current public health approach. *Int J Environ Res Public Health* **7**, 765-783, doi:10.3390/ijerph7030765 (2010).

21 Campisi, J. Aging, cellular senescence, and cancer. *Annu Rev Physiol* **75**, 685-705, doi:10.1146/annurev-physiol-030212-183653 (2013).

22 Campisi, J. & d'Adda di Fagagna, F. Cellular senescence: when bad things happen to good cells. *Nat Rev Mol Cell Biol* **8**, 729-740, doi:10.1038/nrm2233 (2007).

23 Sedelnikova, O. A. *et al.* Senescing human cells and ageing mice accumulate DNA lesions with unrepairable double-strand breaks. *Nat Cell Biol* **6**, 168-170, doi:10.1038/ncb1095 (2004).

24 Nakamura, A. J. *et al.* Both telomeric and non-telomeric DNA damage are determinants of mammalian cellular senescence. *Epigenetics Chromatin* **1**, 6, doi:10.1186/1756-8935-1-6 (2008).

25 Schmitt, E., Paquet, C., Beauchemin, M. & Bertrand, R. DNA-damage response network at the crossroads of cell-cycle checkpoints, cellular senescence and apoptosis. *J Zhejiang Univ Sci B* **8**, 377-397, doi:10.1631/jzus.2007.B0377 (2007).

26 Sulli, G., Di Micco, R. & d'Adda di Fagagna, F. Crosstalk between chromatin state and DNA damage response in cellular senescence and cancer. *Nat Rev Cancer* **12**, 709-720, doi:10.1038/nrc3344 (2012).

27 Minamino, T. & Komuro, I. Vascular cell senescence: contribution to atherosclerosis. *Circ Res* **100**, 15-26, doi:10.1161/01.RES.0000256837.40544.4a (2007).

28 Minamino, T. Endothelial Cell Senescence in Human Atherosclerosis: Role of Telomere in Endothelial Dysfunction. *Circulation* **105**, 1541-1544, doi:10.1161/01.cir.0000013836.85741.17 (2002).

29 Kuilman, T., Michaloglou, C., Mooi, W. J. & Peeper, D. S. The essence of senescence. *Genes Dev* **24**, 2463-2479, doi:10.1101/gad.1971610 (2010).

30 Yaswen, P. & Stampfer, M. R. Molecular changes accompanying senescence and immortalization of cultured human mammary epithelial cells. *The International Journal of Biochemistry & Cell Biology* **34**, 1382–1394 (2002).

31 Parrinello, S. *et al.* Oxygen sensitivity severely limits the replicative lifespan of murine fibroblasts. *NATURE CELL BIOLOGY* **5** (2003).

32 Liu, C., La Rosa, S. & Hagos, E. G. Oxidative DNA damage causes premature senescence in mouse embryonic fibroblasts deficient for Kruppel-like factor 4. *Mol Carcinog* **54**, 889-899, doi:10.1002/mc.22161 (2015).

33 Raghuram, G. V. & Mishra, P. K. Stress induced premature senescence : a new culprit in ovarian tumorigenesis? *The Indian Journal of Medical Research* **140**, S120-S129 (2014).

34 Suzuki, M. & Boothman, D. A. Stress-induced Premature Senescence (SIPS). *Journal of Radiation Research* **49**, 105-112, doi:10.1269/jrr.07081 (2008).

35 Grune, T., Shringarpure, R., Sitte, N. & Davies, K. Age-Related Changes in Protein Oxidation and Proteolysis in Mammalian Cells. *Journal of Gerontology: BIOLOGICAL SCIENCES* **56A**, B459–B467 (2001).

36 Reeg, S. & Grune, T. Protein Oxidation in Aging: Does It Play a Role in Aging Progression? *Antioxid Redox Signal* **23**, 239-255, doi:10.1089/ars.2014.6062 (2015).

37 Farhat, N. *et al.* Stress-induced senescence predominates in endothelial cells isolated from atherosclerotic chronic smokers. *Can J Physiol Pharmacol* **86**, 761-769, doi:10.1139/Y08-082 (2008).

38 Coleman, P. R. *et al.* Age-associated stresses induce an anti-inflammatory senescent phenotype in endothelial cells. *AGING,* **5**, 913-924 (2013).

39 Maeda, M., Hayashi, T., Mizuno, N., Hattori, Y. & Kuzuya, M. Intermittent high glucose implements stress-induced senescence in human vascular endothelial cells: role of superoxide production by NADPH oxidase. *PLoS One* **10**, e0123169, doi:10.1371/journal.pone.0123169 (2015).

40 Nilsson, P. M. Early vascular aging (EVA): consequences and prevention. *Vascular Health and Risk Management* **4**, 547-552 (2008).

41 Matsui-Hirai, H. *et al.* Dose-dependent modulatory effects of insulin on glucose-induced endothelial senescence in vitro and in vivo: a relationship between telomeres and nitric oxide. *J Pharmacol Exp Ther* **337**, 591-599, doi:10.1124/jpet.110.177584 (2011).

42 Balasubramanyam, M., Adaikalakoteswari, A., Finny Monickaraj, S. & V., M. Telomere shortening & metabolic/vascular diseases. *Indian J Med Res* **125**, pp 441-450 (2007).

43 Tominaga, K. The emerging role of senescent cells in tissue homeostasis and pathophysiology. *Pathobiol Aging Age Relat Dis* **5**, 27743, doi:10.3402/pba.v5.27743 (2015).

44 Gerardo, F. Barriers to Ras transformation. *NATURE CELL BIOLOGY* **9**, 483-485 (2007).

45 Turrens, J. F. Mitochondrial formation of reactive oxygen species. *J Physiol* **552**, 335-344, doi:10.1113/jphysiol.2003.049478 (2003).

46 Aldebasi, Y. H., Rahmani, Arshad H., Khan, A. A. & Salah, M. A. The effect of vascular endothelial growth factor in the progression of bladder cancer and diabetic retinopathy. *Int J Clin Exp Med* **6**, :239-251 (2013).

47 Passos, J. F., Saretzki, G. & von Zglinicki, T. DNA damage in telomeres and mitochondria during cellular senescence: is there a connection? *Nucleic Acids Res* **35**, 7505-7513, doi:10.1093/nar/gkm893 (2007).

48 Ben-Porath, I. & Weinberg, R. A. The signals and pathways activating cellular senescence. *Int J Biochem Cell Biol* **37**, 961-976, doi:10.1016/j.biocel.2004.10.013 (2005).

49 Xua, D., Richard Nevilleb, R. & Finkela, T. Homocysteine accelerates endothelial cell senescence. *FEBS Letters* **470**, 20-24 (2000).

50 Erusalimsky, J. D. & Skene, C. Mechanisms of endothelial senescence. *Exp Physiol* **94**, 299-304, doi:10.1113/expphysiol.2008.043133 (2008).

51 Furumoto, K., Inoue, E., Nagao, N., Hiyama, E. & Miwa, N. Molecular changes accompanying senescence and immortalization of cultured human mammary epithelial cells. *Life Sciences* **63**, 935448,931998 (1998).

52 Erusalimsky, J. D. Vascular endothelial senescence: from mechanisms to pathophysiology. *J Appl Physiol (1985)* **106**, 326-332, doi:10.1152/japplphysiol.91353.2008 (2009).

53 Bhattacharyya, A., Chattopadhyay, R., Mitra, S. & Crowe, S. E. Oxidative stress: an essential factor in the pathogenesis of gastrointestinal mucosal diseases. *Physiol Rev* **94**, 329-354, doi:10.1152/physrev.00040.2012 (2014).

54 Szabo, C., Ischiropoulos, H. & Radi, R. Peroxynitrite: biochemistry, pathophysiology and development of therapeutics. *Nat Rev Drug Discov* **6**, 662-680, doi:10.1038/nrd2222 (2007).

55 Calado, R. T. & Dumitriu, B. Telomere dynamics in mice and humans. *Semin Hematol* **50**, 165-174, doi:10.1053/j.seminhematol.2013.03.030 (2013).

56 Perez-Rivero, G. *et al.* Mice deficient in telomerase activity develop hypertension because of an excess of endothelin production. *Circulation* **114**, 309-317, doi:10.1161/CIRCULATIONAHA.105.611111 (2006).

57 Perez-Rivero, G. *et al.* Telomerase deficiency promotes oxidative stress by reducing catalase activity. *Free Radic Biol Med* **45**, 1243-1251, doi:10.1016/j.freeradbiomed.2008.07.017 (2008).

58 Napier, C. E. *et al.* Mild hyperoxia limits hTR levels, telomerase activity, and telomere length maintenance in hTERT-transduced bone marrow endothelial cells. *Biochim Biophys Acta* **1803**, 1142-1153, doi:10.1016/j.bbamcr.2010.06.010 (2010).

59 Vasa, M., Breitschopf, K., Zeiher, A. M. & Dimmeler, S. Nitric oxide activates telomerase and delays endothelial cell senescence. *Circ Res.* **87** (2000).

60 Liang, F.-Q. & Godley, B. F. Oxidative stress-induced mitochondrial DNA damage in human retinal pigment epithelial cells: a possible mechanism for RPE aging and age-related macular degeneration. *Experimental Eye Research* **76**, 397-403, doi:10.1016/s0014-4835(03)00023-x (2003).

61 Dromparis, P. & Michelakis, E. D. Mitochondria in vascular health and disease. *Annu Rev Physiol* **75**, 95-126, doi:10.1146/annurev-physiol-030212-183804 (2013).

62 Kluge, M. A., Fetterman, J. L. & Vita, J. A. Mitochondria and endothelial function. *Circ Res* **112**, 1171-1188, doi:10.1161/CIRCRESAHA.111.300233 (2013).

63 Ziegler, D. V., Wiley, C. D. & Velarde, M. C. Mitochondrial effectors of cellular senescence: beyond the free radical theory of aging. *Aging Cell* **14**, 1-7 (2015).

64 Miyauchi, H. *et al.* Akt negatively regulates the in vitro lifespan of human endothelial cells via a p53/p21-dependent pathway. *The EMBO Journal* **23**, 212–220, doi:10.1038/ (2004).

65 Spyridopoulos, I., Isner, J. M. & Losordo, D. W. Oncogenic ras induces premature senescence in endothelial cells: role of p21Cip1/Waf1. *Basic Res Cardiol* **97**.

66 Deshpande, S. S. Constitutive Activation of rac1 Results in Mitochondrial Oxidative Stress and Induces Premature Endothelial Cell Senescence. *Arteriosclerosis, Thrombosis, and Vascular Biology* **23**, 1e-6, doi:10.1161/01.atv.0000047869.13737.53 (2002).

67 Serrano, M. *et al.* Oncogenic ras Provokes Premature Cell Senescence Associated with Accumulation of p53 and p16INK4a. *Cell* **88**, 593-602.

68 Moiseeva, O., Bourdeau, V., Roux, A., Deschenes-Simard, X. & Ferbeyre, G. Mitochondrial dysfunction contributes to oncogene-induced senescence. *Mol Cell Biol* **29**, 4495-4507, doi:10.1128/MCB.01868-08 (2009).

69 van den Oever, I. A., Raterman, H. G., Nurmohamed, M. T. & Simsek, S. Endothelial dysfunction, inflammation, and apoptosis in diabetes mellitus. *Mediators Inflamm* **2010**, 792393, doi:10.1155/2010/792393 (2010).

70 Correia-Melo, C. *et al.* Mitochondria are required for pro-ageing features of the senescent phenotype. *EMBO J* **35**, 724-742, doi:10.15252/embj.201592862 (2016).

71 Passos, J. F. *et al.* Mitochondrial dysfunction accounts for the stochastic heterogeneity in telomere-dependent senescence. *PLoS Biol* **5**, e110, doi:10.1371/journal.pbio.0050110 (2007).

72 Wolff, S., Weissman, J. S. & Dillin, A. Differential scales of protein quality control. *Cell* **157**, 52-64, doi:10.1016/j.cell.2014.03.007 (2014).

73 Cuanalo-Contreras, K., Mukherjee, A. & Soto, C. Role of protein misfolding and proteostasis deficiency in protein misfolding diseases and aging. *Int J Cell Biol* **2013**, 638083, doi:10.1155/2013/638083 (2013).

74 Vendruscolo, M., Knowles, T. P. & Dobson, C. M. Protein solubility and protein homeostasis: a generic view of protein misfolding disorders. *Cold Spring Harb Perspect Biol* **3**, doi:10.1101/cshperspect.a010454 (2011).

75 Lilienbaum, A. Relationship between the proteasomal system and autophagy. *Int J Biochem Mol Biol* 2152-4114 (2013).

76 Wójcik, C. & DeMartino, G. N. Intracellular localization of proteasomes. *The International Journal of Biochemistry & Cell Biology* **35**, 579-589, doi:10.1016/s1357-2725(02)00380-1 (2003).

77 Wojcik, C. & Di Napoli, M. Ubiquitin-proteasome system and proteasome inhibition: new strategies in stroke therapy. *Stroke* **35**, 1506-1518, doi:10.1161/01.STR.0000126891.93919.4e (2004).

78 Pickering, A. M. *et al.* The immunoproteasome, the 20S proteasome and the PA28alphabeta proteasome regulator are oxidative-stress-adaptive proteolytic complexes. *Biochem J* **432**, 585-594, doi:10.1042/BJ20100878 (2010).

79 Goldberg, A. L. Protein degradation and protection against misfolded or damaged proteins. *Nature* **426**, 895-899 (2003).

80 Myung, J., Kim, K. B. & Crews, C. M. The Ubiquitin-Proteasome Pathway and Proteasome Inhibitors. *Med Res Rev* **21**, 245-273 (2008).

81 Murata, S., Yashiroda, H. & Tanaka, K. Molecular mechanisms of proteasome assembly. *Nat Rev Mol Cell Biol* **10**, 104-115, doi:10.1038/nrm2630 (2009).

82 Groll, M., Berkers, C. R., Ploegh, H. L. & Ovaa, H. Crystal structure of the boronic acid-based proteasome inhibitor bortezomib in complex with the yeast 20S proteasome. *Structure* **14**, 451-456, doi:10.1016/j.str.2005.11.019 (2006).

83 Davies, K. J. A. Degradation of oxidized proteins by the 20S proteasome. *Biochimie* **83**, 301-310 (2001).

84 Jung, T., Hohn, A. & Grune, T. The proteasome and the degradation of oxidized proteins: Part II - protein oxidation and proteasomal degradation. *Redox Biol* **2C**, 99-104, doi:10.1016/j.redox.2013.12.008 (2013).

85 Saeki, Y., Toh, E. A., Kudo, T., Kawamura, H. & Tanaka, K. Multiple proteasome-interacting proteins assist the assembly of the yeast 19S regulatory particle. *Cell* **137**, 900-913, doi:10.1016/j.cell.2009.05.005 (2009).

86 Isono, E. *et al.* The assembly pathway of the 19S regulatory particle of the yeast 26S proteasome. *Mol Biol Cell* **18**, 569-580, doi:10.1091/mbc.E06-07-0635 (2007).

87 Bar-Nun, S. & Glickman, M. H. Proteasomal AAA-ATPases: structure and function. *Biochim Biophys Acta* **1823**, 67-82, doi:10.1016/j.bbamcr.2011.07.009 (2012).

88 Finley, D. Recognition and processing of ubiquitin-protein conjugates by the proteasome. *Annu Rev Biochem* **78**, 477-513, doi:10.1146/annurev.biochem.78.081507.101607 (2009).

89 Ben-Nissan, G. & Sharon, M. Regulating the 20S proteasome ubiquitin-independent degradation pathway. *Biomolecules* **4**, 862-884, doi:10.3390/biom4030862 (2014).

90 Ciechanover, A. & Schwartz, A. L. The ubiquitin-proteasome pathway: The complexity and myriad functions of proteins death. *Proc. Natl. Acad. Sci. USA* **95**, 2727–2730 (1998).

91 Walden, H., Podgorski, M. S. & Schulman, B. A. Insights into the ubiquitin transfer cascade from the structure of the activating enzyme for NEDD8. *NATURE* **422** (2003).

92 Cascio, P., Call, M., M.Petre, B., Walz, T. & Goldberg, A. L. Properties of te hybrid from of the 26S proteasome containing both 19S and PA28 complexes. *The EMBO Journal* **21**, 26636-22645 (2002).

93 Sijts, E. J. & Kloetzel, P. M. The role of the proteasome in the generation of MHC class I ligands and immune responses. *Cell Mol Life Sci* **68**, 1491-1502, doi:10.1007/s00018-011-0657-y (2011).

94 Ferrington, D. A. & Gregerson, D. S. Immunoproteasomes: structure, function, and antigen presentation. *Prog Mol Biol Transl Sci* **109**, 75-112, doi:10.1016/B978-0-12-397863-9.00003-1 (2012).

95 Jang, E. R. *et al.* Revisiting the role of the immunoproteasome in the activation of the canonical NF-kappaB pathway. *Mol Biosyst* **8**, 2295-2302, doi:10.1039/c2mb25125f (2012).

96 Friguet, B. Oxidized protein degradation and repair in ageing and oxidative stress. *FEBS Lett* **580**, 2910-2916, doi:10.1016/j.febslet.2006.03.028 (2006).

97 Kotamraju, S. *et al.* Upregulation of immunoproteasomes by nitric oxide: potential antioxidative mechanism in endothelial cells. *Free Radic Biol Med* **40**, 1034-1044, doi:10.1016/j.freeradbiomed.2005.10.052 (2006).

98 Kalogeris, T., Bao, Y. & Korthuis, R. J. Mitochondrial reactive oxygen species: a double edged sword in ischemia/reperfusion vs preconditioning. *Redox Biol* **2**, 702-714, doi:10.1016/j.redox.2014.05.006 (2014).

99 Rahman, T., Hosen, I., Islam, M. M. T. & Shekhar, H. U. Oxidative stress and human health. *Advances in Bioscience and Biotechnology* **03**, 997-1019, doi:10.4236/abb.2012.327123 (2012).

100 Berlett, B. S. & Stadtman, E. R. Protein Oxidation in Aging, Disease, and Oxidative Stress*. *THE JOURNAL OF BIOLOGICAL CHEMISTRY* **272**, 20313–20316 (1997).

101 STADTMAN, E. R. & LEVINE, R. L. Protein Oxidation. *ANNALS NEW YORK ACADEMY OF SCIENCES* **899**, 899:191-208; (2000).

102 Madian, A. G. & Regnier, F. E. Proteomic identification of carbonylated proteins and their oxidation sites. *J Proteome Res* **9**, 3766-3780, doi:10.1021/pr1002609 (2010).

103 PACHER, P., BECKMAN, J. S. & LIAUDET, L. Nitric Oxide and Peroxynitrite in Health and Disease. *Physiol Rev.* (2008).

104 Pastore, A. & Temussi, P. Protein aggregation and misfolding: good or evil? *J Phys Condens Matter* **24**, 244101, doi:10.1088/0953-8984/24/24/244101 (2012).

105 Chaudhuri, T. K. & Paul, S. Protein-misfolding diseases and chaperone-based therapeutic approaches. *FEBS J* **273**, 1331-1349, doi:10.1111/j.1742-4658.2006.05181.x (2006).

106 Trachootham, D., Lu, W., Ogasawara, M. A., Nilsa, R. D. & Huang, P. Redox regulation of cell survival. *Antioxid Redox Signal* **10**, 1343-1374, doi:10.1089/ars.2007.1957 (2008).

107 Jung, T., Bader, N. & Grune, T. Lipofuscin: formation, distribution, and metabolic consequences. *Ann N Y Acad Sci* **1119**, 97-111, doi:10.1196/annals.1404.008 (2007).

108 Terman, A., Gustafsson, B. & Brunk, U. T. Autophagy, organelles and ageing. *J Pathol* **211**, 134-143, doi:10.1002/path.2094 (2007).

109 Friguet, B. & Szweda, L. I. Inhibition of the multicatalytic proteinase (proteasome) by 4-hydroxy-2-nonenal cross-linked protein. *FEBS Letters* **405**, 21-25, doi:10.1016/s0014-5793(97)00148-8 (1997).

110 SITTE, N. *et al.* Proteasome inhibition by lipofuscin/ceroid during postmitotic aging of fibroblast. *The FASEB Journal* **14** (2000).

111 TERMAN, A. & BRUNK, U. T. Lipofuscin: Mechanisms of formation and increase with age. *APMIS* **106**, 265-276 (1998).

112 Hohn, A. *et al.* Lipofuscin inhibits the proteasome by binding to surface motifs. *Free Radic Biol Med* **50**, 585-591, doi:10.1016/j.freeradbiomed.2010.12.011 (2011).

113 Grune, T., Jung, T., Merker, K. & Davies, K. J. Decreased proteolysis caused by protein aggregates, inclusion bodies, plaques, lipofuscin, ceroid, and 'aggresomes' during oxidative stress, aging, and disease. *Int J Biochem Cell Biol* **36**, 2519-2530, doi:10.1016/j.biocel.2004.04.020 (2004).

114 Chondrogianni, N. & Gonos, E. S. Proteasome dysfunction in mammalian aging: steps and factors involved. *Exp Gerontol* **40**, 931-938, doi:10.1016/j.exger.2005.09.004 (2005).

115 Bulteau, A. L., Szweda, L. I. & Friguet, B. Mitochondrial protein oxidation and degradation in response to oxidative stress and aging. *Exp Gerontol* **41**, 653-657, doi:10.1016/j.exger.2006.03.013 (2006).

116 Elleder, M., Sokolová, J. & Hřebíček, M. Follow-up study of subunit c of mitochondrial ATP synthase (SCMAS) in Batten disease and in unrelated lysosomal disorders. *Acta Neuropathologica* **93**, 379-390, doi:10.1007/s004010050629 (1997).

117 Stangl, K. & Stangl, V. The ubiquitin-proteasome pathway and endothelial (dys)function. *Cardiovasc Res* **85**, 281-290, doi:10.1093/cvr/cvp315 (2010).

118 Muratani, M. & Tansey, W. P. How the ubiquitin-proteasome system controls transcription. *Nat Rev Mol Cell Biol* **4**, 192-201, doi:10.1038/nrm1049 (2003).

119 Voorhees, P. M. & Orlowski, R. Z. The proteasome and proteasome inhibitors in cancer therapy. *Annu Rev Pharmacol Toxicol* **46**, 189-213, doi:10.1146/annurev.pharmtox.46.120604.141300 (2006).

120 Meiners, S. *et al.* Ubiquitin-Proteasome Pathway as a New Target for the Prevention of Restenosis. *Circulation* **105**, 483-489 (2002).

121 Elliott, P. J., Zollner, T. M. & Boehncke, W. H. Proteasome inhibition: a new anti-inflammatory strategy. *J Mol Med (Berl)* **81**, 235-245, doi:10.1007/s00109-003-0422-2 (2003).

122 Lorenz, M. *et al.* Proteasome inhibition prevents experimentally-induced endothelial dysfunction. *Life Sci* **84**, 929-934, doi:10.1016/j.lfs.2009.04.016 (2009).

123 Dreger, H. *et al.* Nrf2-dependent upregulation of antioxidative enzymes: a novel pathway for proteasome inhibitor-mediated cardioprotection. *Cardiovasc Res* **83**, 354-361, doi:10.1093/cvr/cvp107 (2009).

124 Meiners, S., Ludwig, A., Stangl, V. & Stangl, K. Proteasome inhibitors: poisons and remedies. *Med Res Rev* **28**, 309-327, doi:10.1002/med.20111 (2008).

125 Singh, R. & Cuervo, A. M. Lipophagy: connecting autophagy and lipid metabolism. *Int J Cell Biol* **2012**, 282041, doi:10.1155/2012/282041 (2012).

126 McCarthy, M. K. & Weinberg, J. B. The immunoproteasome and viral infection: a complex regulator of inflammation. *Front Microbiol* **6**, 21, doi:10.3389/fmicb.2015.00021 (2015).

127 Kapeta, S., Chondrogianni, N. & Gonos, E. S. Nuclear erythroid factor 2-mediated proteasome activation delays senescence in human fibroblasts. *J Biol Chem* **285**, 8171-8184, doi:10.1074/jbc.M109.031575 (2010).

128 Tang, J., Gordon, G. M., Nickoloff, B. J. & Foreman, K. E. The Helix–Loop–Helix Protein Id-1 Delays Onset of Replicative Senescence in Human Endothelial Cells. *Laboratory Investigation* **82**, 1073-1079, doi:10.1097/01.lab.0000022223.65962.3a (2002).

129 Herbig, U., Jobling, W. A., Chen, B. P. C., Chen, D. J. & Sedivy, J. M. Telomere Shortening Triggers Senescence of Human Cells through a Pathway Involving ATM, p53, and p21CIP1 , but Not p16INK4a. *Molecular Cell, Vol. 14, 501–513, May 21, 2004, Copyright ©2004 by Cell Press* **14**, 501–513, (2004).

130 Bayreuther, K. *et al.* Human skin fibroblasts in vitro differentiate along a terminal cell lineage. *Proc. Natl. Acad. Sci. USA* **85**, 5112-5116 (1988).

131 Loayza-Puch, F. *et al.* p53 induces transcriptional and translational programs to suppress cell proliferation and growth. *Genome Biol* **14**, R32, doi:10.1186/gb-2013-14-4-r32 (2013).

132 Grune, T., Merker, K., Sandig, G. & Davies, K. J. A. Selective degradation of oxidatively modified protein substrates by the proteasome. *Biochemical and Biophysical Research Communications* **305**, 709-718, doi:10.1016/s0006-291x(03)00809-x (2003).

133 Bota, D. A. & Davies, K. J. Lon protease preferentially degrades oxidized mitochondrial aconitase by an ATP-stimulated mechanism. *Nat Cell Biol* **4**, 674-680, doi:10.1038/ncb836 (2002).

134 Nystrom, T. Role of oxidative carbonylation in protein quality control and senescence. *The EMBO Journal* **24**, 1311–1317, doi:10.1038/ (2005).

135 Kurz, D. J. *et al.* Chronic oxidative stress compromises telomere integrity and accelerates the onset of senescence in human endothelial cells. *Journal of cell Science* **117**, 2417-2426 P, doi:10.1242/jcs (2004).

136 Furumoto, K., Inoue, E., Nagao, N., Hiyama, E. & Miwa, N. AGE-DEPENDENT TELOMERE SHORTENING IS SLOWED DOWNBY ENRICHMENT OF INTRACELLULAR VITAMIN C VIA SUPPRESSION OF OXIDATIVE STRESS. *Life Sciences* **63**, 935-948 (1998).

137 Xu, D., Neville, R. & Finkel, T. Homocysteine accelerates endothelial cell senescence. *FEBS J* **470**, 20-24 (2000).

138 Tang, X., Luo, Y.-X., ChenHou-Zao. & Liu, D.-P. Mitochondria, endothelial cell function, and vascular diseases. *Frontiers in Physiology* **5**, doi:10.3389/fphys.2014.00175 (2014).

139 Zhou, S. *et al.* Repression of P66Shc expression by SIRT1 contributes to the prevention of hyperglycemia-induced endothelial dysfunction. *Circ Res* **109**, 639-648, doi:10.1161/CIRCRESAHA.111.243592 (2011).

140 Ungvari, Z. *et al.* Dysregulation of mitochondrial biogenesis in vascular endothelial and smooth muscle cells of aged rats. *Am J Physiol Heart Circ Physiol* **294**, H2121-2128, doi:10.1152/ajpheart.00012.2008 (2008).

141 Dai, D. F., Rabinovitch, P. S. & Ungvari, Z. Mitochondria and cardiovascular aging. *Circ Res* **110**, 1109-1124, doi:10.1161/CIRCRESAHA.111.246140 (2012).

142 Zhang, J., Block, E. R. & Patel, J. M. Down-regulation of mitochondrial cytochrome c oxidase in senescent porcine pulmonary artery endothelial cells *Mechanisms of Ageing and Development* **123**, 1363–1374 (2002).

143 Rogers, S. C., Zhang, X., Azhar, G., Luo, S. & Wei, J. Y. Exposure to high or low glucose levels accelerates the appearance of markers of endothelial cell senescence and induces dysregulation of nitric oxide synthase. *J Gerontol A Biol Sci Med Sci* **68**, 1469-1481, doi:10.1093/gerona/glt033 (2013).

144 Csiszar, A. Aging-Induced Phenotypic Changes and Oxidative Stress Impair Coronary Arteriolar Function. *Circulation Research* **90**, 1159-1166, doi:10.1161/01.res.0000020401.61826.ea (2002).

145 Collins, C. & Tzima, E. Hemodynamic forces in endothelial dysfunction and vascular aging. *Exp Gerontol* **46**, 185-188, doi:10.1016/j.exger.2010.09.010 (2011).

146 Katusic, Z. S. Mechanisms of endothelial dysfunction induced by aging: role of arginase I. *Circ Res* **101**, 640-641, doi:10.1161/CIRCRESAHA.107.162701 (2007).

147 Mason, E. F. & Rathmell, J. C. Cell metabolism: an essential link between cell growth and apoptosis. *Biochim Biophys Acta* **1813**, 645-654, doi:10.1016/j.bbamcr.2010.08.011 (2011).

148 Faubert, B. *et al.* AMPK is a negative regulator of the Warburg effect and suppresses tumor growth in vivo. *Cell Metab* **17**, 113-124, doi:10.1016/j.cmet.2012.12.001 (2013).

149 Herzog, R. *et al.* Senescence-Associated Changes in Proteome and O-GlcNAcylation Pattern in Human Peritoneal Mesothelial Cells. *Biomed Res Int* **2015**, 382652, doi:10.1155/2015/382652 (2015).

150 Cole, N. B. *et al.* Lipid droplet binding and oligomerization properties of the Parkinson's disease protein alpha-synuclein. *J Biol Chem* **277**, 6344-6352, doi:10.1074/jbc.M108414200 (2002).

151 Kolattukudy, P. E. & Niu, J. Inflammation, endoplasmic reticulum stress, autophagy, and the monocyte chemoattractant protein-1/CCR2 pathway. *Circ Res* **110**, 174-189, doi:10.1161/CIRCRESAHA.111.243212 (2012).

152 Keembiyehetty, C. N., Krzeslak, A., Love, D. C. & Hanover, J. A. A lipid-droplet-targeted O-GlcNAcase isoform is a key regulator of the proteasome. *Journal of Cell Science* **124**, 2851-2860, doi:10.1242/jcs (2011).

153 Zhang, H. *et al.* Role of TNF-alpha in vascular dysfunction. *Clin Sci (Lond)* **116**, 219-230, doi:10.1042/CS20080196 (2009).

154 Breitschopf, K., Zieher, A. M. & Dimmeler, S. Pro-atherogenic factors induce telomerase incativation in endothelial cells throught an Akt-dependent mechanism. *FEBS J* **493**, 21-25 (2001).

155 Hohn, T. J. & Grune, T. The proteasome and the degradation of oxidized proteins: part III-Redox regulation of the proteasomal system. *Redox Biol* **2**, 388-394, doi:10.1016/j.redox.2013.12.029 (2014).

156 Hershko, A. & Ciechanover, A. THE UBIQUITIN SYSTEM. *Annu. Rev. Biochem. 1998. 67:425–79* **67**, 425-479 (1998).

157 de Bruin, G. *et al.* A Set of Activity-Based Probes to Visualize Human (Immuno)proteasome Activities. *Angew Chem Int Ed Engl* **55**, 4199-4203, doi:10.1002/anie.201509092 (2016).

158 Keller, J. N., Hanni, K. B. & Markesbery, W. R. Possible involvement of proteasome inhibition in aging: implications for oxidative stress. *Mechanisms of Ageing and Development* **113**, 61-67 (1999).

159 Chondrogianni, N., Sakellari, M., Lefaki, M., Papaevgeniou, N. & Gonos, E. S. Proteasome activation delays aging in vitro and in vivo. *Free Radic Biol Med* **71**, 303-320, doi:10.1016/j.freeradbiomed.2014.03.031 (2014).

160 Dahlmann, B. Role of proteasomes in disease. *BMC Biochem* **8 Suppl 1**, S3, doi:10.1186/1471-2091-8-S1-S3 (2007).

161 Breusing, N. *et al.* Inverse correlation of protein oxidation and proteasome activity in liver and lung. *Mech Ageing Dev* **130**, 748-753, doi:10.1016/j.mad.2009.09.004 (2009).

162 Fonseca, D. B., Sheehy, M. R., Blackman, N., Shelton, P. M. & Prior, A. E. Reversal of a hallmark of brain ageing: lipofuscin accumulation. *Neurobiol Aging* **26**, 69-76, doi:10.1016/j.neurobiolaging.2004.02.013 (2005).

163 Terman, A., Dalen, H., Eaton, J., Neuzil, J. & Brunk, U. Aging of cardiac myocytes in culture: oxidative stress, lipofuscin accumulation, and mitochondrial turnover. *Ann N Y Acad Sci* **1019**, 70-77 (2004).

164 Krouwer, V. J. D., Hekking, L. H. P., Makkinje, M. L., Klapisz, E. R. & Post, J. A. Endothelial cell senescence is associated with disrupted cell-cell junctions and increased monolayer permeability. *Vascular Cell* **4** (2012).

165 Sitte, N., Merker, K., Grune, T. & Zglinicki, T. Lipofuscin accumulation in proliferating fibroblasts in vitro: an indicator of oxidative stress. *Experimental Gerontoiogy* **36**, 475-486 (2001).

166 Petropoulos, I. *et al.* Increase of Oxidatively Modified Protein Is Associated With a Decrease of Proteasome Activity and Content in Aging Epidermal Cells. *Journal of Gerontology: BIOLOGICAL SCIENCES* **55A**, 220-227 (2000).

167 Chondrogianni, N. *et al.* Central role of the proteasome in senescence and survival of human fibroblasts: induction of a senescence-like phenotype upon its inhibition and resistance to stress upon its activation. *J Biol Chem* **278**, 28026-28037, doi:10.1074/jbc.M301048200 (2003).

168 Bulteau, A. L., Szweda, L. I. & Friguet, B. Age-dependent declines in proteasome activity in the heart. *Arch Biochem Biophys* **397**, 298-304, doi:10.1006/abbi.2001.2663 (2002).

169 Merker, K., Ullrich, O., Schmidt, H., Sitte, N. & Grune, T. Stability of the nuclear protein turnover during cellular senescence of human fibroblasts. *The FASEB Journal* (2003).

170 Enenkel, C. Nuclear transport of yeast proteasomes. *Biomolecules* **4**, 940-955, doi:10.3390/biom4040940 (2014).

171 Burcoglu, J., Zhao, L. & Enenkel, C. Nuclear Import of Yeast Proteasomes. *Cells* **4**, 387-405, doi:10.3390/cells4030387 (2015).

172 Mikecz, A., Chen, M., Rockel, T. & Scharf, A. in *The Nucleus: Volume 1: Nuclei and Subnuclear Components* (ed Ronald Hancock) 191-202 (Humana Press, 2008).

173 Pickering, A. M., Linder, R. A., Zhang, H., Forman, H. J. & Davies, K. J. Nrf2-dependent induction of proteasome and Pa28alphabeta regulator are required for adaptation to oxidative stress. *J Biol Chem* **287**, 10021-10031, doi:10.1074/jbc.M111.277145 (2012).

174 Chapple, S. J., Siow, R. C. & Mann, G. E. Crosstalk between Nrf2 and the proteasome: therapeutic potential of Nrf2 inducers in vascular disease and aging. *Int J Biochem Cell Biol* **44**, 1315-1320, doi:10.1016/j.biocel.2012.04.021 (2012).

175 Kwak, M. K., Wakabayashi, N., Greenlaw, J. L., Yamamoto, M. & Kensler, T. W. Antioxidants Enhance Mammalian Proteasome Expression through the Keap1-Nrf2 Signaling Pathway. *Molecular and Cellular Biology* **23**, 8786-8794, doi:10.1128/mcb.23.23.8786-8794.2003 (2003).

176 Vangala, J. R., Dudem, S., Jain, N. & Kalivendi, S. V. Regulation of PSMB5 protein and beta subunits of mammalian proteasome by constitutively activated signal transducer and activator of transcription 3 (STAT3): potential role in bortezomib-mediated anticancer therapy. *J Biol Chem* **289**, 12612-12622, doi:10.1074/jbc.M113.542829 (2014).

177 Baraibar, M. A. & Friguet, B. in *Progress in Molecular Biology and Translational Science* Vol. Volume 109 (ed Grune Tilman) 249-275 (Academic Press, 2012).

178 Chondrogianni, N. *et al.* Overexpression of proteasome beta5 assembled subunit increases the amount of proteasome and confers ameliorated response to oxidative stress and higher survival rates. *J Biol Chem* **280**, 11840-11850, doi:10.1074/jbc.M413007200 (2005).

179 Okada, K. *et al.* 4-Hydroxy-2-nonenal-mediated Impairment of Intracellular Proteolysis during Oxidative Stress IDENTIFICATION OF PROTEASOMES AS TARGET MOLECULES. *THE JOURNAL OF BIOLOGICAL CHEMISTRY* **274**, 23787–23793 (1999).

180 Okada, K. *et al.* 4-Hydroxy-2-nonenal-mediated Impairment of Intracellular Proteolysis during Oxidative Stress. *THE JOURNAL OF BIOLOGICAL CHEMISTRY* **274**, 23787–22379 (1999).

181 REINHECKEL, T. *et al.* Comparative resistance of the 20S and 26S proteasome to oxidative stress. *Biochem. J.* **335**, 637–642 (1998).

182 Reinheckel, T., Ullrich, O., Sitte, N. & Grune, T. Differential impairment of 20S and 26S proteasome activities in human hematopoietic K562 cells during oxidative stress. *Arch Biochem Biophys* **377**, 65-68, doi:10.1006/abbi.2000.1717 (2000).

183 Aiken, C. T., Kaake, R. M., Wang, X. & Huang, L. Oxidative stress-mediated regulation of proteasome complexes. *Mol Cell Proteomics* **10**, R110 006924, doi:10.1074/mcp.M110.006924 (2011).

184 Keller, J. N., Huang, F. F. & Markesbery, W. R. Decreased levels of proteasome activity and proteasome expression in aging spinal cord. *Neuroscience* **98**, 149-156, doi:http://dx.doi.org/10.1016/S0306-4522(00)00067-1 (2000).

185 Demasi, M., Shringarpure, R. & Davies, K. J. Glutathiolation of the proteasome is enhanced by proteolytic inhibitors. *Arch Biochem Biophys* **389**, 254-263, doi:10.1006/abbi.2001.2332 (2001).

186 Demasi, M., Silva, G. M. & Netto, L. E. 20 S proteasome from Saccharomyces cerevisiae is responsive to redox modifications and is S-glutathionylated. *J Biol Chem* **278**, 679-685, doi:10.1074/jbc.M209282200 (2003).

187 Thomas, S., Kotamraju, S., Zielonka, J., Harder, D. R. & Kalyanaraman, B. Hydrogen peroxide induces nitric oxide and proteosome activity in endothelial cells: a bell-shaped signaling response. *Free Radic Biol Med* **42**, 1049-1061, doi:10.1016/j.freeradbiomed.2007.01.005 (2007).

188 Katsiki, M., Chondrogianni, N., Chinou, I., Rivett, A. J. & Gonos, E. S. The Olive constituent oleruopein exhibits proteasome stimulatory properties in vitro and confirms life span extension of human embryonic fibroblasts. *Rejuvenation Res.*, 157-172 (2007).

189 Micucci, M. *et al.* 2015. *Oxid Med Cell Longev* **2015**, doi:10.1155/2015/318125.

190 Kuckelkorn, U. *et al.* Incorporation of major histocompatibility complex – encoded subunits LMP2 and LMP7 changes the quality of the 20S proteasome polypeptide processing products independent of interferon-γ. *European Journal of Immunology* **25**, 2605-2611, doi:10.1002/eji.1830250930 (1995).

191 Caniard, A. *et al.* Proteasome function is not impaired in healthy aging of the lung. *Aging* **7**, 776-787 (2015).

192 Stratford, F. L., Chondrogianni, N., Trougakos, I. P., Gonos, E. S. & Rivett, A. J. Proteasome response to interferon-gamma is altered in senescent human fibroblasts. *FEBS Lett* **580**, 3989-3994, doi:10.1016/j.febslet.2006.06.029 (2006).

193 Giannini, C. *et al.* Poly-Ub-substrate-degradative activity of 26S proteasome is not impaired in the aging rat brain. *PLoS One* **8**, e64042, doi:10.1371/journal.pone.0064042 (2013).

194 Ferrington, D. A., Husom, A. D. & Thompson, L. V. Altered proteasome structure, function, and oxidation in aged muscle. *The FASEB Journal* **19**, 644-668 (2005).

195 Kotamraju, S. *et al.* Nitric oxide inhibits H2O2-induced transferrin receptor-dependent apoptosis in endothelial cells: Role of ubiquitin-proteasome pathway. *Proc Natl Acad Sci U S A* **100**, 10653-10658, doi:10.1073/pnas.1933581100 (2003).

196 Hasler, P. & Zouali, M. Immune receptor signaling, aging, and autoimmunity. *Cell Immunol* **233**, 102-108, doi:10.1016/j.cellimm.2005.04.012 (2005).

197 Hussong, S. A., Kapphahn, R. J., Phillips, S. L., Maldonado, M. & Ferrington, D. A. Immunoproteasome deficiency alters retinal proteasome's response to stress. *J Neurochem* **113**, 1481-1490, doi:10.1111/j.1471-4159.2010.06688.x (2010).

198 Sagiv, A. & Krizhanovsky, V. Immunosurveillance of senescent cells: the bright side of the senescence program. *Biogerontology* **14**, 617-628, doi:10.1007/s10522-013-9473-0 (2013).

199 Lujambio, A. To clear, or not to clear (senescent cells)? That is the question. *Inside the Cell* **1**, 87-95, doi:10.1002/icl3.1046 (2016).

200 Zhu, Y. *et al.* The Achilles' heel of senescent cells: from transcriptome to senolytic drugs. *Aging Cell* **14**, 644-658, doi:10.1111/acel.12344 (2015).

201 Baker, D. J. *et al.* Clearance of p16Ink4a-positive senescent cells delays ageing-associated disorders. *Nature* **479**, 232-236, doi:10.1038/nature10600 (2011).

202 Baker, D. J. *et al.* Naturally occurring p16(Ink4a)-positive cells shorten healthy lifespan. *Nature* **530**, 184-189, doi:10.1038/nature16932 (2016).

203 Zhu, Y. *et al.* Identification of a Novel Senolytic Agent, Navitoclax, Targeting the Bcl-2 Family of Anti-Apoptotic Factors. *Aging Cell* (2015).

204 Chondrogianni, N., Trougakos, I. P., Kletsas, D., Chen, Q. M. & Gonos, E. S. Partial proteasome inhibition in human fibroblasts triggers accelerated M1 senescence or M2 crisis depending on p53 and Rb status. *Aging Cell* **7** (2008).

205 Ding, Q., Dimayuga, E., Markesbery, W. R. & Keller, J. N. Proteasome inhibition increases DNA and RNA oxidation in astrocyte and neuron cultures. *J Neurochem* **91**, 1211-1218, doi:10.1111/j.1471-4159.2004.02802.x (2004).

206 Sullivan, P. G. *et al.* Proteasome inhibition alters neural mitochondrial homeostasis and mitochondria turnover. *J Biol Chem* **279**, 20699-20707, doi:10.1074/jbc.M313579200 (2004).

207 Patil, C. & Walter, P. Intracellular signaling from the endoplasmic reticulum to the nucleus: the unfolded protein response in yeast and mammals. *Current Opinion in Cell Biology* **13**, 349-355, doi:http://dx.doi.org/10.1016/S0955-0674(00)00219-2 (2001).

208 Seluanov, A. *et al.* Change of the death pathway in senescent human fibroblasts in response to DNA damage is caused by an inability to stabilize p53. *Mol Cell Biol* **21**, 1552-1564, doi:10.1128/MCB.21.5.1552-1564.2001 (2001).

209 AZIRI, H. & BENCHIMOL, S. FROM TELOMERE LOSS TO P53 INDUCTION AND ACTIVATION OF A DNA-DAMAGE PATHWAY AT SENESCENCE: THE TELOMERE LOSS/DNA DAMAGE MODEL OF CELL AGING. *Experimental Gerontoiogy* **31**, 295-301 (1996).

210 Periz, G. *et al.* Regulation of protein quality control by UBE4B and LSD1 through p53-mediated transcription. *PLoS Biol* **13**, e1002114, doi:10.1371/journal.pbio.1002114 (2015).

211 Gansauge, S. *et al.* The induction of apoptosis in proliferating human fibroblasts by oxygen radicals is associated with a p53- and p21WAF1CIP1induction. *FEBS Letters* **404**, 6-10, doi:10.1016/s0014-5793(97)00059-8 (1997).

212 Wang, E. Senescent Human Fibroblasts Resist Programmed Cell Death, and Failure to Suppress bctl Is Involved *CANCER RESEARCH* **55**, 2284-2292 (1995).

213 WEBLEY, K. *et al.* Posttranslational Modifications of p53 in Replicative Senescence Overlapping but Distinct from Those Induced by DNA Damage. *MOLECULAR AND CELLULAR BIOLOGY* **20**, 2803–2808 (2000).

9 Ehrenwörtliche Erklärung

Hiermit versichere ich,

(1) dass mir die Promotionsordnung der Fakultät bekannt ist,

(2) dass ich die vorliegende Dissertation selbständig angefertigt habe, und alle verwendeten Quellen, Hilfsmittel und persönlichen Informationen als solche gekennzeichnet habe,

(3) dass mich Prof. Dr. Regine Heller sowie Prof. Dr. Tilman Grune bei der Auswahl und Anfertigung des Materials sowie Manuskriptes unterstützt haben,

(4) dass ich weder die Hilfe eines Promotionsberaters in Anspruch genommen habe, noch andere Personen unmittelbare oder mittelbare geldwerte Leistungen von mir erhalten haben, die im Zusammenhang mit dem Inhalt der vorgelegten Dissertation stehen,

(5) dass ich die Dissertation noch nicht als Prüfungsarbeit für eine staatliche oder andere wissenschaftliche Prüfung eingereicht habe

(6) dass ich zu keinem Zeitpunkt die gleiche, eine in wesentlichen Teilen ähnliche oder eine andere Abhandlung als Dissertation an einer anderen Hochschule eingereicht habe.

Jena 16.11.2016

Europass Curriculum Vitae

Personal information

First name(s) / Surname(s)	**Odeta Meçe**
Address(es)	Neugasse 26, App11, Jena 07743, Germany
Telephone(s)	+4917684290351
E-mail	Odeta.Mece@med.uni-jena.de odetamece@hotmail.com
Nationality	Albanian
Date of birth	08.05.1987
Gender	Female

Education and training

Dates	**03/2012-**
Title of qualification	PhD student at the Institute of Molecular Cell Biology, Centre for Molecular Biomedicine, Jena, Germany
Principal subjects/occupational skills covered	Molecular Cell Biology
Name and type of organisation providing education and training	Jena University Hospital, Centre for Molecular Biomedicine, Institute of Molecular Cell Biology, Hans-Knöll-Str. 2, 07745 Jena, Germany
Level in national or international classification	Aims the academic title PhD
Dates	**2008-2010**
Title of qualification	Master degree in Biology
Principal subjects/occupational skills covered	Cell biology, Immunology
Name and type of organisation providing education and training	University of Tirana, Albania Faculty of Natural Science, Department of Biology

Dates	**2005-2008**
Title of qualification	Undergraduate degree in Biology
Principal subjects/occupational skills covered	Cell Biology, Genetics, Physiology
Name and type of organisation providing education and training	University of Tirana, Albania Faculty of Natural Science, Department of Biology
Level in national or international classification	Undergraduate degree

Work experience

Dates	**10/2010-10/2011**
Occupation or position held	Assistant of Prof. Dr. Stelian Buzo in the course of Clinical Biochemistry
Main activities and responsibilities	Tutoring student seminars and practical courses of Biology and Clinical Biochemistry
Name and address of the employer	Universiteti Logos, Rruga "Dritan Hoxha" Pallatet Komfort , Tirane, Albania
Type of business or sector	Logos University (Degree awarding educational institution in Clinical Biochemistry)

Personal skills and competences

Mother tongue(s) **Albanian**

Other language(s)

Self-assessment	Understanding		Speaking		Writing
European level (*)	Listening	Reading	Spoken interaction	Spoken production	
English	Excellent	Excellent	Excellent	Excellent	Excellent
German	Very good	Very good	Good	Good	Good
Greek	Very good	Good	Very good	Very good	Good

Social skills and competences	Good team spirit, adaptability and collaboration capabilities
Organisational skills and competences	Ability to organize well time and effort, commitment and seriousness at work and projects I involve myself in
Technical skills and competences	Cell culture and transfection, proteins and mRNA extraction, western blotting, qPCR, microscopy and flow Cytometry
Computer skills and competences	Knowledge of Microsoft applications and office: MS word, MS excel, Ms PowerPoint, Adobe Ilustrator, GraphPAD PRISM, Image J etc…

Published abstracts

Odeta Meçe, Nderim Kryeziu, Tilman Grune, Regine Heller, The role of proteasomal protein degradation in endothelial Senescence, *Perfusion, 1, 2015, p.39*

Katrin Spengler, Nderim Kryeziu, Silke Lindenmüller, **Odeta Meçe**, Anne Weiland, Lars-Oliver Klotz, Regine Heller, Angiogenesis is dependent on endothelial autophagy – the role of AMPK, *Perfusion, 1, 2015, p.47*

Odeta Meçe, Tilman Grune, Regine Heller, Premature senescence and proteolytic activities in endothelial cells, *Perfusion, 1, 2014, p41*

Conference contributions

Odeta Meçe, Nderim Kryeziu, Tilman Grune, Regine Heller Premature Senescence and proteolytic activities in endothelial cells. Stress und Altern Chancen und Risken September 24th-27th 2014, University Hospital Halle-Saale **(Oral presentation)**

Odeta Meçe, Tilman Grune, Regine Heller, Premature senescence and proteolytic activities in endothelial cells. Stress and Ageing: From Molecular Biology to Clinical Perspective, September 6th-8th 2013, Heart Center, University Hospital Halle-Saale **(Poster presentation)**

Odeta Meçe, Nderim Kryeziu, Tilman Grune, Regine Heller, Compromised proteasomal activity in endothelial cell senescence. Annual Conference of German Association for Aging Research, Jena 2015 **(Poster presentation)**

Odeta Meçe, Nderim Kryeziu, Tilman Grune, Regine Heller, The role of proteasomal protein degradation in endothelial senescence, Annual meeting of the DGAF, Rauischholzhausen, March 2013 **(Poster Presentation)**

Katrin Spengler, Nderim Kryeziu, Silke Lindenmüller, **Odeta Meçe**, Anne Weiland, Lars-Oliver Klotz, Regine Heller, Angiogenesis is dependent on endothelial autophagy – the role of AMPK, Annual meeting of the DGAF, Rauischholzhausen, March 2015 **(Poster Presentation)**

Honors and awards

DAAD scholarship winner for a research grant for 3 years for doctoral candidates and researchers

Winner of "Hans Kaffarnic" award given for the best poster presentation, March 2015, Annual Meeting of the German association for Atherosclerosis research

Additional information

1. **7th Proteasome and Autophagy workshop**, 6th – 8th April 2016, Clermont-Ferrand, France.
2. **Summer School of Molecular Medicine**, hosted by the Interdisiplinary Center for Clinical Research, Jena University Hospital, Germany from August 29 till September 29, 2011, Insights (practical and theoretical) into research topics of molecular medicine

3. **Summer School of Free Radical Biology,** Spetces, Greece, SFRR, September 2012

4. **EFIS-EJI South East European Immunology School**, Arandjelovac, Serbia, October 2011
5. Participation and thesis presentation at the **International Congres of Ecosystems,** Tirana, June 4-6, 2011
6. **International Training in Reproductive sciences and Technologies** held at the Friedrich Schiller University of Jena, Germany, November 2010
7. Participation in **"18th Balkan Clinical Laboratory Federation Meeting",** Tirana, 22-25 August 2010
8. Participation at the **International Summer School of Applied Spectroscopy** held at the University of Novi Sad, Faculty of Technology, Serbia, July 2010